

A comprehensive proteomic and bioinformatics analysis of human spinal cord injury plasma identifies proteins associated with the complement cascade and liver function as potential prognostic indicators of neurological outcome

1 Abstract

1.1 Introduction

Spinal Cord Injury (SCI) is a major cause of disability, with complications post-injury often leading to life-long health issues with need of extensive treatment. Neurological outcome post-SCI can be variable and difficult to predict, particularly in incomplete injured patients. The identification of specific SCI biomarkers in blood, may be able to improve prognostics in the field. This study has utilised proteomic and bioinformatics methodologies to investigate differentially expressed proteins in plasma samples across human SCI cohorts with the aim of identifying prognostic biomarkers and biological pathway alterations that relate to neurological outcome.

1.2 Methods and Materials

Blood samples were taken, following informed consent, from ASIA impairment scale (AIS) grade C "Improvers" (AIS grade improvement) and "Non-Improvers" (No AIS change), and AIS grade A and D at <2 weeks ("Acute") and approx. 3 months ("Sub-acute") post-injury. The total protein concentration from each sample was extracted, with pooled samples being labelled and non-pooled samples treated with ProteoMiner™ beads. Samples were then analysed using two 4-plex isobaric tag for relative and absolute quantification (iTRAQ) analyses and a label-free experiment for comparison, before quantifying with mass spectrometry.

Proteomic datasets were analysed using OpenMS (version 2.6.0). R (version 4.1.4) and in particular, the R packages MSstats (version 4.0.1), STRINGdb (version 2.4.2) and pathview (version 1.32.0) were used for downstream analysis. Proteins of interest identified from this analysis were further validated by enzyme-linked immunosorbent assay (ELISA).

1.3 Results

The data demonstrated proteomic differences between the cohorts, with the results from the iTRAQ approach supporting those of the label-free analysis. A total of 79 and 87 differentially abundant proteins across AIS and longitudinal groups were identified from the iTRAQ and label-free analyses, respectively. Alpha-2-macroglobulin (A2M), retinol binding protein 4 (RBP4), serum

34 amyloid A1 (SAA1), Peroxiredoxin 2, alipoprotein A1 (ApoA1) and several immunoglobulins were
35 identified as biologically relevant and differentially abundant, with potential as individual prognos-
36 tic biomarkers of neurological outcome. Bioinformatics analyses revealed that the majority of dif-
37 ferentially abundant proteins were components of the complement cascade and most interacted
38 directly with the liver.

39 **1.4 Conclusions**

40 Many of the proteins of interest identified using proteomics were detected only in a single group
41 and therefore have potential as a binary (present or absent) biomarkers, RBP4 and PRX-2 in particu-
42 lar. Additional investigations into the chronology of these proteins, and their levels in other tissues
43 (cerebrospinal fluid in particular) are needed to better understand the underlying pathophysiol-
44 ogy, including any potentially modifiable targets. Pathway analysis highlighted the complement
45 cascade as being significant across groups of differential functional recovery.

46 **2 Introduction**

47 Spinal cord injury (SCI) is the transient or permanent loss of normal spinal sensory, motor or au-
48 tonomic function, and is a major cause of disability. Globally, SCI affects around 500,000 people
49 each year and is most commonly the result of road traffic accidents or falls.(Crozier-Shaw, Den-
50 ton, and Morris 2020) Patients typically require extensive medical, rehabilitative and social care at
51 high financial cost to healthcare providers. The lifetime cost of care in the UK is estimated to be
52 £1.12 million (mean value) per SCI, with the total cost of SCI in the UK to the NHS being £1.43 bil-
53 lion in 2016.(McDaid et al. 2019) Individuals with SCI show markedly higher rates of mental illness
54 relative to the general population.(Furlan, Gulasingam, and Craven 2017) Complications arising
55 post-SCI can be long-lasting and often include pain, spasticity and cardiovascular disease, where
56 the systemic inflammatory response that follows SCI can frequently result in organ complications,
57 particularly in the liver and kidneys.(Gris, Hamilton, and Weaver 2008; Sun et al. 2016; Hagen 2015)

58 The recovery of neurological function post-SCI is highly variable, requiring any clinical trials to have
59 an impractically large sample size to prove efficacy, hence the translation of novel efficacious ther-
60 apies is challenging and expensive.(Spiess et al. 2009) Being able to more accurately predict patient
61 outcomes would aid clinical decisions and facilitate future clinical trials. Therefore, novel biomark-
62 ers that allow for stratification of injury severity and capacity for neurological recovery would be
63 of high value to the field.

64 Biomarkers studies in SCI often investigate protein changes in cerebral spinal fluid (CSF) as the
65 closer proximity of this medium is thought to be more reflective of the parenchymal injury.(Brian
66 K. Kwon et al. 2019; Hulme et al. 2017) Whilst this makes CSF potentially more informative for
67 elucidating the pathology of SCI, the repeated use of CSF for routine analysis presents challenges
68 in clinical care due to the risk and expense associated with the invasiveness of the collection pro-
69 cedure. In contrast, systemic biomarkers measurable in the blood represent a source of information
70 that can be accessed and interpreted both a lower cost and risk. Studies of traumatic brain in-
71 jury have demonstrated that protein markers identified in CSF are also detectable in both plasma
72 and serum.(Wang et al. 2018) More recently, circulating white blood cell populations have also
73 been identified as potential SCI injury biomarkers, with a 2021 study showing that elevated levels
74 of neutrophils were associated with no AIS grade conversion, while conversely an increase in lym-
75 phocytes during the first week post-SCI were associated with an AIS grade improvement.(Jogia et
76 al. 2021)

77 A number of individual proteins have been shown to be altered in the bloods post-SCI, including
78 multiple interleukins (IL), tumour necrosis factor alpha (TNF- α) and C-reactive protein (CRP).(Segal

79 et al. 1997; Hayes et al. 2002; Frost et al. 2005)

80 Further, changes in inflammatory marker levels detected in acute SCI patients were found to
81 be mirrored in donor-matched blood and CSF, albeit at lower absolute concentrations systemi-
82 cally.(Brian K. Kwon et al. 2010)

83 Previously, we have shown that routinely collected blood measures associated with liver function
84 and inflammation added predictive value to AIS motor and sensor outcomes at discharge and 12-
85 months post-injury.(Bernardo Harrington et al. 2020; Brown et al. 2019) The current study uses
86 an unbiased shotgun proteomic approach to investigate differentially expressed proteins in SCI
87 patients, coupled with bioinformatics pathway and network analyses.

88 3 Methods and Materials

Table 1. Patient demographics. ± denotes interquartile range

	n	Percent
Polytrauma		
Yes	16	41
No	23	59
Gender		
F	13	33
M	26	67
Diabetes		
Yes	7	18
No	32	82
Neurological level		
C	26	67
L	4	10
T	9	23
AIS change		
A	11	28
C	7	18
C->D	10	26
D	11	28
Age at injury (Median years±IQR)	53±26	-

89 3.1 Patients

90 Blood samples were taken from SCI patients who had provided informed consent and in accord-
91 ance to ethical provided by the National Research Ethics Service [NRES] Committee North West
92 Liverpool East [11/NW/0876]. “Improvers” were defined as individuals who experienced an AIS
93 grade improvement from admission to a year post-injury, whereas “non-improvers” were defined
94 as patients who saw no change in AIS grade in the same period.

95 3.2 Plasma collection and storage

96 Plasma samples were collected within 2 weeks of injury (acute) and at approximately 3 months
97 post-injury (subacute). Upon collection in EDTA (ethylenediaminetetraacetic acid) coated tubes
98 samples were centrifuged at 600g for 15 minutes, to pellet erythrocytes and the resultant plasma

99 fraction was aspirated and divided into aliquots for long-term storage in -80°C briefly and liquid
100 nitrogen in the longer term.

101 **3.3 Sample preparation and analysis using iTRAQ proteomics**

102 Thawed plasma samples ($2\mu\text{l}$) each were diluted with distilled water ($98\mu\text{l}$). Total protein was
103 quantified using a Pierce™ 660nm Protein Assay (Thermo Fisher Scientific, Hemel Hempstead,
104 UK)(Stoscheck 1987).

105 A total of 100mg of plasma protein was taken from each sample and pooled equally to form a
106 patient test group. For example, the AIS C improver group was pooled from 10 separate patient
107 samples, 10mg of protein per patient.

108 The pooled plasma samples were precipitated by incubation of the sample in six times the volume
109 of chilled acetone for 1 hour at -20°C. The samples were then centrifuged at 6,000G for 10 minutes
110 at 4°C, and re-suspended in $200\mu\text{l}$ of triethylammonium bicarbonate buffer. Sequencing Grade
111 Modified Trypsin ($10\mu\text{g} \cdot 85\mu\text{g}$ of protein; Promega, Madison, WI, USA) was then added to the sam-
112 ples for overnight digestion at 37°C. Peptides underwent reduction and alkylation (according to
113 the manufacturer's instructions; Applied Biosystems, Bleiswijk, The Netherlands). Tryptic digests
114 were labelled with iTRAQ tags (again according to the manufacturer's instructions for the iTRAQ
115 kit), before being pooled into test groups and dried in a vacuum centrifuge. Two individual iTRAQ
116 experiments were set up, the first to assess acute and sub-acute improvers or non-improvers and
117 the second to assess acute improvers and non-improvers to AIS grade A and D patients. The follow-
118 ing tags were used for each group of patient samples 114 tag - acute improvers, 115 tag - sub-acute
119 improvers, 116 tag - acute non-improvers and 117 tag - sub-acute non-improvers for run 1 and 114
120 tag - acute improvers, 115 tag - acute non-improvers, 116 tag - AIS grade A and 117 tag - AIS grade
121 D for run 2.

122 **3.3.0.1 iTRAQ mass spectrometry analysis** The samples were analysed at the BSRC St. An-
123 drews University Mass Spectrometry and Proteomics Facility. A total of 12 SCX fractions were
124 analysed by nano-electrospray ionisation-liquid chromatography/tandem mass spectrometry (LC-
125 MS/MS) using a TripleTOF 5600 tandem mass spectrometer (AB Sciex, Framingham, MA, USA) as
126 described previously.(Fuller et al. 2015) Each fraction ($10\mu\text{l}$) was then analysed by nanoflow LC-ESI-
127 MSMS, as described previously.

128 **3.3.1 Sample preparation and analysis using label-free proteomics**

129 No sample pooling was used, and so each of the 73 samples were maintained separately through-
130 out protein equalisation, mass spectrometry, and label-free quantification steps. Thus, protein
131 abundance was quantified for each sample, whereupon mean protein abundance across experi-
132 mental groups was calculated to assess protein changes.

133 To reduce the dynamic range of proteins, ProteoMiner™ beads (BioRad, Hemel Hempstead, UK)
134 were used.(Boschetti and Righetti 2008) Total protein was quantitated with a Pierce™ 660nm Pro-
135 tein Assay (Thermo Fisher Scientific, Hemel Hempstead, UK), whereupon 5 mg of total protein was
136 applied to ProteoMiner™ beads, and processed as described previously.(Stoscheck 1987; Peffers
137 et al. 2015)

138 **3.3.1.1 Label free mass spectrometry analysis** Tryptic peptides were subjected to LC-MC/MC
139 via a 2-h gradient on a NanoAcuity™ ultraperformance LC (Waters, Manchester, UK) connected to
140 a Q-Exactive Quadrupole-Orbitrap instrument (Thermo-Fisher Scientific Hemel Hempstead, UK).

141 The Q-Exactive was operated in a data dependent positive electrospray ionisation mode, automatically
142 switching between full scan MS and MS/MS acquisition. Survey full scan MS spectra (*m/z*
143 300–2000) were acquired in the Orbitrap with 70,000 resolution (*m/z* 200) following accumulation
144 of ions to 1×10^6 target value based on the predictive automatic gain control values from the previous
145 full scan. Dynamic exclusion was set to 20s, the 10 most intense multiply charged ions (≥ 2)
146 were sequentially isolated and fragmented in the octopole collision cell by higher energy collisional
147 dissociation (HCD), with a fixed injection time of 100ms and 35,000 resolution. The following
148 mass spectrometric conditions were used: spray voltage, 1.9kV, no sheath or axillary gas flow;
149 normalised HCD collision energy 30%; heated capillary temperature, 250°C. MS/MS ion selection
150 threshold was set to 1×10^4 count and 2Da isolation width was set.

151 **3.3.2 iTRAQ OpenMS analysis**

152 TripleTOF 5600 tandem mass spectrometer output files produced in the ABSciex proprietary .wiff
153 file format were converted to an open file format, .mzML for analysis with OpenMS (version 2.6.0).
154 The docker image of ProteoWizard version 3.0.20287 was used for conversion, and peak picking
155 was applied on conversion (Chambers et al. 2012). OpenMS version 2.6.0 was used for further anal-
156 ysis.(Röst et al. 2016) Unless otherwise stated, default arguments were used. The 12 fraction files
157 were merged and sorted by retention time. A decoy database was generated with DecoyDatabase
158 and the -enzyme flag set to Trypsin, the human reference proteome was taken from Uniprot (Pro-
159 teome ID: UP000005640, downloaded: 2020-10-01), as was the .fasta for porcine trypsin (Entry:
160 P00761, downloaded: 2020-10-01).(The UniProt Consortium 2021)

161 The MSFQPlusAdapter was used to run the search. For the -fixed_modifications "Methylthio (C)"
162 and "iTRAQ4plex (N-term)" were passed due to the alkylating agent used in sample preparation
163 and to account for the N-terminus modifications made by iTRAQ tags. "Oxidation (M)" was passed
164 to -variable_modifications to reflect the likely occurrence of methionine oxidation. To reflect the
165 instrument the following flags were also set: -precursor_mass_tolerance 20 -enzyme Trypsin/P
166 -protocol iTRAQ -instrument high_res.

167 To annotate the search results PeptideIndexer and PSMFeatureExtractor were used. For peptide
168 level score estimation and filtering PercolatorAdapter was used with the following arguments:
169 -score_type q-value -enzyme trypsinp. IDFfilter was used to filter to a peptide score of 0.05
170 with -score:pep 0.05

171 IsobaricAnalyzer with -type itraq4plex was used with the merged .mzML files to assign protein-
172 peptide identifications to features or consensus features with IDMapper. The files for each run
173 output by IDMapper were then merged with FileMerger. Bayesian score estimation and protein
174 inference was performed with Epifany and the following flags: -greedy_group_resolution
175 remove_proteins_wo_evidence -algorithm:keep_best_PSM_only false Decoys were removed
176 and 0.05 FDR filtering was done via IDFfilter with -score:protgroup 0.05 -remove_decoys.
177 Finally, IDConflictResolver was used to resolve ambiguous annotations of features with peptide
178 identifications, before quantification with ProteinQuantifier.

179 **3.3.3 Label free OpenMS analysis**

180 For quantification, the raw spectra files were analysed via OpenMS (version 2.6.0) command line
181 tools, with the workflow from the prior section (3.3.2) adapted to suit a label-free analysis. The
182 files were first converted from the proprietary .Raw format to the open .mzML standard with the
183 FileConverter tool via the open-source ThermoRawFileParser.(Röst et al. 2016; Hulstaert et al.
184 2020) Unless otherwise stated, default arguments were used throughout.

185 The decoy database generated in the prior section (iTRAQ OpenMS analysis) was also re-used. The

186 CometAdapter was used to run the search.(Eng, Jahan, and Hoopmann 2013) Fixed modifications
187 were set to "Carbamidomethyl (C)" and "Oxidation (M)" was set as a variable modification. To reflect
188 the instrument the following flags were also set: -precursor_mass_tolerance 20 -isotope_error
189 0/1.

190 To annotate the identified peptides with proteins the PeptideIndexer tool was used. PeptideIndexer
191 and PSMFeatureExtractor were used for annotation. For peptide level score estimation and fil-
192 tering PercolatorAdapter was used with the following flags: -score_type q-value -enzyme
193 trypsin. IDFFilter was used to filter to a peptide score of 0.01 with -score:pep 0.01 followed
194 by IDScoreSwitcher with the following flags: -new_score "MS:1001493" -new_score_orientation
195 lower_better -new_score_type "pep" -old_score "q-value". The ProteomicsLFQ was used for
196 subsequent processing with the flags: -proteinFDR 0.05 -targeted_only true. The -out_msstats
197 flag was also used to produce quantitative data for downstream statistical analysis with the R
198 package MSstats.(Choi et al. 2014)

199 **3.3.4 Network and pathway analysis**

200 The Bioconductor package ReactomePA, which employs the open-source, open access, manually
201 curated and peer-reviewed pathway database Reactome was used for network analysis.(Yu and
202 He 2016; Jassal et al. 2020)

203 **3.3.5 Enzyme-linked immunosorbent assays**

204 Four proteins identified by the iTRAQ analysis were measured by enzyme-linked immunoab-
205 sorbent assay (ELISA) from non-pooled samples to validate the iTRAQ findings.

206 These proteins were alpha-2-macroglobulin (A2M), retinol binding protein 4 (RBP4), serum amy-
207 loid A1 (SAA1) and apolipoprotein A1 (ApoA1). They were selected for their biological relevance
208 and differential abundance between AIS C improvers and non-improvers, implying potential as
209 biomarkers of neurological outcome prediction. A2M, RBP4 and SAA1 were assessed using a hu-
210 man DuoSet® ELISAs (R&D Systems, Abingdon, UK). ApoA1 was assessed using a human Quan-
211 tikine® ELISA (R&D Systems, Abingdon, UK). Samples were diluted 1:600,000 for A2M and RBP4,
212 1:100 for SAA1 and 1:20,000 for ApoA1 in the respective assay kit diluent. Samples that were above
213 the assay detection limit were rerun at 1:300 and 1:40,000 for SAA1 and ApoA1 respectively. All
214 ELISAs were carried out according to the manufacturer's protocol. Protein concentrations were
215 normalised to the sample dilution factor. Statistical analysis was performed using the statistical
216 programming language R version 4.1.3 (2022-03-10). Pairwise t tests with bonferroni adjusted P-
217 values with the R rstatix package were used to assess differential abundance.

218 **4 Results**

219 **4.1 Results**

220 Plasma from American Spinal Injury Association (ASIA) grade C SCI patients (total n=17) contrasting
221 those who experienced an ASIA grade conversion (n=10), and those who did not (n=7) collected
222 within 2 weeks, and at approximately 3 months post-injury (Improvers n=9 vs Non-improvers n=6).
223 Relative protein abundance in AIS grade A (n=10) and grade D (n=11) patients was also examined.

224 In the interest of brevity, only the plots of acute and subacute AIS C improvers VS non-improvers
225 are included here, please see the supplemental data for the other comparisons (section 5).

²²⁶ **4.1.1 Comparing OpenMS and ProteinPilot**

²²⁷ The AIS A group had 56 and 26 more abundant and 9 and 6 less abundant proteins respectively.
²²⁸ Acutely, AIS C improvers relative to AIS A and D had 21 and 53 more abundant and 46 and 12 less
²²⁹ abundant for OpenMS, whereas ProteinPilot had 5 and 19 more abundant proteins, and 18 and 6
²³⁰ less abundant.

²³¹ **4.1.2 iTRAQ analyses**

²³² **4.1.3 Differential protein abundances**

²³³ AIS C improvers had 18 more abundant proteins and 49 less abundant proteins at the acute phase
²³⁴ relative to non-improvers. Similarly, at the subacute phase, AIS C improvers had 34 more abun-
²³⁵ dant proteins and 34 less abundant proteins relative to non-improvers. The AIS A group had 56
²³⁶ more abundant and 9 less abundant proteins respectively relative to non-improvers. Acutely, AIS
²³⁷ C improvers relative to AIS A and D had 21 and 53 more abundant and 46 and 12 less abundant
²³⁸ proteins. Please see the appendix for a full list of protein changes.

²³⁹ **4.1.4 Heatmaps**

²⁴⁰ The majority of the pathways associated with the proteins identified by these iTRAQ experiments
²⁴¹ are related to the complement cascade and platelet activity (Figure 1, 2, S1, S2, S3, S4, S5, S6, S7, S8).
²⁴² There are also several pathways implicated in metabolic processes, particularly with apolipopro-
²⁴³ teins and retinoids.

Acute AIS C Improvers VS non-Improvers

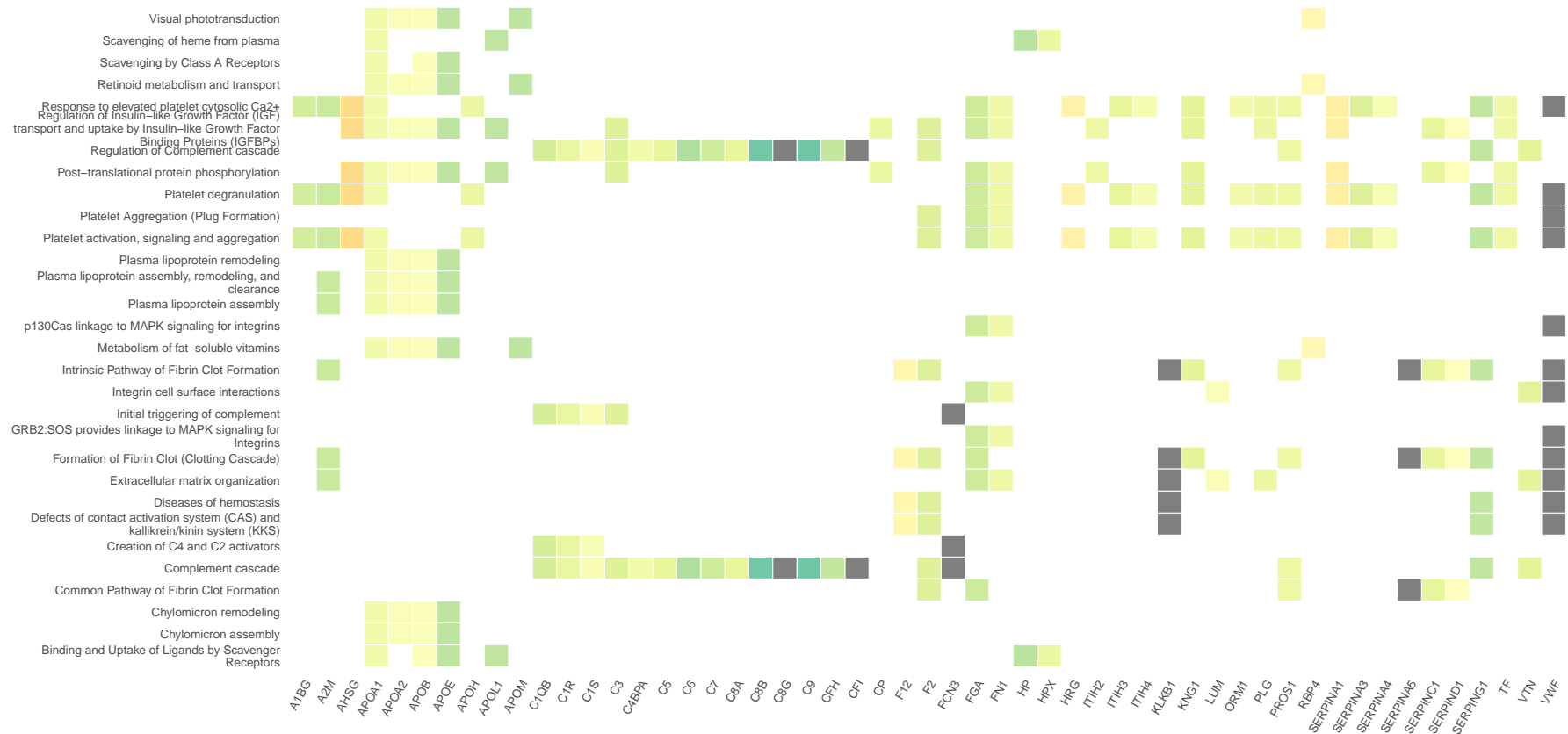


Figure 1. Heatmap denoting the log₂ fold change of proteins in plasma collected 2-weeks post-injury, and the biological pathways these proteins are associated with on Reactome. This compares AIS C SCI patients who experienced an AIS grade improvement and those who did not.

Subacute AIS C Improvers VS non-Improvers

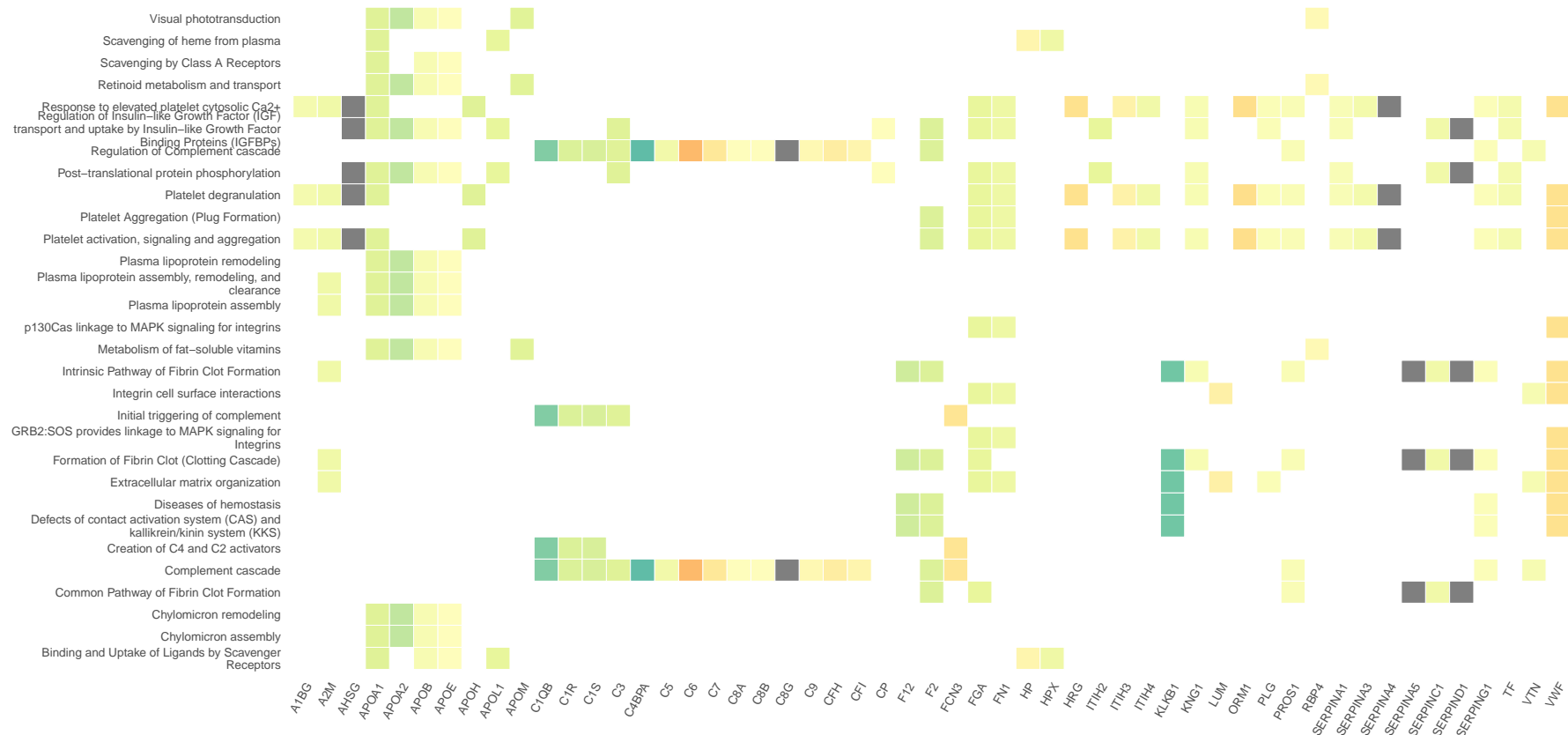


Figure 2. Heatmap denoting the log₂ fold change of proteins in plasma collected 3-months post-injury, and the biological pathways these proteins are associated with on Reactome. This compares AIS C SCI patients who experienced an AIS grade improvement and those who did not.

²⁴⁴ Similarly to the iTRAQ data, many of the Reactome pathways are associated with the complement cascade and platelets activation (Figures 3, 4, S9, S10, S11, S12, S13, S14, S15).

²⁴⁵ Please see appendix section 5.3 for additional plots.

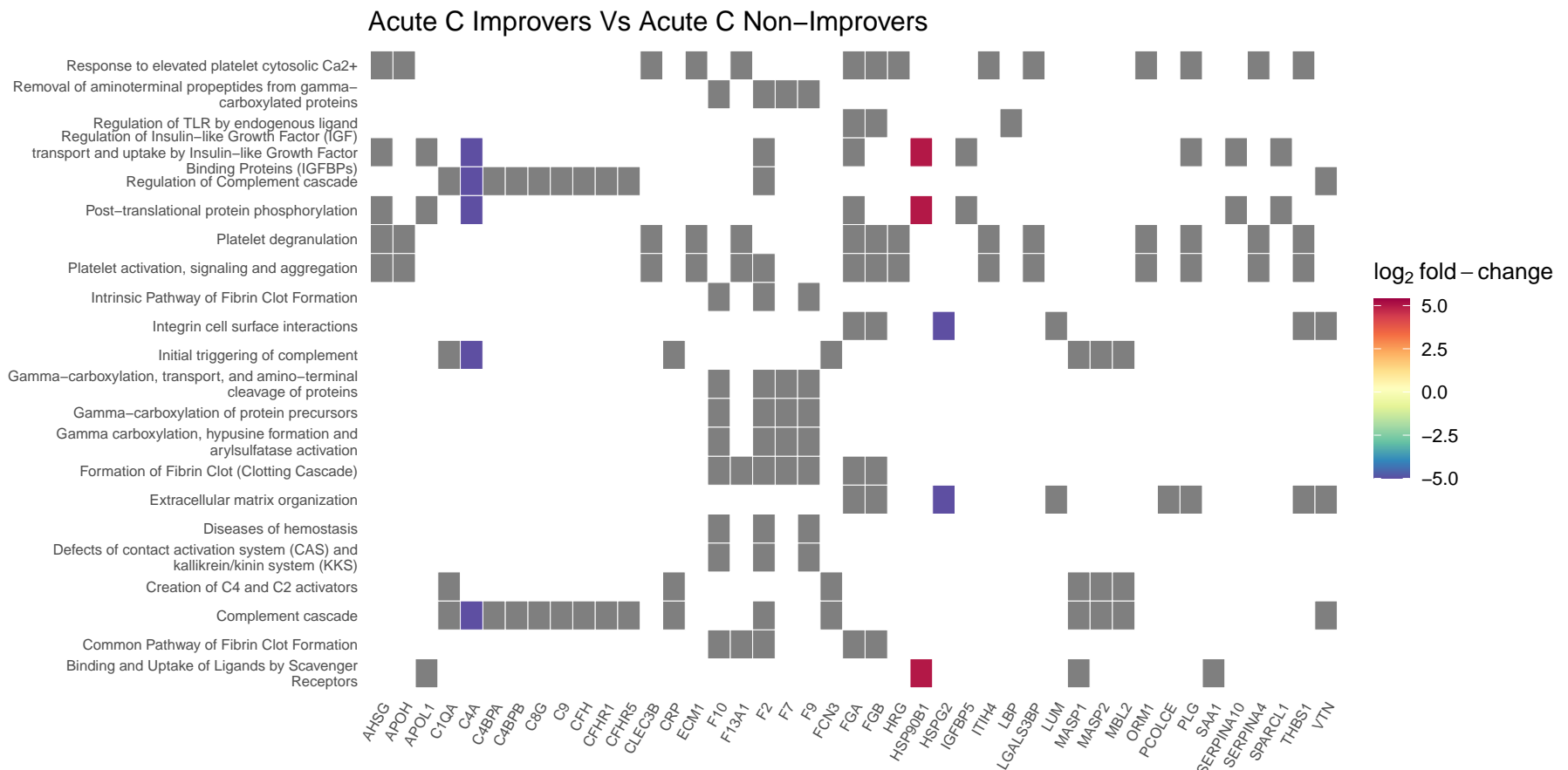


Figure 3. Heatmap denoting the \log_2 fold change of proteins in plasma collected 2-weeks post-injury, and the biological pathways these proteins are associated with on Reactome. This compares AIS C SCI patients who experienced an AIS grade improvement and those who did not. Grey blocks denote proteins not present in the comparison.

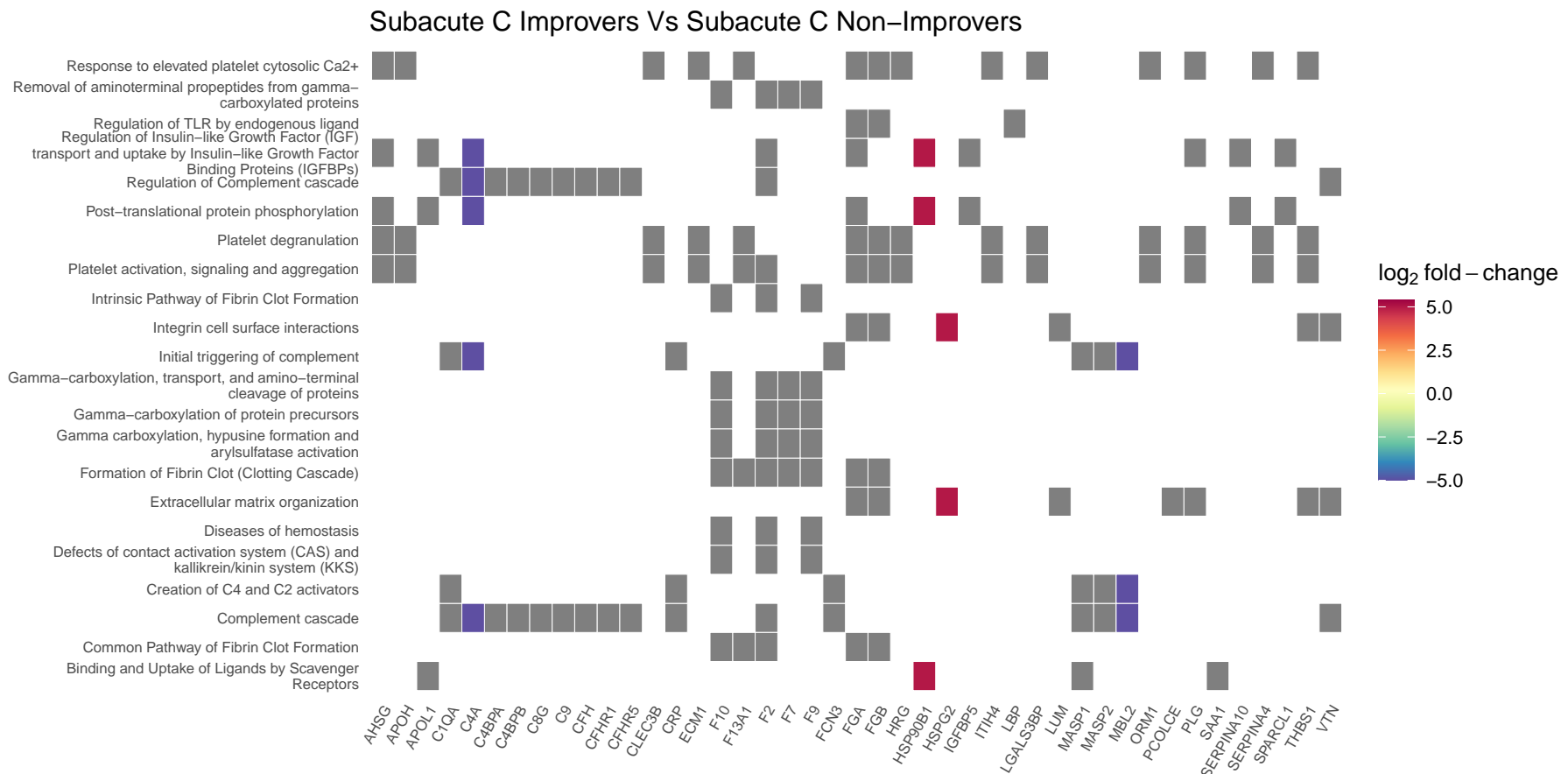


Figure 4. Heatmap denoting the \log_2 fold change of proteins in plasma collected 3-months post-injury, and the biological pathways these proteins are associated with on Reactome. This compares AIS C SCI patients who experienced an AIS grade improvement and those who did not. Grey blocks denote proteins not present in the comparison.

²⁴⁷ **4.1.5 Network analysis of Differentially Abundant Proteins between AIS C improvers and
248 non-improvers**

²⁴⁹ Similar to the heatmaps, network plots highlighted that the majority of proteins changes were
250 associated with the complement cascade and pathways linked to platelet activity (Figure 5, 6, S16,
251 S17, S18, S19, S20, S21, S22, S23). Several proteins were also associated with the regulation of
252 insulin-like growth factor.

Acute AIS C Improvers VS non-Improvers

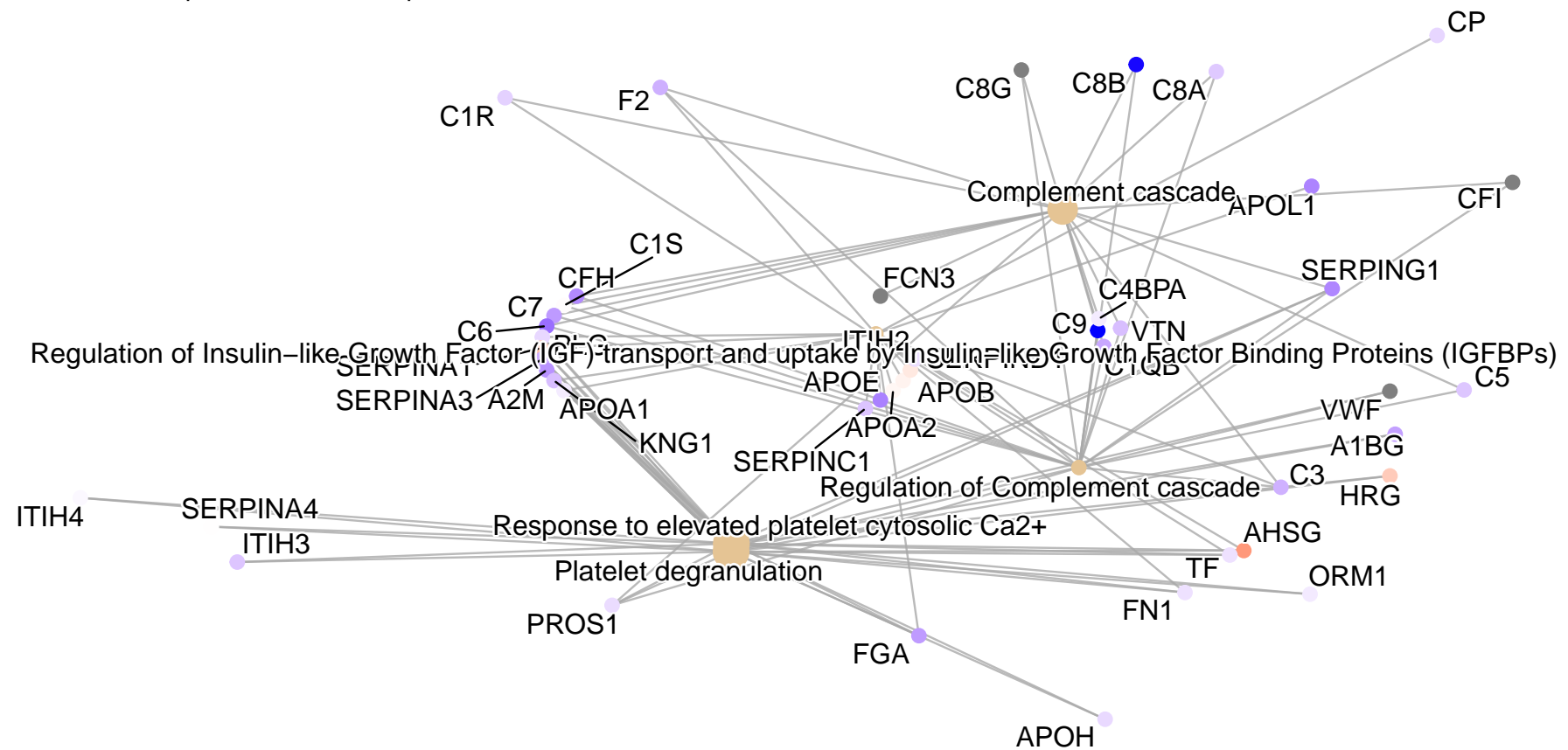


Figure 5. Network plot denoting the \log_2 fold change of proteins in plasma collected 2-weeks post-injury, and the biological pathways these proteins are associated with on Reactome. This compares AIS C SCI patients who experienced an AIS grade improvement and those who did not.

Subacute AIS C Improvers VS non-Improvers

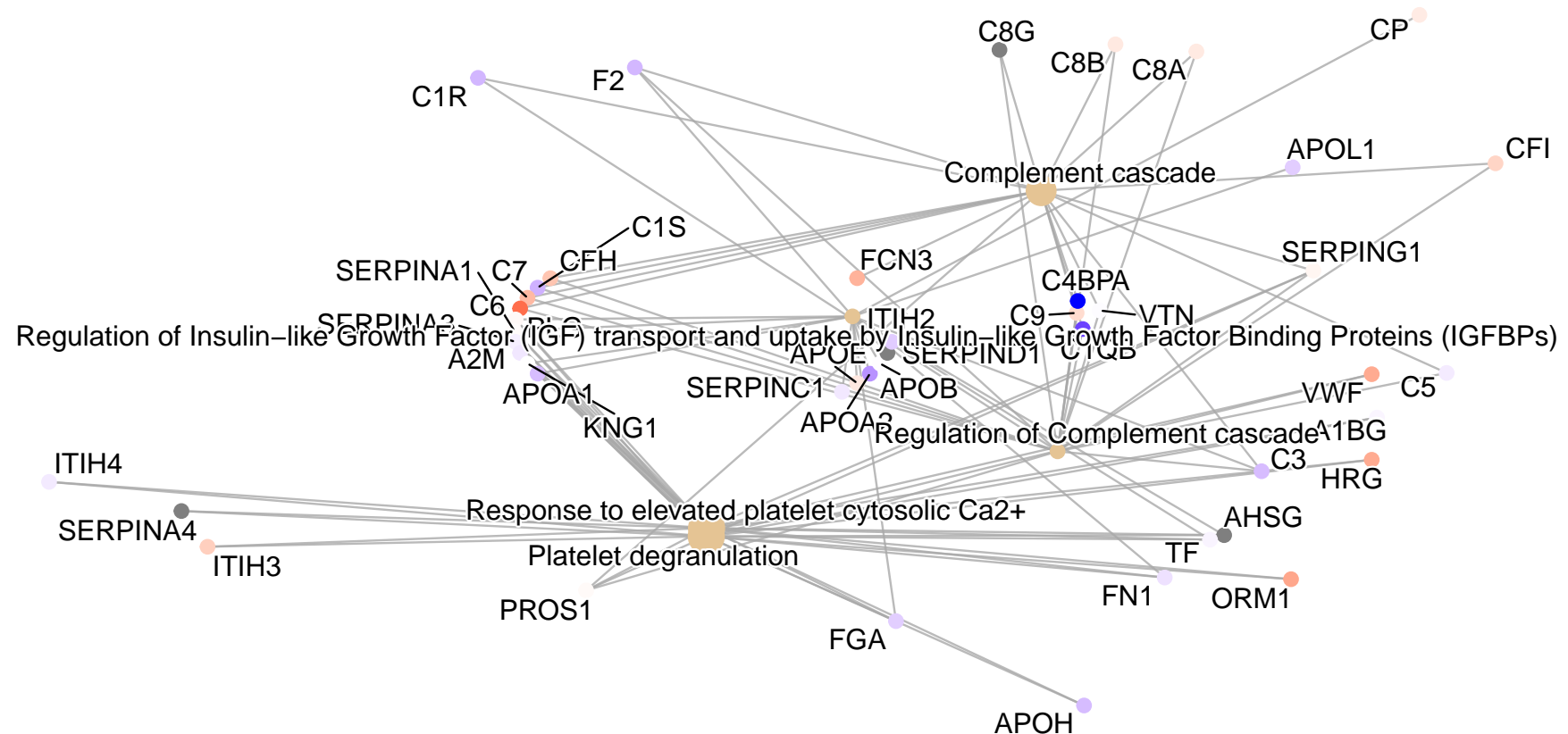


Figure 6. Network plot denoting the \log_2 fold change of proteins in plasma collected 3-months post-injury, and the biological pathways these proteins are associated with on Reactome. This compares AIS C SCI patients who experienced an AIS grade improvement and those who did not.

- ²⁵³ Similarly to the heatmaps and the iTRAQ data, network plots derived using the label-free data
²⁵⁴ highlight the majority of differential proteins are associated with the complement cascade and
²⁵⁵ pathways linked to platelets (Figures 7, 8, S24, S25, S26, S27, S28, S29, S30).
- ²⁵⁶ Please see appendix section 5.4 for additional plots.

Acute C Improvers Vs Acute C Non-Improvers

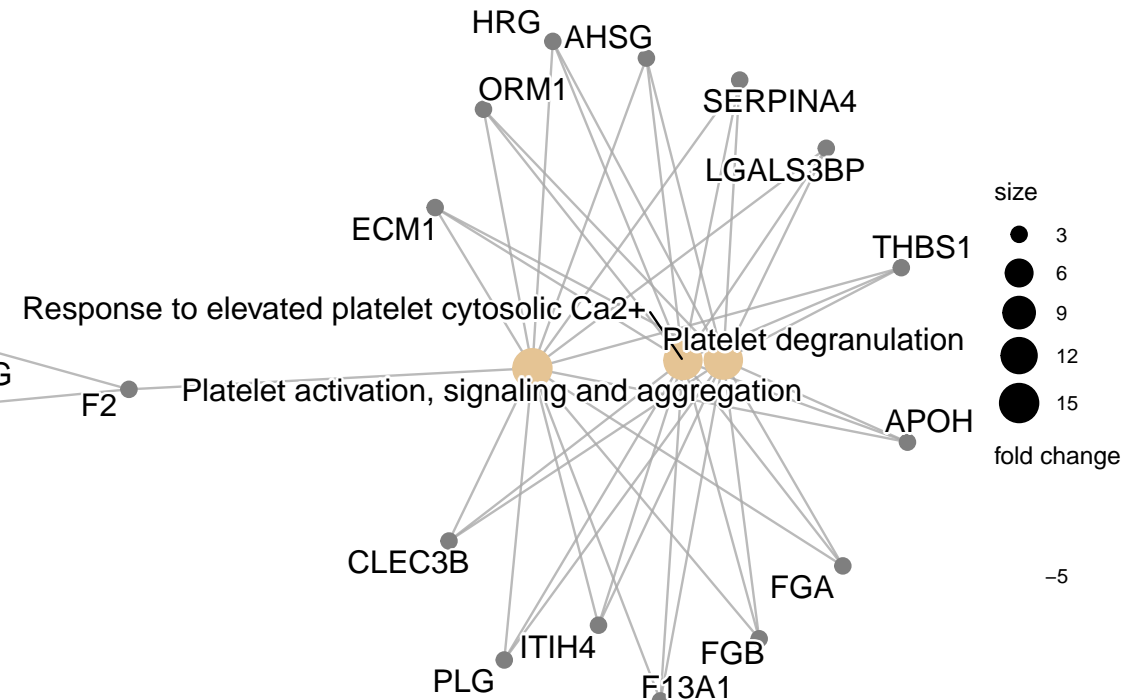
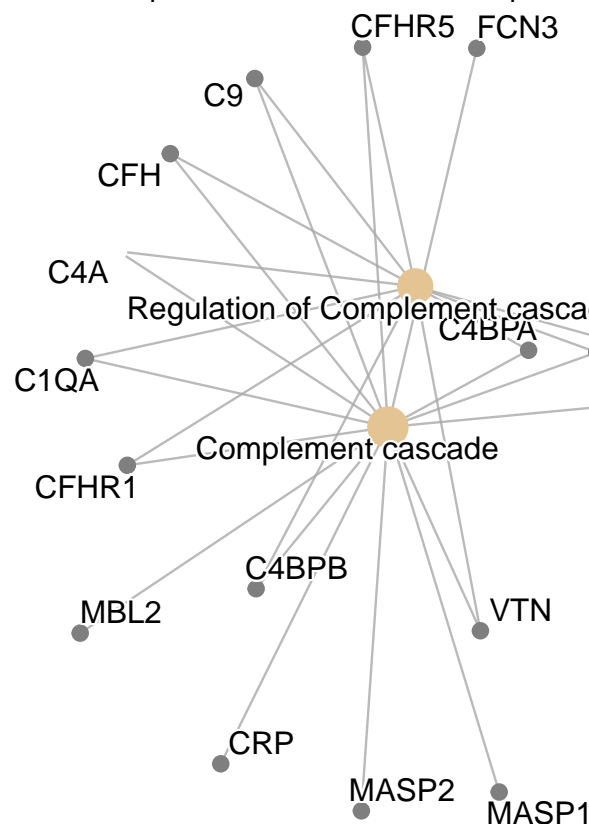
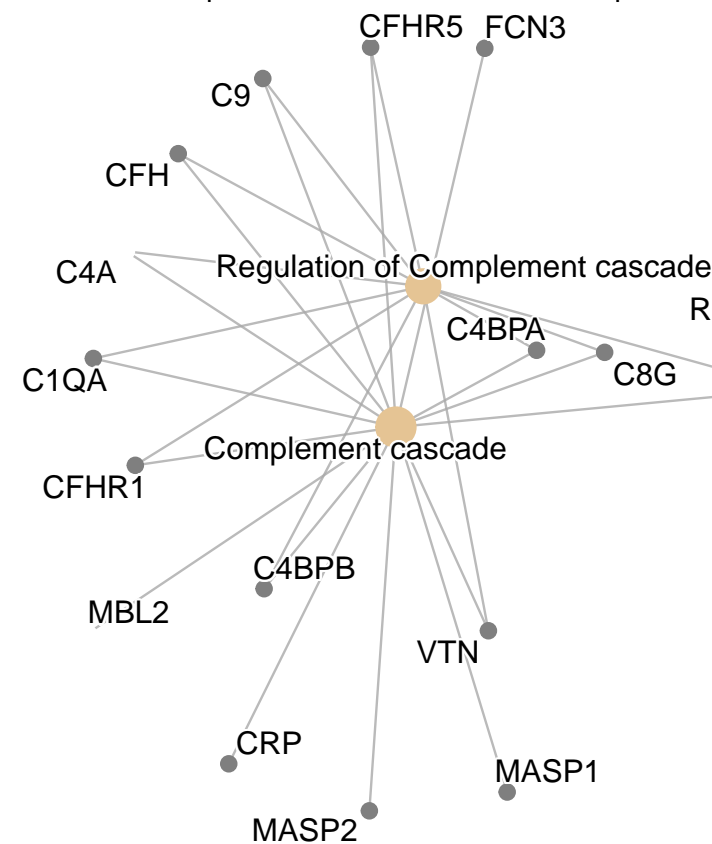


Figure 7. Network plot denoting the \log_2 fold change of proteins in plasma collected 2-weeks post-injury, and the biological pathways these proteins are associated with on Reactome. This compares AIS C SCI patients who experienced an AIS grade improvement and those who did not.

Subacute C Improvers Vs Subacute C Non-Improvers



Response to elevated platelet cytosolic Ca²⁺ / Platelet activation, signaling and aggregation

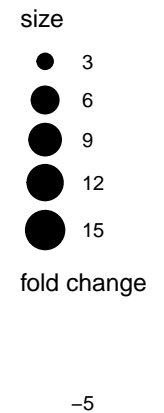
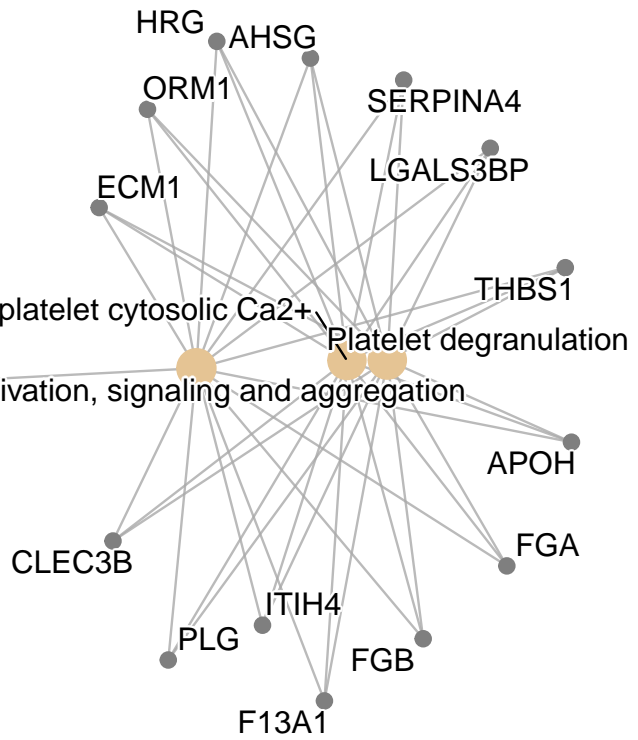


Figure 8. Network plot denoting the log₂ fold change of proteins in plasma collected 3-months post-injury, and the biological pathways these proteins are associated with on Reactome. This compares AIS C SCI patients who experienced an AIS grade improvement and those who did not.

4.1.6 Pathway analysis of Differentially Abundant Proteins between AIS C improvers and non-improvers

Pathway analysis via the *pathview* R package returned the complement and coagulation cascade to be on the sole significant KEGG pathway to derive from the OpenMS analysed data. The majority of the proteins present in this pathway were less abundant in the 2-week post-injury plasma of AIS C patients who experienced an AIS grade conversion and those who did not (Figure 9).

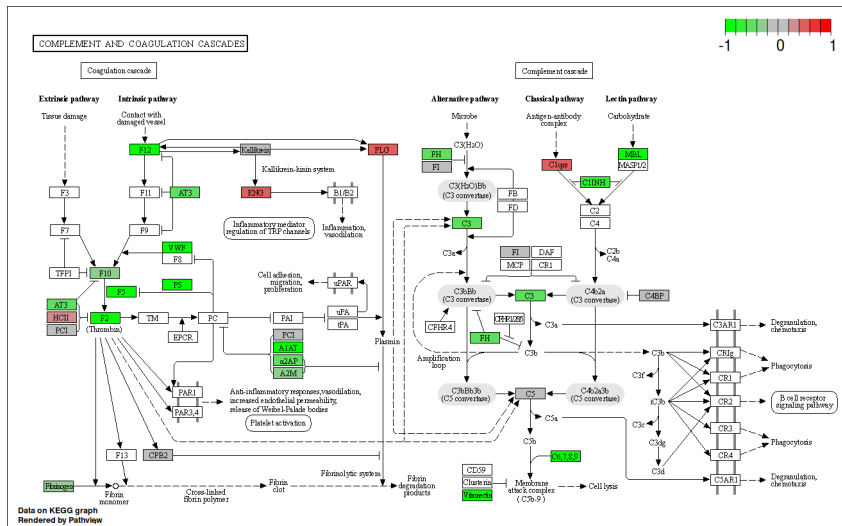


Figure 9. KEGG complement cascade pathway annotated with log₂ fold change of proteins in plasma collected 2-weeks post-injury. This compares AIS C SCI patients who experienced an AIS grade improvement and those who did not.

Similarly to the iTRAQ pathway analysis, the label free data analysed via the pathview R package returned the complement and coagulation cascade to be the sole significant KEGG pathway derived from the OpenMS analysed data. The majority of the proteins present in this pathway were less abundant 2-weeks post-injury in the plasma of AIS C patients who experienced an AIS grade conversion than those who did not (Figure 10).

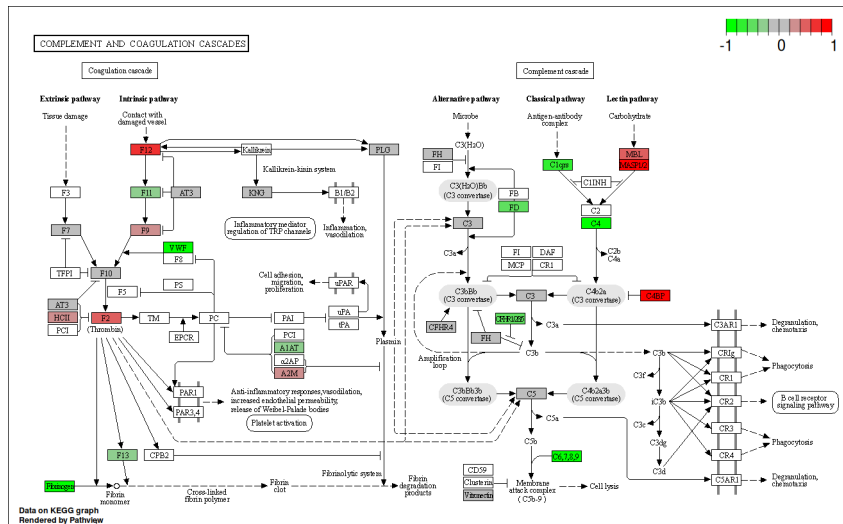


Figure 10. KEGG complement cascade pathway annotated with log₂ fold change of proteins in plasma collected 2-weeks post-injury. This compares AIS C SCI patients who experienced an AIS grade improvement and those who did not.

4.1.7 Validation of Proteomic Data using ELISA

No statistically significant difference between groups for A2M abundance in plasma via DuoSet® ELISAs, though there were outliers in the AIS A and D groups, and particularly in the AIS C patients at 3-months who did not experience an AIS grade conversion (Figure 11).

A significant difference was found between AIS C non-improvers at 2-weeks and AIS D for SAA1, with outliers in AIS C non-improvers at 2-weeks, and both AIS C improvers and non-improvers at 3-months post-injury (Figure 11). For ApoA1 plasma abundance estimated via Quantikine® ELISAs, statistically significant differences were found between AIS C improvers at 2-weeks and both AIS C improvers and non-improvers at 3-months, AIS C 3-month improvers and AIS A and D, and AIS C 3-month non-improvers and AIS A and D (Figure 11). A statistically significant difference was also found between AIS C improvers and non-improvers at 2-weeks post-injury for RBP4 (Figure 11).

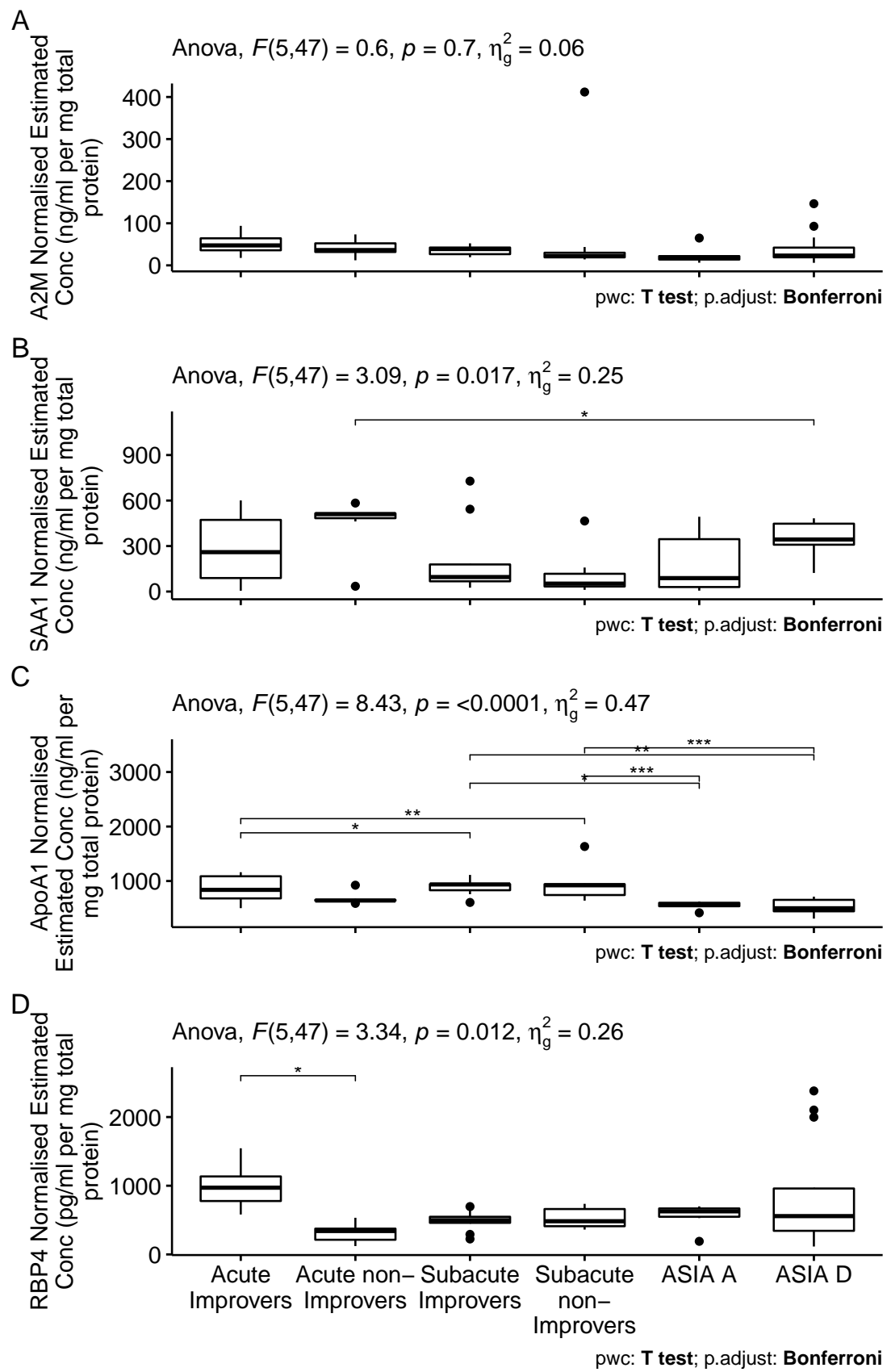


Figure 11. Normalised estimated concentration of α -2-macroglobulin (A), serum amyloid A1 (B), apolipoprotein A1 (C) and retinol binding protein 4 (D). Estimates were calculated from the optical density of a standard curve produced via a DuoSet® ELISA. Plasma from each patient that made up the pooled iTRAQ samples was assayed and pairwise t-tests with bonferroni adjusted P-values were performed to assess differential abundance.

279 **4.1.8 STRINGdb plots**

280 Network interaction plots generated from the OpenMS processed data via STRINGdb revealed that
281 all test groups contained similar proteins, albeit with different abundances, with no distinct group-
282 specific networks observed (Figures S31, S32, S33, S34, S35, S36, S37, S38 and S39).

283 Network interaction plots generated of the significant proteins via STRINGdb revealed that all groups
284 contained similarly smaller networks, with many proteins with no known interactions in the STRING
285 database (Figures S40, S41, S42, S43, S44, S45, S46, S47, S48).

286 **4.1.9 Volcano plots**

287 The mean number of down-regulated and up-regulated significant proteins in each group is 10.6,
288 and 6.8. Between AIS C improvers and non-improvers, 8 and 4 proteins were up- and down-
289 regulated acutely, whereas 6 and 6 were up- and down-regulated subacutely (Figures S49 and
290 S50). Longitudinally, AIS C acute improvers had 10 up-regulated and 7 down-regulated proteins
291 relative to subacute improvers, while for non-improvers 6 and 12 were up- and down-regulated
292 respectively (Figures S51 and S52).

293 **4.1.10 Comparing iTRAQ and label-free proteins**

294 A total of 87 and 79 unique proteins were identified across the label-free and iTRAQ experiments
295 respectively, with a modest overlap of 26 proteins found using both techniques.

296 **5 Discussion**

297 This is the first study, to our knowledge, to investigate the plasma proteome in SCI patients whose
298 AIS scores either improved or did not improve post injury and also to compare these to AIS grade
299 A and D patients. We have used two proteomic techniques allowing us to profile both high and low
300 abundance proteins, in order to identify protein candidate biomarkers which may have potential to
301 predict neurological improvement within the acute setting. Moreover, this data can better inform
302 us of the biology underlying neurological improvement or stability in a cohort of patients being
303 conservatively managed post SCI.

304 Briefly, for processing of proteomic data, we compared the performance of the mass spectrometry
305 vendor (ABSciex) provided ProteinPilot (version 4.5) and OpenMS (version 2.6.0). As there were only
306 modest difference in both the proteins identified and the respective fold changes (data not shown),
307 we opted to use OpenMS for the greater transparency and reproducibility it offers as open-source
308 software.

309 This study has highlighted a number of proteins that may be able to discriminate in, the acute
310 phase following injury, between AIS grade C patients who either improve or do not improve by
311 an AIS grade following SCI. The most promising of these is Retinol Binding Protein 4 (RBP4) which
312 was demonstrated to be increased in non-improvers compared to improvers in the acute phase.
313 Further this change could be confirmed using ELISA, which may provide a more clinically useful
314 means of assessment on a wide scale.

315 RBP4 is synthesised in the liver and binds retinol that is released following vitamin A de-
316 deficiency.(Peterson 1971) Once delivered to target cells, retinol can either be converted to
317 retinaldehyde, which is required for functional vision, or oxidised to retinoic acid, which is a
318 ligand for nuclear receptors, thus regulating gene expression.(Lane and Bailey 2005; Balmer and
319 Blomhoff 2002) The role of retinoid signalling in spinal cord and motor neuron differentiation,
320 including development of regions of the spinal cord has been outlined, and implies a possible

321 involvement in maintaining motor neuron integrity.(Colbert et al. 1995; Sockanathan and Jessell
322 1998) The mRNA of a rodent homologue of RBP was found to be up-regulated at 24 hours post-SCI
323 and may promote cell proliferation and regeneration by increasing retinoid metabolism.(Song et
324 al. 2001; Hurst et al. 1999)

325 Another study of amyotrophic lateral sclerosis (ALS), a neurodegenerative disease, comparing gene
326 expression between post-mortem spinal cord samples of ALS and controls similarly observed up-
327 regulation of RBP1 in ALS spinal cord.(Malaspina, Kaushik, and Belleroche 2001) Furthermore, a
328 transgenic mouse study reported retinoid signalling may contribute to the retained plasticity and
329 regenerative potential of the mature spinal cord.(Haskell et al. 2002) Collectively, these results
330 might support a hypothesis that AIS C improvers have increased levels of RBP4 and this relates to
331 improved capacity for neuronal regeneration/plasticity. Whether this is due to increased expres-
332 sion or due to higher vitamin A dietary intake is unclear from this data.

333 Alongside RBP4, a number of other protein abundance differences across the different biological
334 comparisons were identified in proteins associated with liver function. Our previous work investi-
335 gating the potential of routinely measured haematological analytes for predicting neurological
336 outcome in SCI patients also highlighted several proteins that were linked with liver function; thus
337 providing further support to the theory that liver status is relevant to differential functional re-
338 cover.(Brown et al. 2019; Bernardo Harrington et al. 2020) The pathway analysis specifically indi-
339 cated that the acute phase response (APR) is implicated.

340 The APR is the bodies first response to infection or injury, including SCI. This systemic response
341 is largely coordinated by factors released from the liver, but the APRs effects extend to multiple
342 peripheral organs including the kidneys, lungs and spleen.(Bao et al. 2012; Campbell, Zahid, et
343 al. 2008; Fleming et al. 2012; Gris, Hamilton, and Weaver 2008) This hepatic response is typically
344 transient and quickly fades, but prolonged liver inflammation and pathology has been observed in
345 rodent SCI models.(Goodus et al. 2018; **sauerbeck_spinal_2015?**) Basic liver functions are chrono-
346 cally impaired by SCI, including metabolising carbohydrates, fats and proteins, storage of minerals
347 vitamins and glycogen and filtering blood from the digestive tract.(García-López et al. 2007; DeLeve
348 2007; Farkas and Gater 2018; Chow et al. 2012; **sauerbeck_spinal_2015?**)

349 The acute (1-7 days) liver response to SCI is well documented; the inflammatory cytokines in-
350 cluding TNF α , IL-1 α , IL-1 β and IL-6, released at the injury site, reach the liver through the blood-
351 stream.(Fleming et al. 2012; Hundt et al. 2011) This provokes the liver to enter the APR and produce
352 acute phase proteins thus stimulating a greater immune response.(Anthony and Couch 2014; Flem-
353 ing et al. 2012) The hepatocytes that make up the majority of the liver biomass, express receptors
354 that bind the aforementioned inflammatory cytokines; similarly the hepatic macrophage Kupffer
355 cells also bind these cytokines, complement proteins and lipopolysaccharide (LPS) and swiftly re-
356 move microorganisms, endotoxins and other debris from the blood.(Yang et al. 2013; Szalai et
357 al. 2000; Crispe 2016; Campbell et al. 2005) Furthermore, it has been suggested that liver inflam-
358 mation and Kupffer cells activity promote recruitment of leukocytes to the injury site in brain or
359 spinal trauma, potentially enhancing CNS injury.(Anthony and Couch 2014; Campbell et al. 2005)
360 For example, a rodent study demonstrated depletion of Kupffer cells prior to injury resulted in few
361 neutrophils infiltrating the injury site.(Campbell, Zahid, et al. 2008; Campbell, Anthony, et al. 2008)

362 • MH NOTE: PRX-2 was one of the most promising proteins from the label-free data. We didn't
363 do any elisas for it, but I think we can argue that the label-free is more statistically robust due
364 to the biological and technical replicates. We could argue that it may not have turned up in
365 the iTRAQ as we didn't use the proteominer beads too I suppose

366 Another protein that our label-free proteomic data highlights is Peroxiredoxin 2 (PRX-2), which
367 was detected acutely in AIS C improvers and AIS D patients, and subacutely in AIS A and AIS D.
368 Peroxiredoxins are a large and highly conserved family of enzymes that reduce peroxides. PRX-2

369 is highly abundant in RBCs and intracellularly serves as an important anti-oxidant role in various
370 cells types, including neurons.(Low, Hampton, and Winterbourn 2008) By contrast, extracellular
371 PRX-2 has been suggested to act as an inflammatory DAMP, leading microglia and macrophages
372 to release a plethora of pro-inflammatory factors.(Salzano et al. 2014; Garcia-Bonilla and Iadecola
373 2012; Shichita et al. 2012) An *in vitro* primary neurons and microglia co-culture study reported
374 PRX-2 activating microglia via TLR-4, potentially leading to neuronal apoptosis.(Lu et al. 2018) A
375 murine study found over-expression of PRX-2 attenuated oxidative stress and neuronal apoptosis
376 following subarachnoid haemorrhage.(Lu et al. 2019) Over-expression of PRX-2 is speculated to
377 protect again ischaemic neuronal injury by modulating the redox-sensitive thioredoxin-apoptosis
378 signal-regulating kinase (ASK) 1 signalling complex.(Gan et al. 2012) Several molecular chaperones
379 can interact with ASK1, including thioredoxin and TNF receptor-associated factor 6.(Matsuzawa et
380 al. 2005) The dissociation of the thioredoxin-ASK1 complex activates ASK1. PRX-2 is oxidised after
381 scavenging free radicals, whereupon its antioxidant activity is reduced. This inactivation can be
382 reversed by the thioredoxin-thioredoxin reductase system, whereby oxidised PRX-2 can regain its
383 activity by reducing thioredoxin, leading to the dissociation of the thioredoxin-ASK1 complex.(Rhee
384 and Woo 2011) Additionally, oxidised PRX-1 can inhibit ASK1-induced apoptosis via the thioredoxin-
385 binding domain on ASK1.(Kim, Kim, and Lee 2008)

386 The presence of PRX-2 in acute AIS C improvers and absence in acute C non-improvers suggests the
387 protein could indicate a more protective action against oxidative stress, and implies the protein has
388 potential value as a biomarker of functional outcomes. Similarly, PRX-2 may be acting as a healthy
389 response to trauma-induced oxidative stress in both acute AIS D, although the persistence to the
390 subacute time-point is less clear. Likewise, the presence of PRX-2 in AIS A subacutely, but not
391 acutely is more perplexing. It should be noted that as plasma was used and cells were lysed, there
392 is no distinction between intracellular and extracellular PRX-2 in this data. Perhaps in the more
393 severe AIS A injury, secondary injuries, including oxidative stress, are greater and so persist to the
394 subacute time-point. The acute absence may be a result of an overwhelmed physiology unable to
395 respond or prioritise managing oxidative stress.

396 Pathway analysis from both the iTRAQ and label-free experiments identified the complement and
397 coagulation cascades as a significant pathway of interest. More broadly, the trend in this data is for
398 proteins in the complement pathway is lower abundance, or inhibitory proteins such as C4BP to be
399 more abundant, in the acute improvers. C3 for instance, cleavage of which is vital for complement
400 activation, was less abundant in acute AIS C improvers relative to non-improvers. This finding is
401 in line with a genetic C3 knockout study in mice which reported better neurological scores 2 days
402 post-injury, reduced residual consolidated neurological deficit at 21 days and display minor change
403 in reduced gliosis (20% decrease at 1h timepoint) but a three-to-fourfold decrease in neutrophil in-
404 filtration, resulting in enhanced regeneration of axons.(Qiao et al. 2006) Another study using a
405 similar C3 knockout model reported improved neurological scores at acute and long-term time
406 points.(Guo et al. 2010) These results imply that the complement cascade is a particularly impor-
407 tant component of a differential response to neurological injury which ultimately leads to greater
408 functional recovery. Given the complexity of the complement cascade and the limited time points
409 in this study, further work is needed to elucidate which facets of the cascade are outcome modify-
410 ing, and at which stages post-injury.

411 The small number of statistically significant proteins speaks to the variability of human plasma
412 samples, and is likely exacerbated by the inconstant timing of sample collection relative to injury.
413 Thus, a repeat of this experiment with a larger sample size will likely reveal many more proteins of
414 potential interest. Regardless, this study has highlighted RPB4 and PRX-2 as potential biomarkers
415 of functional recover. We have also highlighted the complement cascade as being a particularly
416 important pathway in differential recovery. Additional investigation of these proteins, but also the
417 complement cascade more broadly, particularly at more acute time points, would also be valuable.

⁴¹⁸ Furthermore, a metabolomic analysis with a similar samples would greatly compliment this work,
⁴¹⁹ particularly with regards to investigating further links to the livers role in neurological recovery.

420 **Supplementary material**

421 **5.1 Session Information**

```
422 ##          -
423 ## platform      aarch64-apple-darwin20
424 ## arch         aarch64
425 ## os           darwin20
426 ## system       aarch64, darwin20
427 ## status
428 ## major        4
429 ## minor        1.3
430 ## year         2022
431 ## month        03
432 ## day          10
433 ## svn rev      81868
434 ## language     R
435 ## version.string R version 4.1.3 (2022-03-10)
436 ## nickname     One Push-Up

437 Packages Used
438 package
439 version
440 date
441 base
442 4.1.3
443 2022-03-18
444 MSstats
445 4.2.0
446 2021-05-31
447 STRINGdb
448 2.6.5
449 2020-01-10
450 ReactomePA
451 1.38.0
452 2021-10-26
453 rlang
454 1.0.2
455 2022-03-04
456 bookdown
457 0.26
```

```
458 2022-04-15
459 lime
460 0.5.2
461 2021-02-24
462 RColorBrewer
463 1.1.3
464 2022-04-03
465 ggVennDiagram
466 1.2.0
467 2021-10-19
468 DiagrammeR
469 1.0.9
470 2022-03-04
471 lubridate
472 1.8.0
473 2021-10-03
474 patchwork
475 1.1.1
476 2020-12-15
477 cowplot
478 1.1.1
479 2020-12-15
480 readxl
481 1.4.0
482 2022-03-28
483 BiocManager
484 1.30.18
485 2022-05-18
486 knitr
487 1.39
488 2022-04-26
489 data.table
490 1.14.2
491 2021-09-23
```

```
492 naniar
493 0.6.1
494 2021-05-14
495 psych
496 2.2.5
497 2022-05-01
498 Hmisc
499 4.7.0
500 2022-04-12
501 Formula
502 1.2.4
503 2020-10-16
504 survival
505 3.3.1
506 2022-02-20
507 lattice
508 0.20.45
509 2021-09-18
510 bibtex
511 0.4.2.3
512 2020-09-19
513 captioner
514 2.2.3
515 2015-07-15
516forcats
517 0.5.1
518 2021-01-27
519 stringr
520 1.4.0
521 2019-02-09
522 dplyr
523 1.0.9
524 2022-04-27
525 purrr
```

```
526  0.3.4
527  2020-04-16
528  readr
529  2.1.2
530  2022-01-30
531  tidyverse
532  1.2.0
533  2022-01-27
534  tibble
535  3.1.7
536  2022-04-26
537  ggplot2
538  3.3.6
539  2022-04-27
540  tidyverse
541  1.3.1
542  2021-04-15
543  kableExtra
544  1.3.4
545  2021-02-19
546  rmarkdown
547  2.14
548  2022-04-25
```


Table S1. OpenMS log₂ fold changes in the plasma proteome of SCI patients. 'Acute' and 'Subacute' samples collected within 2 week and approximately 3-months post-injury respectively.

gene	Acute AIS C improvers vs non-improvers	Subacute AIS C improvers vs non-improvers	AIS C improvers acute vs subacute	AIS C non-improvers acute vs subacute	AIS C improvers vs non-improvers	AIS A vs D	AIS C improvers vs A	AIS C improvers vs D	AIS C non-improvers vs A	AIS C non-improvers vs D
A1BG	-0.9031824	-0.1017534	-0.6087849	0.1926441	0.2252650	0.7937347	-0.3497633	0.4439714	-0.5750284	0.2187064
A2M	-1.0385788	-0.2464392	-0.6760613	0.1160783	-1.2300968	1.4247538	-1.6029796	-0.1782258	-0.3728828	1.0518710
AFM	-0.3788476	-1.2248641	0.4815192	-0.3644973	0.5517904	1.1923601	-1.2566085	-0.0642484	-1.8083989	-0.6160388
AHSG	1.1794532	NA	-0.5545288	NA	NA	NA	NA	NA	NA	NA
AMBP	0.6562004	-0.3433433	0.8606588	-0.1388849	-0.9023293	NA	1.2037841	NA	2.1061134	NA
APCS	0.1498290	0.2108936	-0.0114011	0.0496636	NA	0.3557242	NA	NA	-0.0494567	0.3062675
APOA1	-0.1816744	-0.6923621	-0.2337557	-0.7444434	-0.7677301	0.6941282	-1.3172834	-0.6231553	-0.5495533	0.1445749
APOA2	0.0900143	-1.1461360	-0.6667620	-1.9029124	NA	NA	NA	NA	NA	NA
APOA4	0.1295961	0.9636781	-1.2312803	-0.3971983	-1.3254088	0.7876011	-1.3346720	-0.5470709	-0.0092632	0.7783379
APOB	0.1379231	-0.0164100	-0.6332751	-0.7876082	-0.8570393	0.5260041	-1.2345864	-0.7085823	-0.3775471	0.1484570
APOE	-1.2133754	0.2930673	-0.6884490	0.8179937	-0.9078302	0.7746514	-1.5477490	-0.7730977	-0.6399188	0.1347326
APOH	-0.3600286	-0.7024687	-0.6444887	-0.9867188	-0.9996639	2.8143614	-1.0091799	1.8051815	-0.0095159	2.8048455
APOL1	-1.1790763	-0.5193515	-1.0440264	-0.3843015	-0.1152769	0.5652696	0.1299333	0.6952029	0.2452102	0.8104799
APOM	-1.2167971	-0.6819883	0.6934807	1.2282895	NA	0.6561807	NA	NA	0.6664954	1.3226762
ATRN	NA	NA	-1.0062957	NA	NA	NA	NA	NA	NA	NA
AZGP1	1.2191679	1.0251503	0.0811400	-0.1128776	-3.3889514	-3.6440501	0.3702887	-3.2737614	3.7592401	0.1151900
C1QB	-0.8410072	-2.0020393	0.7071113	-0.4539208	-1.9729191	1.3563310	-2.0066282	-0.6502972	-0.0337090	1.3226219
C1R	-0.4335115	-0.7632158	0.0366498	-0.2930545	-0.1467491	0.7976066	0.3564300	1.1540366	0.5031791	1.3007857
C1S	0.0295224	-0.8193739	0.1679558	-0.6809404	NA	NA	NA	NA	NA	NA
C2	NA	NA	NA	NA	-2.5581036	2.5640965	-2.5952702	-0.0311737	-0.0371665	2.5269300
C3	-0.7440620	-0.6968585	0.0652375	0.1124410	-1.0730763	1.2388421	-2.1616420	-0.9227999	-1.0885657	0.1502764
C4BPA	-0.1810388	-2.4454980	1.6627662	-0.6016930	-1.2378707	1.5489731	-1.8448914	-0.2959183	-0.6070207	0.9419523
C5	-0.5447843	-0.2031226	0.9230001	1.2646617	-0.7200022	1.2710496	-1.6768797	-0.4058301	-0.9568775	0.3141721
C6	-1.3936214	1.7817023	-1.3097108	1.8656129	-3.0451914	1.7642372	-3.2550019	-1.4907647	-0.2098105	1.5544267
C7	-0.9642124	0.8848082	-0.7827165	1.0663041	0.9970185	0.0708650	-1.1136320	-1.0427670	-2.1106505	-2.0397855
C8A	-0.5117891	0.2736564	-0.7630145	0.0224310	-2.8108340	0.1731241	-2.1285385	-1.9554144	0.6822955	0.8554196
C8B	-2.1950427	0.2789045	-1.5954883	0.8784589	-1.8943958	-0.4802611	-0.9597537	-1.4400148	0.9346421	0.4543810
C8G	NA	NA	-1.6304866	NA	NA	NA	NA	NA	NA	NA
C9	-2.2199059	0.4534093	-1.9249790	0.7483361	-0.7345863	0.6495872	-3.2424254	-2.5928382	-2.5078391	-1.8582519
CD5L	-0.9293248	-0.6204735	-0.7145571	-0.4057058	-2.4642871	0.4482534	-2.3260120	-1.8777586	0.1382751	0.5865285
CFH	-1.1239737	0.7406948	-1.6480885	0.2165801	-1.0358708	0.1380093	-1.3260484	-1.1880391	-0.2901776	-0.1521683
CFI	NA	0.5359696	NA	1.2578110	NA	NA	NA	NA	NA	NA
CLU	-1.1958984	-0.8681850	-0.1721921	0.1555214	-1.3664377	0.8251962	-2.1976184	-1.3724222	-0.8311807	-0.0059845
CP	-0.3892064	0.2565411	-0.4537277	0.1920199	-0.6657547	0.4235353	-0.2695812	0.1539541	0.3961736	0.8197089
F12	0.4852010	-0.9397905	0.6702925	-0.7546990	-0.8534307	0.5549559	-1.3145850	-0.7596291	-0.4611543	0.0938016
F2	-0.7493082	-0.7563593	0.0982877	0.0912367	-0.5408805	1.1677146	-1.5476188	-0.3799042	-1.0067383	0.1609763
FCN3	NA	0.9644778	NA	NA	NA	NA	NA	NA	NA	NA

Table S1. OpenMS log₂ fold changes in the plasma proteome of SCI patients. 'Acute' and 'Subacute' samples collected within 2 week and approximately 3-months post-injury respectively. (continued)

gene	Acute AIS C improvers vs non-improvers	Subacute AIS C improvers vs non-improvers	AIS C improvers acute vs subacute	AIS C non-improvers acute vs subacute	AIS C improvers vs non-improvers	AIS A vs D	AIS C improvers vs A	AIS C improvers vs D	AIS C non-improvers vs A	AIS C non-improvers vs D
FGA	-0.9591400	-0.5109050	0.4841704	0.9324054	-1.0155684	1.0486717	-1.4707952	-0.4221236	-0.4552268	0.5934449
FGB	-0.8339088	-0.1253771	0.0684287	0.7769604	-0.8343143	1.0951087	-1.4646547	-0.3695460	-0.6303405	0.4647683
FGG	-1.1432907	-0.0247316	-0.2978078	0.8207513	-0.7191139	0.7606622	-1.0780014	-0.3173392	-0.3588876	0.4017746
FN1	-0.2795610	-0.3153249	0.2899102	0.2541463	-0.5777631	1.1462731	-1.2550759	-0.1088028	-0.6773129	0.4689602
GC	-0.5583474	0.4050629	-0.7950103	0.1684001	-1.8700166	-0.2961353	-1.2641016	-1.5602369	0.6059149	0.3097797
GSN	0.0704855	0.0479440	-0.6709561	-0.6934976	NA	NA	NA	NA	NA	NA
HABP2	NA	NA	NA	NA	-0.5367242	1.4445961	-0.7070902	0.7375059	-0.1703660	1.2742301
HP	-1.2468596	0.5276209	-0.3488061	1.4256744	-0.6393503	0.9683391	-1.2963281	-0.3279890	-0.6569779	0.3113613
HPX	-0.4104644	-0.2880781	-0.7114901	-0.5891038	-0.3597680	0.9360243	-1.1034368	-0.1674125	-0.7436687	0.1923556
HRG	0.5979026	1.0672891	0.0321566	0.5015431	-0.7300739	0.6893699	-0.8231701	-0.1338002	-0.0930962	0.5962737
IGHA1	1.7635882	1.3476620	0.3628909	-0.0530353	-2.0152404	0.4328016	-2.2081140	-1.7753124	-0.1928737	0.2399280
IGHD	NA	NA	NA	NA	-2.4499647	0.4182281	-3.4284738	-3.0102457	-0.9785091	-0.5602810
IGHG1	-0.0855309	0.9292134	-0.4962961	0.5184482	-0.0970233	-1.8091062	0.4814333	-1.3276728	0.5784566	-1.2306496
IGHG2	0.9720422	0.3501681	0.4607992	-0.1610748	-0.6249433	-1.5106734	0.2705475	-1.2401258	0.8954908	-0.6151826
IGHG3	-0.1941508	1.4323226	-0.9309878	0.6954857	-1.8543540	-0.3927284	-1.8870246	-2.2797530	-0.0326705	-0.4253990
IGHM	-0.6318126	-0.8967300	-0.4174693	-0.6823867	-1.1741740	1.7915993	-2.3508710	-0.5592717	-1.1766971	0.6149023
IGKC	-0.0697458	0.0420359	-0.1150304	-0.0032487	-1.1868447	-0.2875492	-1.1765257	-1.4640749	0.0103190	-0.2772302
IGKV3D- 20	NA	NA	NA	NA	-0.3699302	-0.0536821	0.2114801	0.1577980	0.5814103	0.5277282
ITIH1	-0.9766570	0.7057133	-0.5211753	1.1611951	-0.6149247	0.5495684	-0.5039432	0.0456252	0.1109815	0.6605499
ITIH2	-0.3142692	-0.5283214	-0.2363320	-0.4503842	-0.7431549	0.6757214	-1.2136587	-0.5379373	-0.4705037	0.2052177
ITIH3	-0.5456033	0.6138901	0.3512683	1.5107617	-2.0564371	1.2902341	-1.8743188	-0.5840847	0.1821183	1.4723525
ITIH4	-0.0669542	-0.2189363	0.3808668	0.2288847	-1.0843698	0.9773070	-1.8198452	-0.8425382	-0.7354753	0.2418317
KLKB1	NA	-2.2093082	NA	-0.2713600	NA	NA	NA	NA	NA	NA
KNG1	-0.6198162	-0.0025326	-0.0676278	0.5496558	-0.6644071	0.8052877	0.0312278	0.8365155	0.6956349	1.5009226
LRG1	-0.7988007	0.2565104	0.1402188	1.1955298	-0.9515964	1.7017682	-2.1951046	-0.4933364	-1.2435082	0.4582600
LUM	0.0832323	0.6580097	-1.2635566	-0.6887792	NA	NA	NA	NA	NA	NA
ORM1	-0.1974770	1.1178187	-0.2240143	1.0912814	-1.9126407	1.6761382	-1.3025982	0.3735400	0.6100425	2.2861806
PGLYRP2	NA	NA	NA	NA	NA	NA	NA	NA	NA	NA
PLG	-0.3680073	0.0880557	-0.8410370	-0.3849741	-1.0701631	2.7112467	-2.8493306	-0.1380838	-1.7791675	0.9320793
PROS1	-0.3300860	0.0623958	-0.7963440	-0.4038621	-0.5089636	1.5349629	-3.8745298	-2.3395668	-3.3655662	-1.8306032
RBP4	0.4505693	0.4185795	-0.0211740	-0.0531638	-4.0971240	1.4352287	-2.9877294	-1.5525007	1.1093946	2.5446233
SAA1	-2.7778116	2.3463574	-0.5151865	4.6089825	-1.3858800	2.4855048	-2.5593861	-0.0738814	-1.1735062	1.3119986
SERPINA1	0.6825593	0.0481996	1.7824248	1.1480651	-0.0999129	-0.1558972	-1.3635079	-1.5194051	-1.2635950	-1.4194922
SERPINA3	-0.7582369	-0.1617666	0.1836958	0.7801661	-0.7417534	2.2311097	-2.0353461	0.1957637	-1.2935927	0.9375171
SERPINA4	0.0099121	NA	-1.0180116	NA	-1.4473701	NA	-0.6571525	NA	0.7902176	NA
SERPINAS	NA	NA	NA	0.2757029	NA	NA	NA	NA	NA	NA

Table S1. OpenMS log₂ fold changes in the plasma proteome of SCI patients. 'Acute' and 'Subacute' samples collected within 2 week and approximately 3-months post-injury respectively. (continued)

gene	Acute AIS C improvers vs non-improvers	Subacute AIS C improvers vs non-improvers	AIS C improvers acute vs subacute	AIS C non-improvers acute vs subacute	AIS C improvers vs non-improvers	AIS A vs D	AIS C improvers vs A	AIS C improvers vs D	AIS C non-improvers vs A	AIS C non-improvers vs D
SERPINC1	-0.5553486	-0.2339361	-0.5421237	-0.2207112	-0.7720265	1.1066666	-1.3464506	-0.2397839	-0.5744241	0.5322425
SERPIND1	0.2536120	NA	0.0459257	NA	0.3050057	2.3844297	-1.6468854	0.7375442	-1.9518911	0.4325386
SERPING1	-1.1614755	0.1191571	-1.3510892	-0.0704566	-0.9301893	1.0766804	-1.0904641	-0.0137837	-0.1602748	0.9164056
TF	-0.2823635	-0.1105094	-0.4843676	-0.3125135	-0.7681926	0.5875721	-0.9945649	-0.4069929	-0.2263723	0.3611997
VTN	-0.6186100	-0.0323770	-0.2690009	0.3172321	-1.7234623	1.4918535	-2.1517604	-0.6599069	-0.4282982	1.0635554
VWF	NA	1.0585752	NA	1.3917877	-2.5662912	0.5161630	-1.9774026	-1.4612396	0.5888885	1.1050516

Table S2. ProteinPilot fold changes in the plasma proteome of SCI patients. 'Acute' and 'Subacute' samples collected within 2 week and approximately 3-months post-injury respectively.

Protein	AIS C improvers acute vs subacute	Acute AIS C improvers vs non-improvers	Subacute AIS C improvers vs non-improvers	AIS C non-improvers acute vs subacute	AIS C improvers vs non-improvers	AIS C improvers vs A	AIS C improvers vs D	AIS C non-improvers vs A	AIS C non-improvers vs D	AIS C	AIS A vs D
A1BG	-1.644372	-1.472312	NA	NA	NA	NA	NA	NA	NA	NA	NA
A2M	-6.137620	-9.908319	NA	1.380384	-5.861382	-3.467369	NA	1.659587	5.861382	3.564511	
AFM	NA	2.511886	NA	-4.055085	NA	NA	NA	NA	NA	NA	-3.499452
AHSG	NA	NA	NA	-2.249055	NA	NA	NA	NA	NA	NA	NA
APCS	NA	1.870682	NA	NA	NA	4.207266	1.721869	NA	NA	NA	NA
APOA1	-11.803206	-3.698282	NA	-3.250873	-2.884031	-2.884031	-3.801894	NA	-1.406047	NA	
APOA2	-14.321879	NA	NA	-4.965923	NA	NA	NA	NA	NA	NA	NA
APOA4	-11.587774	-5.915616	NA	-2.108628	-2.964831	-1.555966	-2.488857	1.870682	NA	NA	-1.629296
APOB	-2.443430	3.019952	NA	-6.025596	3.732502	-1.282331	1.367729	-4.742420	-2.805434	1.721869	
APOC1	NA	NA	NA	-4.528976	NA	NA	NA	NA	NA	NA	NA
APOC4	NA	NA	NA	NA	NA	1.318257	NA	4.920395	NA	-4.528976	
APOE	NA	NA	-1.527566	-1.753880	NA	-1.836538	-3.019952	-1.803018	-3.019952	NA	
AZGP1	2.269865	2.630268	3.597493	NA	1.819701	4.446313	NA	NA	NA	NA	-4.130475
C1QB	NA	NA	NA	NA	NA	-1.513561	NA	NA	NA	NA	NA
C1R	NA	NA	NA	NA	NA	-4.446313	NA	NA	NA	NA	NA
C3	2.754229	-1.940886	NA	3.981072	-2.398833	-4.365158	1.614359	-1.976970	3.597493	6.546362	
C4B	2.269865	-2.147830	-1.940886	2.654606	NA	NA	NA	NA	NA	NA	NA
C4BPA	NA	-1.419058	NA	NA	NA	NA	1.659587	-2.013724	NA	3.250873	
C5	1.737801	NA	NA	2.228435	NA	-2.333458	NA	-1.770109	NA	2.167704	
C6	1.887991	NA	NA	NA	NA	-2.070141	-2.805434	NA	NA	NA	NA
C9	NA	-2.421029	NA	9.908319	NA	-4.055085	NA	-1.499685	7.177943	9.375620	
CD5L	NA	-2.831392	-3.280953	NA	-1.819701	-1.819701	NA	NA	NA	NA	NA
CFB	NA	-1.674943	2.535129	4.285485	NA	-2.128139	2.032357	-1.690441	2.511886	4.055085	
CFH	NA	NA	NA	2.558586	NA	NA	NA	NA	2.333458	1.803018	
CFI	NA	NA	NA	NA	NA	NA	NA	NA	NA	2.269865	
CLU	NA	NA	NA	NA	NA	NA	NA	-2.582260	NA	NA	
CP	NA	NA	2.582260	3.019952	NA	NA	2.187762	NA	2.779713	NA	
F2	NA	NA	NA	NA	NA	NA	1.674943	NA	NA	1.527566	
FGA	3.467369	-1.644372	NA	12.133888	-3.531832	-2.654606	NA	NA	5.199960	4.092606	
FGB	3.280953	NA	2.443431	9.204495	-2.187762	-1.330454	2.654606	NA	5.248075	3.133286	
FGG	2.032357	-1.958845	NA	9.638290	-2.312065	-1.644372	4.325138	NA	9.204495	6.367955	

Table S2. ProteinPilot fold changes in the plasma proteome of SCI patients. 'Acute' and 'Subacute' samples collected within 2 week and approximately 3-months post-injury respectively. (continued)

Protein	AIS C improvers acute vs subacute	Acute AIS C improvers vs non-improvers	Subacute AIS C improvers vs non-improvers	AIS C non-improvers acute vs subacute	AIS C improvers vs non-improvers	AIS C improvers vs A	AIS C improvers vs D	AIS C non-improvers vs A	AIS C non-improvers vs D	AIS C	AIS A vs D
FN1	2.582260	2.228435	NA	NA	1.940886	-2.466039	1.472312	-4.875285	NA	3.404082	
GC	NA	NA	NA	NA	NA	NA	1.541700	NA	2.606154	2.398833	
GSN	-2.312065	NA	NA	-4.055085	-3.019952	NA	-4.365158	NA	NA	NA	
HBA1	NA	3.133286	NA	-4.017908	NA	NA	NA	NA	-2.654606	-2.535129	
HBB	NA	10.000000	NA	-15.995580	5.058247	2.167704	NA	NA	-6.137620	-2.558586	
HP	3.499452	NA	2.511886	13.427649	NA	-2.964831	NA	NA	4.092606	4.786301	
HPX	NA	-2.147830	NA	NA	NA	NA	1.995262	NA	2.208005	NA	
HRG	NA	NA	NA	NA	NA	3.531832	NA	3.908409	NA	NA	
IGHM	NA	-5.152286	-3.664376	NA	-5.199960	-4.655861	NA	NA	3.221069	2.937650	
IGKC	NA	NA	NA	NA	NA	1.753880	5.649370	1.786488	5.807644	NA	
ITIH1	NA	NA	NA	NA	NA	NA	NA	-3.597493	NA	NA	
ITIH2	NA	NA	NA	-1.629296	NA	-2.089296	-2.208005	-2.070141	-2.208005	NA	
ITIH3	NA	-2.051162	NA	2.466039	NA	NA	NA	NA	2.108628	2.630268	
ITIH4	1.819701	-2.312065	NA	3.104560	-1.836538	-3.104560	NA	-1.737801	2.376840	4.092606	
JCHAIN	NA	NA	-4.130475	NA	-5.011872	NA	NA	NA	NA	NA	
KNG1	NA	NA	NA	NA	NA	NA	2.754229	NA	NA	NA	
LPA	NA	NA	10.764652	14.723126	NA	NA	NA	NA	NA	NA	
LRG1	NA	-2.167704	NA	3.047895	-6.367955	-9.727472	NA	-1.629296	NA	3.311311	
LUM	-4.405549	NA	NA	-3.250873	NA	NA	NA	NA	NA	NA	
ORM1	NA	NA	16.904409	NA	NA	NA	3.630781	NA	NA	2.992265	
PLG	1.555966	NA	NA	NA	2.312065	1.870682	2.937650	NA	NA	NA	
RBP4	NA	5.495408	NA	NA	NA	NA	NA	NA	NA	NA	
SAA1	NA	NA	28.054337	51.522865	NA	NA	NA	NA	NA	NA	
SAA4	NA	NA	NA	NA	NA	-2.805434	NA	NA	NA	1.905461	
SERPINA1	NA	-2.333458	NA	7.585776	-2.754229	-5.597576	NA	-2.187762	3.221069	7.112135	
SERPINA3	2.108628	-1.737801	3.837072	12.705741	-1.976970	-5.915616	NA	-3.250873	4.325138	12.246162	
SERPIN C1	NA	NA	NA	NA	NA	NA	NA	-2.070141	NA	NA	
SERPIN D1	1.770109	NA	NA	NA	2.032357	NA	NA	NA	NA	NA	
SERPIN F1	NA	NA	NA	NA	NA	-4.365158	-5.248075	NA	NA	NA	
SERPIN F2	NA	NA	NA	NA	NA	-4.207266	NA	-3.467369	NA	NA	
SERPIN G1	NA	-2.535129	NA	2.964831	-1.836538	-4.365158	NA	-2.488857	2.187762	5.248075	

Table S2. ProteinPilot fold changes in the plasma proteome of SCI patients. 'Acute' and 'Subacute' samples collected within 2 week and approximately 3-months post-injury respectively. (continued)

Protein	AIS C improvers acute vs subacute	Acute AIS C improvers vs non-improvers	Subacute AIS C improvers vs non-improvers	AIS C non-improvers acute vs subacute	AIS C improvers vs non-improvers	AIS C improvers vs A	AIS C improvers vs D	AIS C non-improvers vs A	AIS C non-improvers vs D	AIS C	AIS A vs D
TF	-2.728978	NA	-1.527566	-5.445027	NA	NA	1.721869	NA	NA	NA	NA
TTN	NA	NA	NA	NA	NA	-1.706082	-2.208005	-1.770109	NA	NA	1.258925

550 **5.3 Heatmaps**

551 **5.3.1 iTRAQ data**

AIS C Improvers acute vs subacute

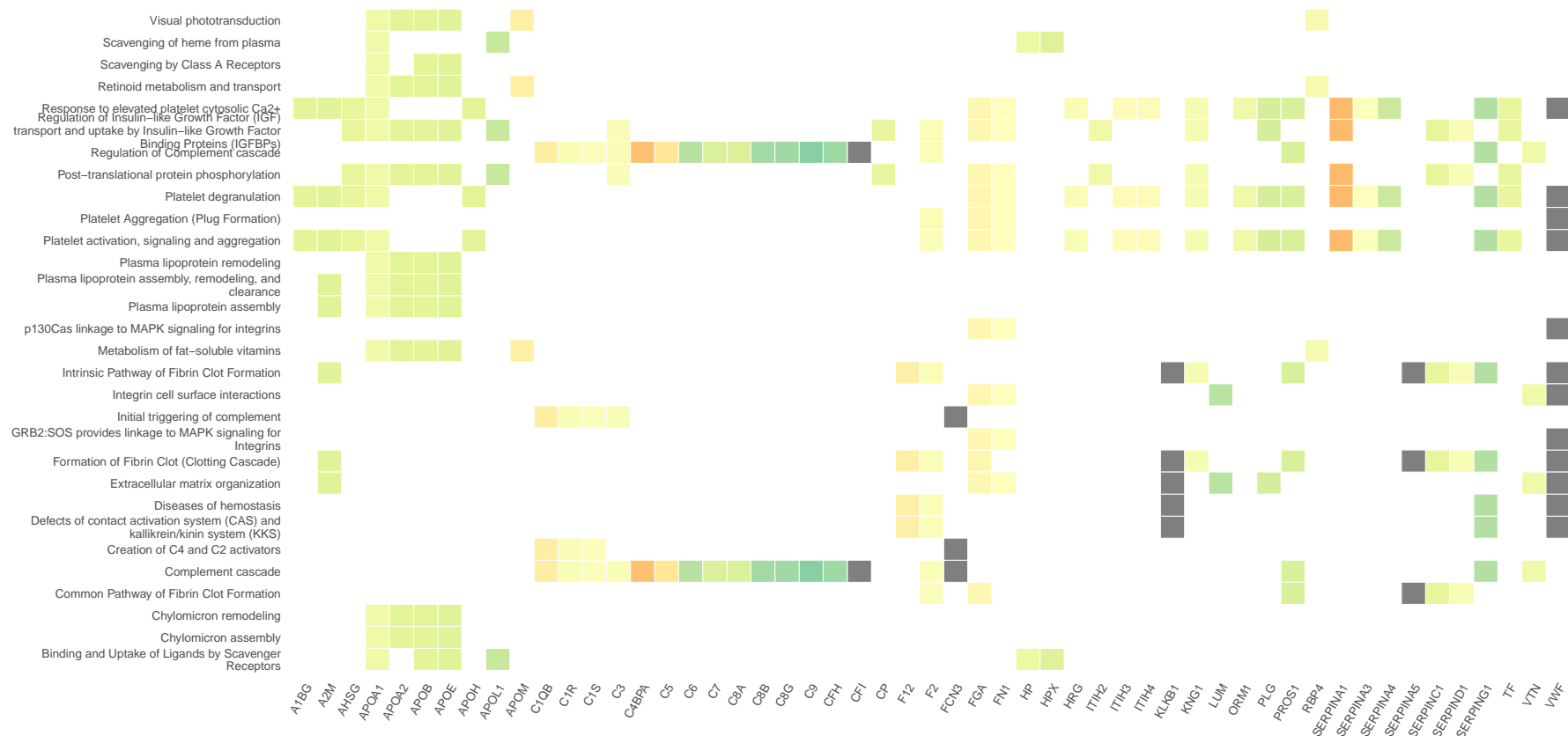


Figure S1. Heatmap denoting the log₂ fold change of proteins in plasma collected 2-weeks and 3-months post-injury, and the biological pathways these proteins are associated with on Reactome. This compares AIS C SCI patients who experienced an AIS grade improvement at 2-weeks and 3-months post-injury.

AIS C non-Improvers acute vs subacute

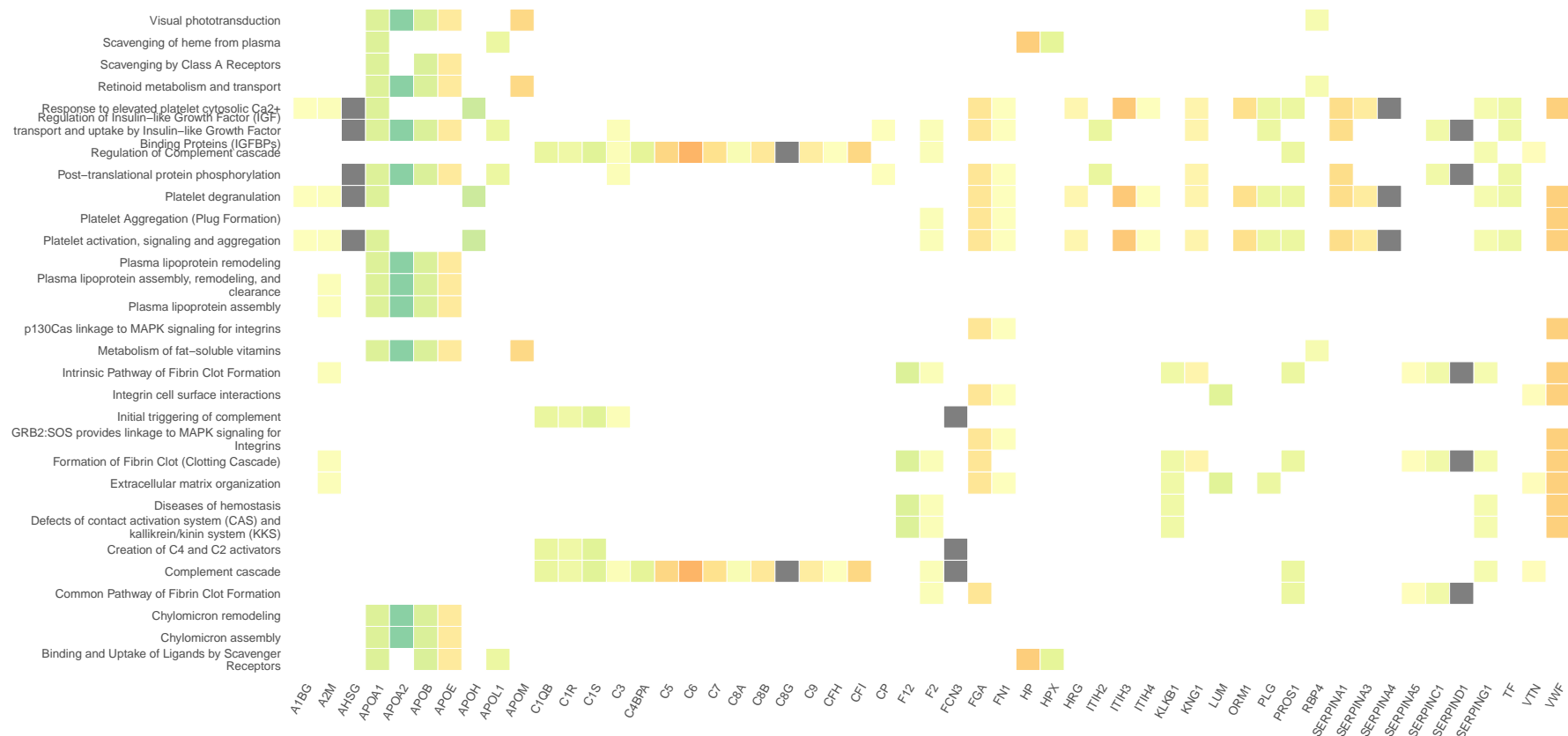


Figure S2. Heatmap denoting the log₂ fold change of proteins in plasma collected 2-weeks and 3-months post-injury, and the biological pathways these proteins are associated with on Reactome. This compares AIS C SCI patients who did not experience an AIS grade improvement at 2-weeks and 3-months post-injury.

Acute AIS C Improvers VS non-Improvers Run 2



Figure S3. Heatmap denoting the log₂ fold change of proteins in plasma collected 2-weeks post-injury, and the biological pathways these proteins are associated with on Reactome. This compares AIS C SCI patients who experienced an AIS grade improvement and those who did not from the second 4-plex iTRAQ experiment.

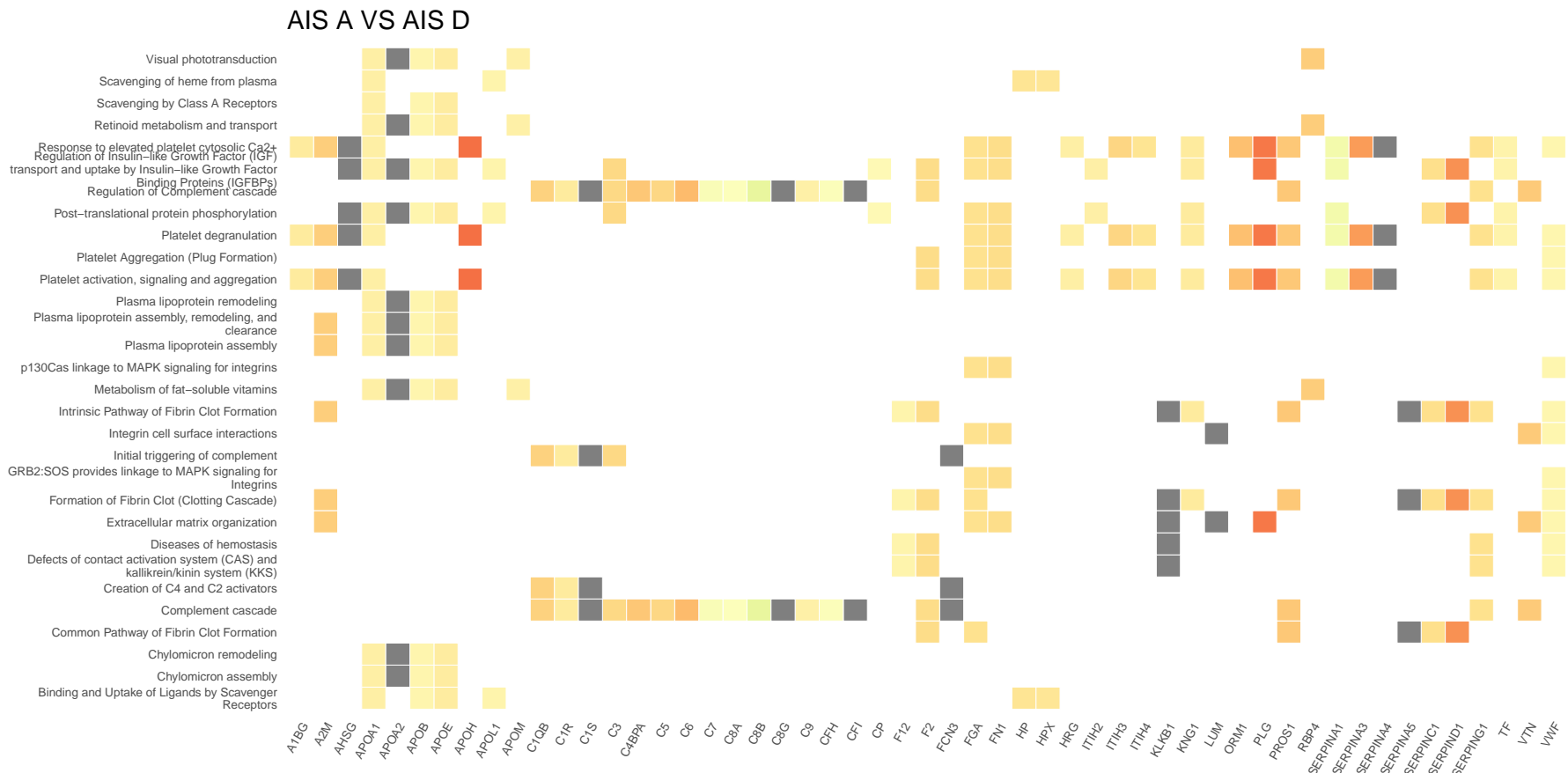


Figure S4. Heatmap denoting the log₂ fold change of proteins in plasma collected 2-weeks post-injury, and the biological pathways these proteins are associated with on Reactome. This compares AIS A and AIS D SCI patients.

Acute AIS C Improvers VS AIS D

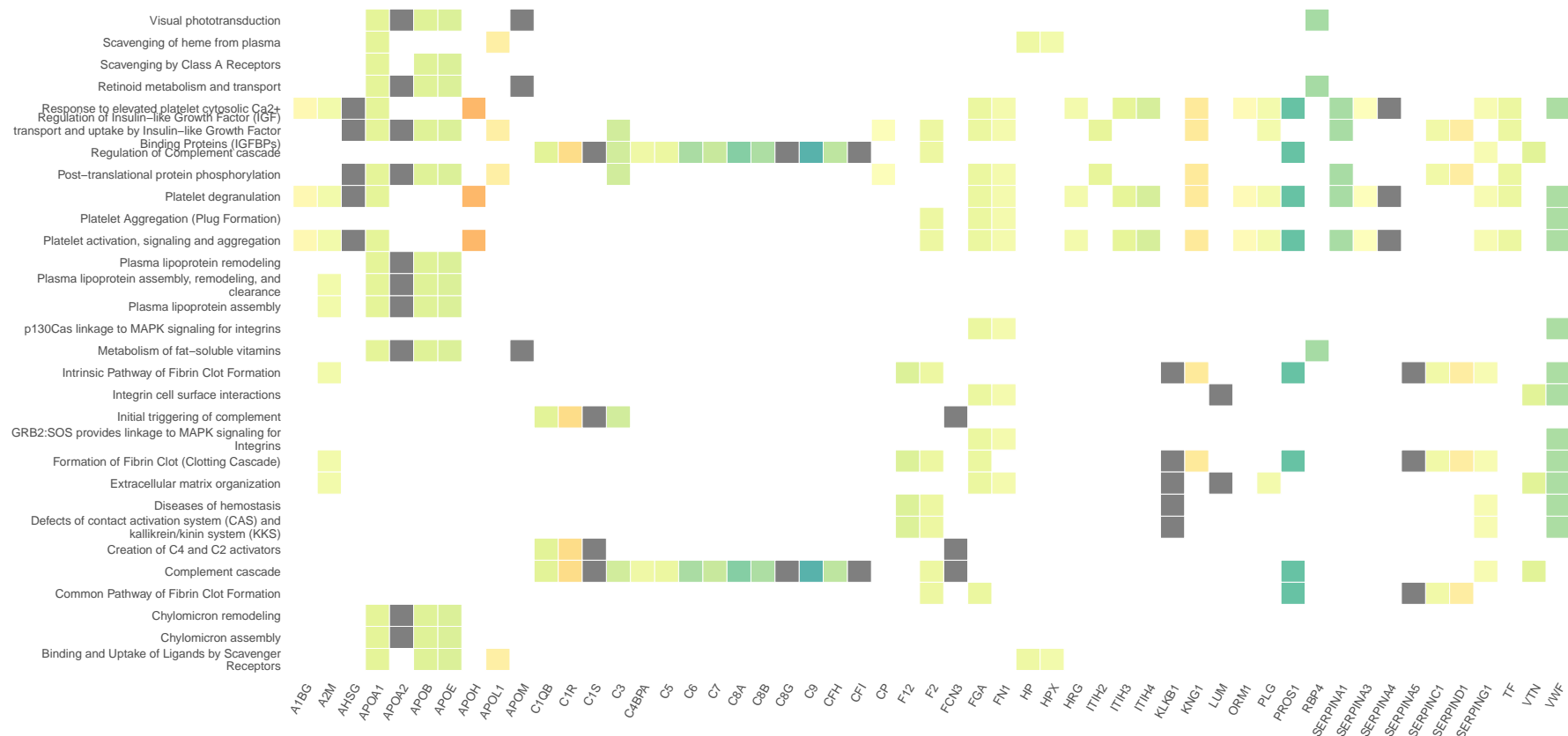


Figure S5. Heatmap denoting the log₂ fold change of proteins in plasma collected 2-weeks post-injury, and the biological pathways these proteins are associated with on Reactome. This compares AIS C SCI patients who experienced an AIS grade improvement and AIS D patients.

Acute AIS C Improvers VS AIS A



Figure S6. Heatmap denoting the log₂ fold change of proteins in plasma collected 2-weeks post-injury, and the biological pathways these proteins are associated with on Reactome. This compares AIS C SCI patients who experienced an AIS grade improvement and AIS A patients.

Acute AIS C non-Improvers VS AIS A



Figure S7. Heatmap denoting the log₂ fold change of proteins in plasma collected 2-weeks post-injury, and the biological pathways these proteins are associated with on Reactome. This compares AIS C SCI patients who did not experience an AIS grade improvement and AIS A patients.

Acute AIS C non-Improvers VS AIS D

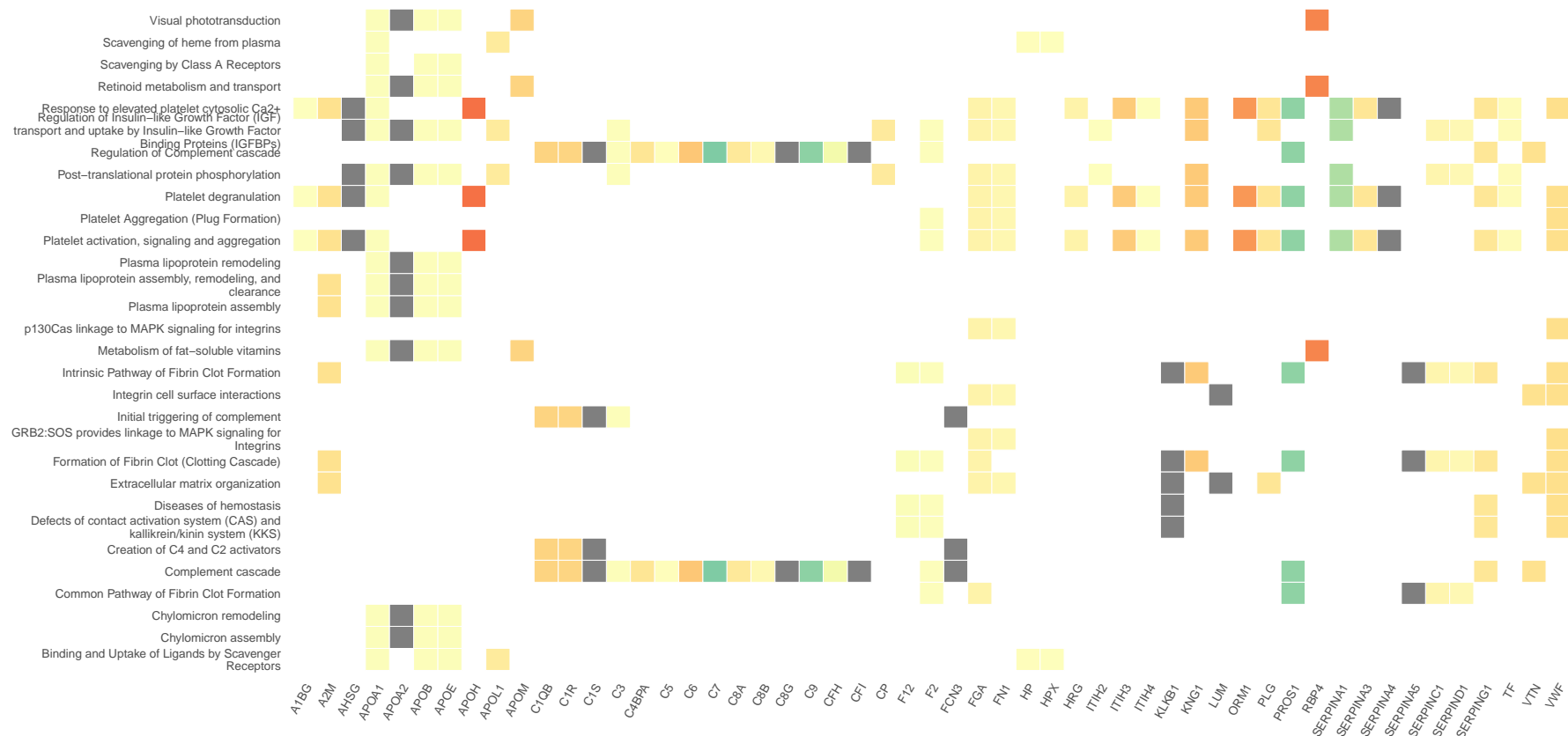


Figure S8. Heatmap denoting the log₂ fold change of proteins in plasma collected 2-weeks post-injury, and the biological pathways these proteins are associated with on Reactome. This compares AIS C SCI patients who did not experience an AIS grade improvement and AIS D patients.

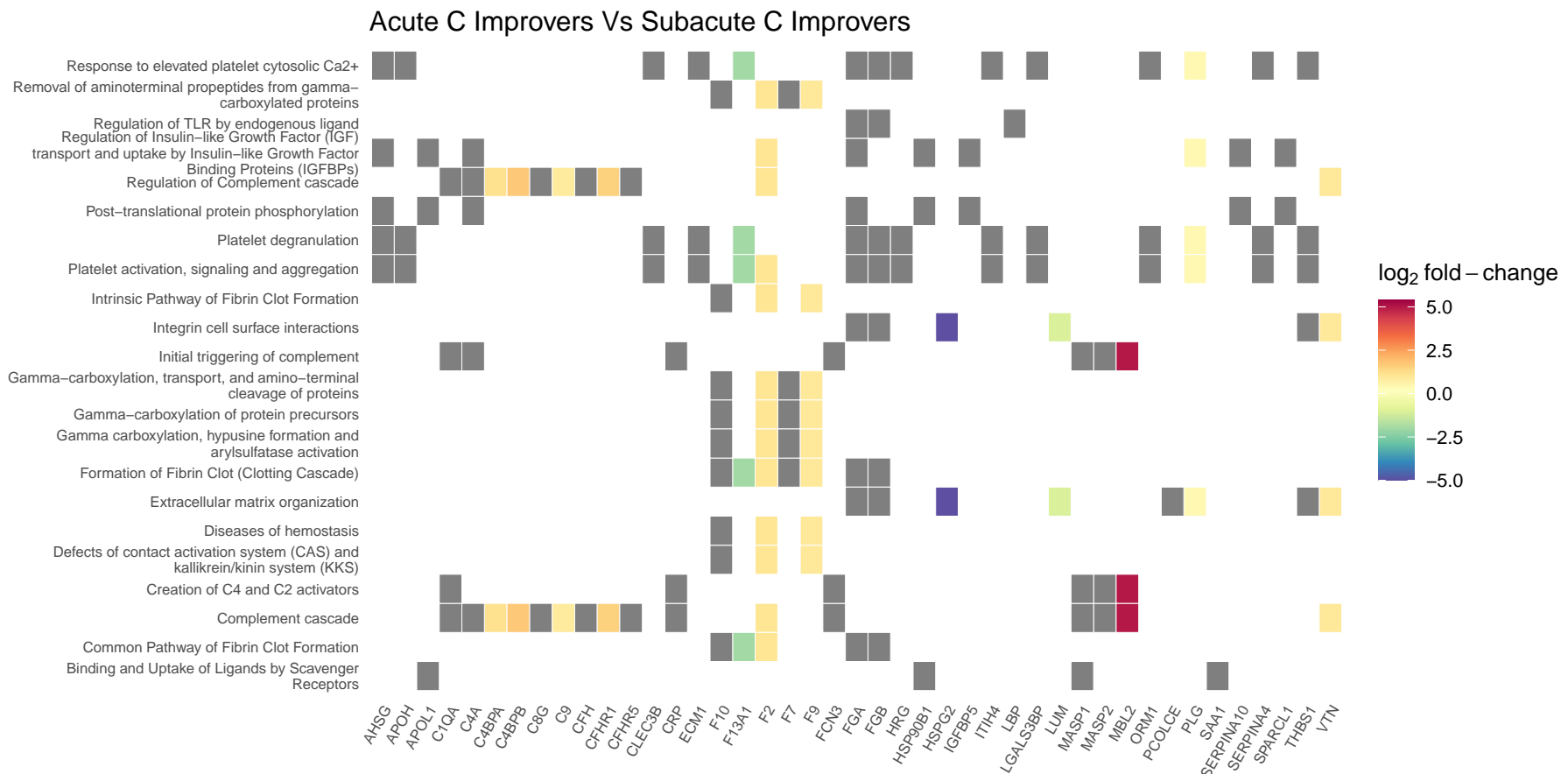


Figure S9. Heatmap denoting the \log_2 fold change of proteins in plasma collected 2-weeks and 3-months post-injury, and the biological pathways these proteins are associated with on Reactome. This compares AIS C SCI patients who experienced an AIS grade improvement at 2-weeks and 3-months post-injury. Grey blocks denote proteins not present in the comparison.

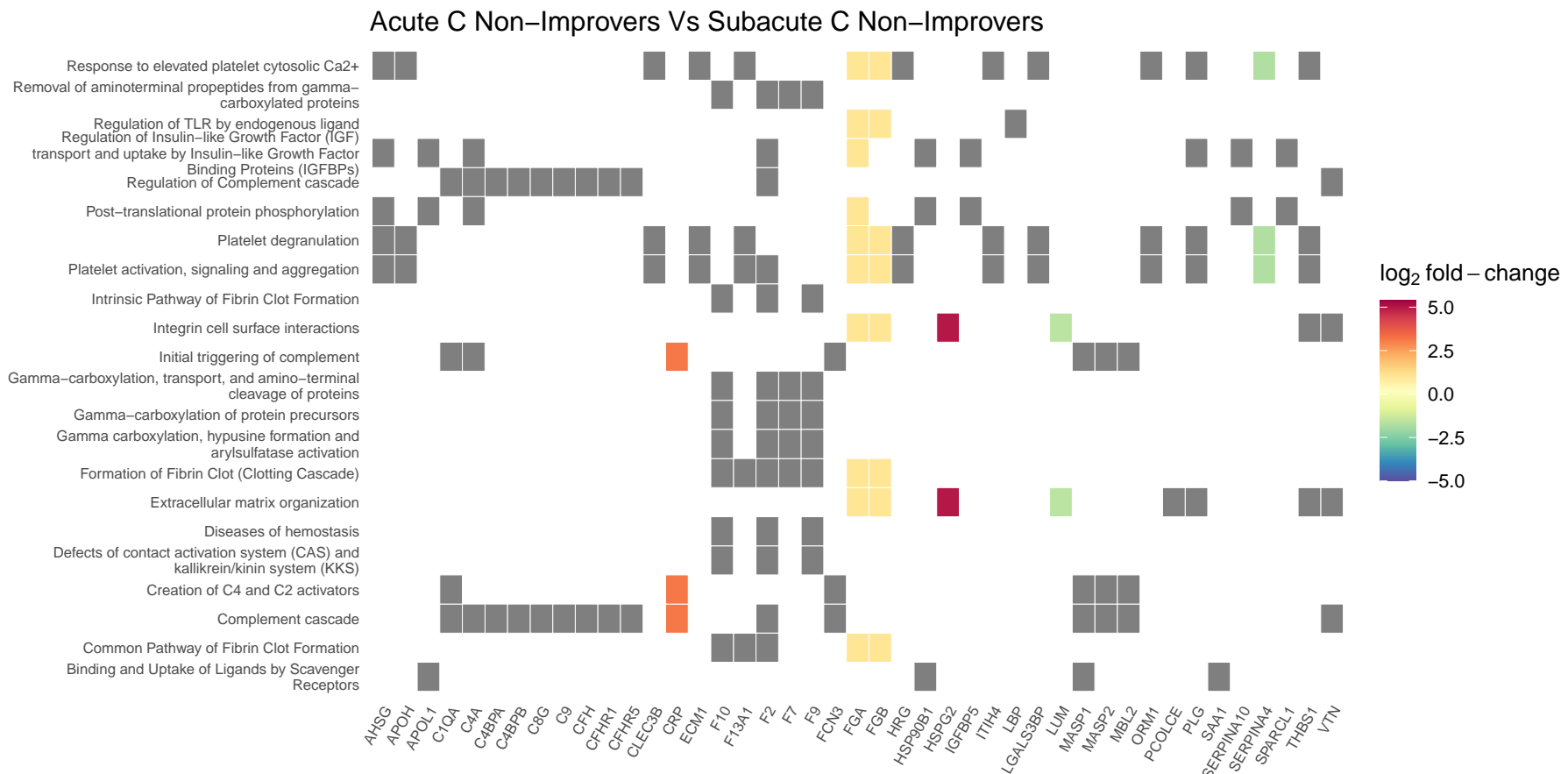


Figure S10. Heatmap denoting the \log_2 fold change of proteins in plasma collected 2-weeks and 3-months post-injury, and the biological pathways these proteins are associated with on Reactome. This compares AIS C SCI patients who did not experience an AIS grade improvement at 2-weeks and 3-months post-injury. Grey blocks denote proteins not present in the comparison.

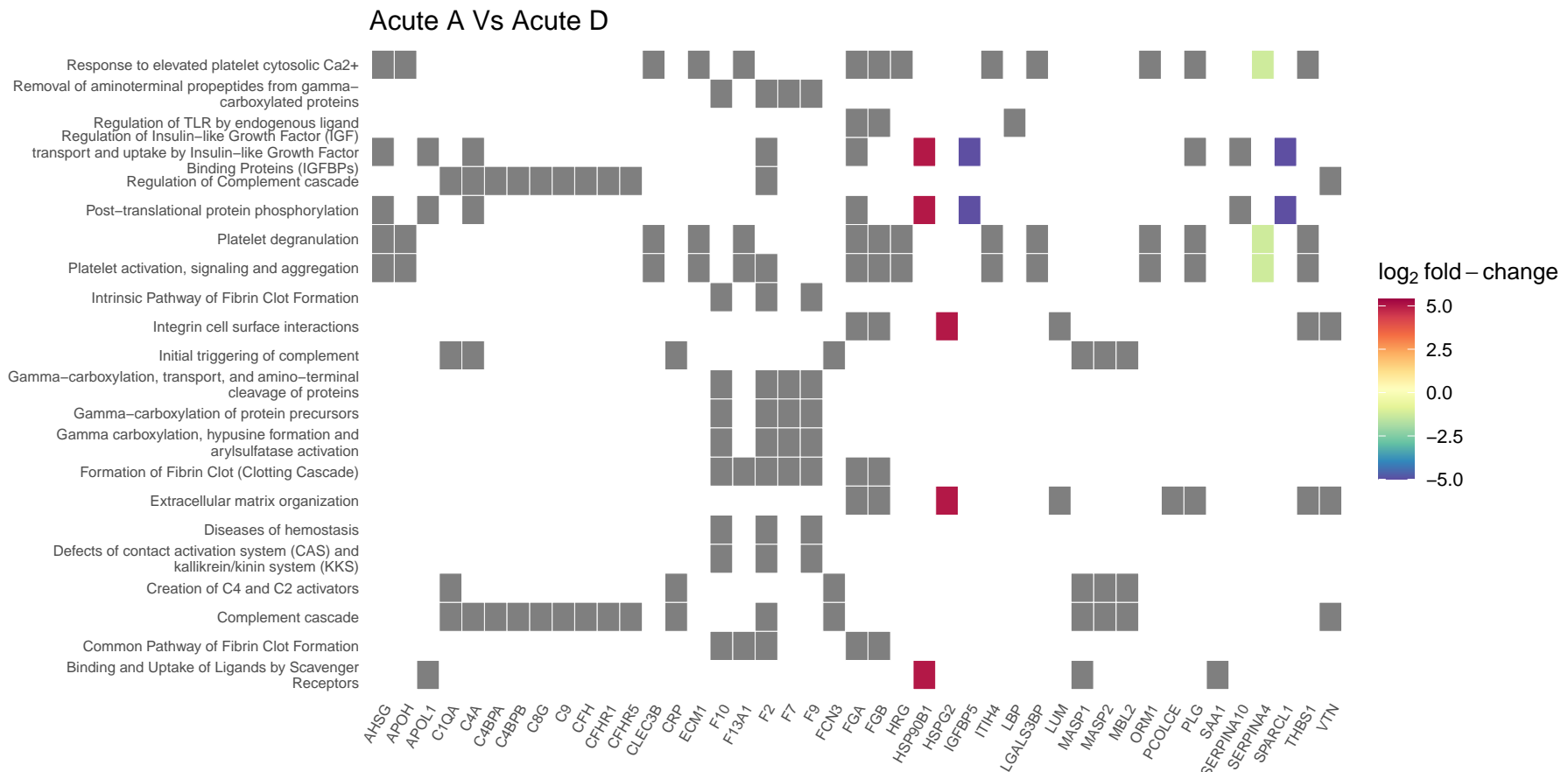


Figure S11. Heatmap denoting the \log_2 fold change of proteins in plasma collected 2-weeks post-injury, and the biological pathways these proteins are associated with on Reactome. This compares AIS A and AIS D SCI patients. Grey blocks denote proteins not present in the comparison.

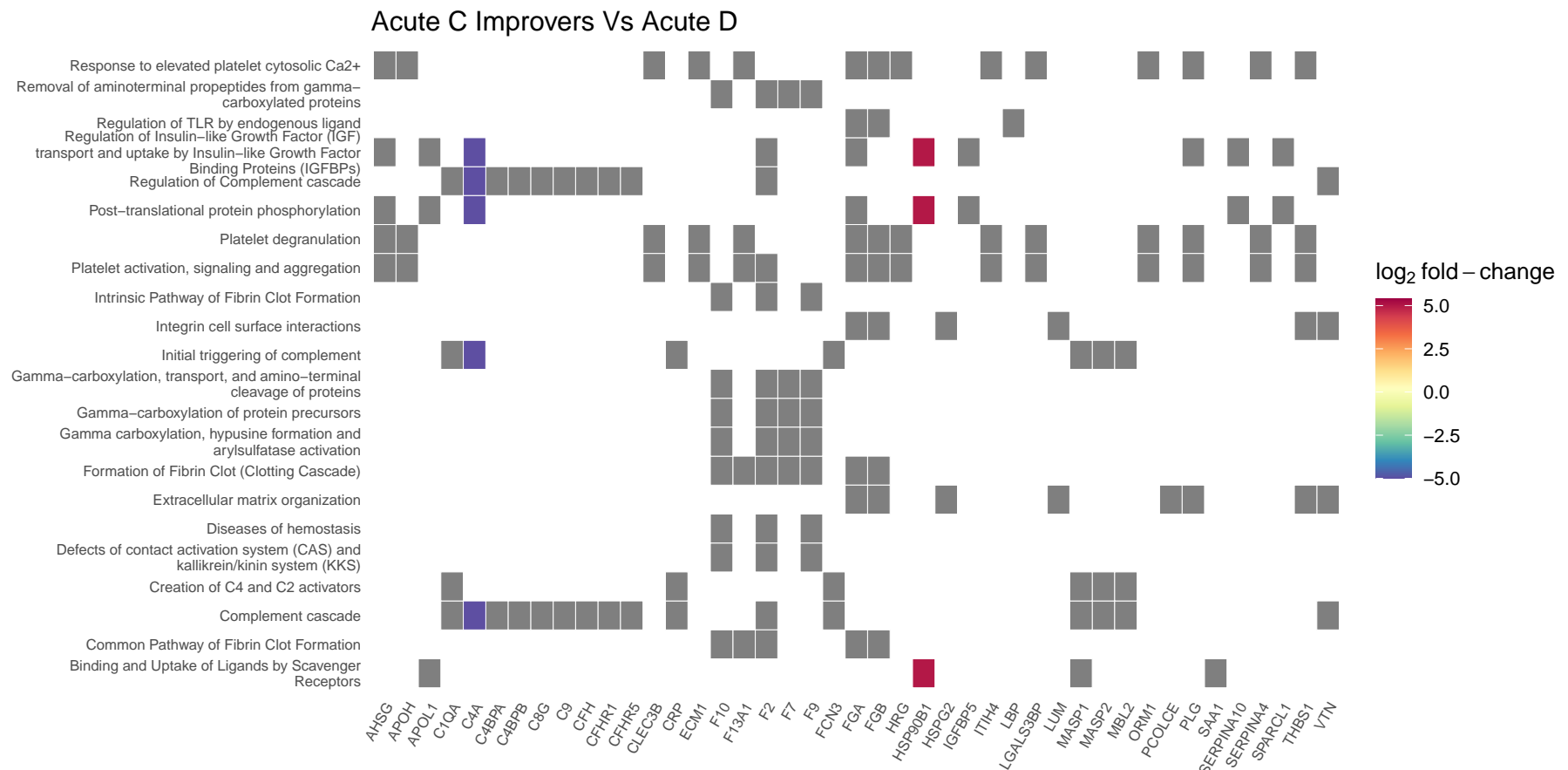


Figure S12. Heatmap denoting the log₂ fold change of proteins in plasma collected 2-weeks post-injury, and the biological pathways these proteins are associated with on Reactome. This compares AIS C SCI patients who experienced an AIS grade improvement and AIS D patients. Grey blocks denote proteins not present in the comparison.

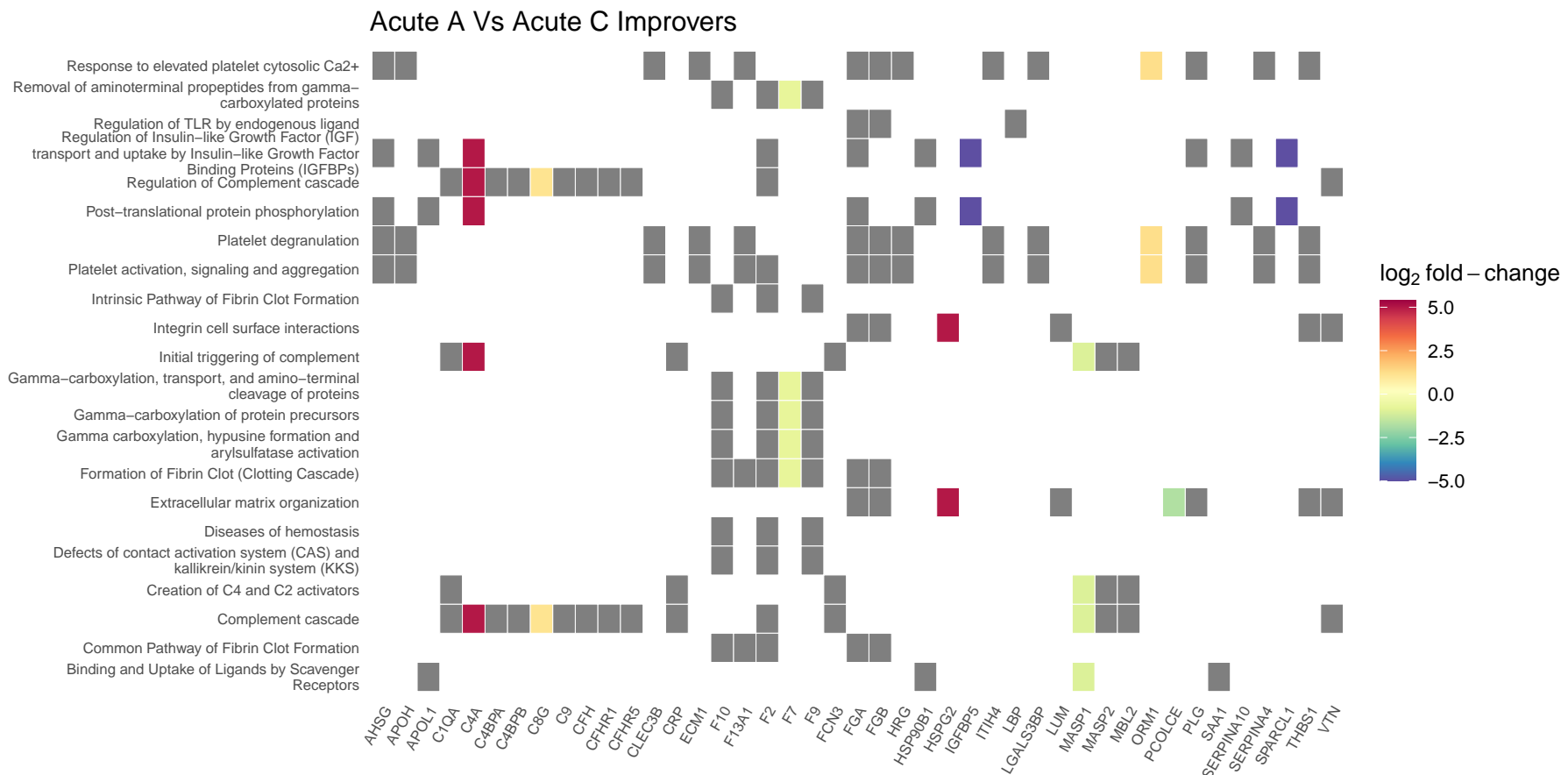


Figure S13. Heatmap denoting the log₂ fold change of proteins in plasma collected 2-weeks post-injury, and the biological pathways these proteins are associated with on Reactome. This compares AIS C SCI patients who experienced an AIS grade improvement and AIS A patients. Grey blocks denote proteins not present in the comparison.

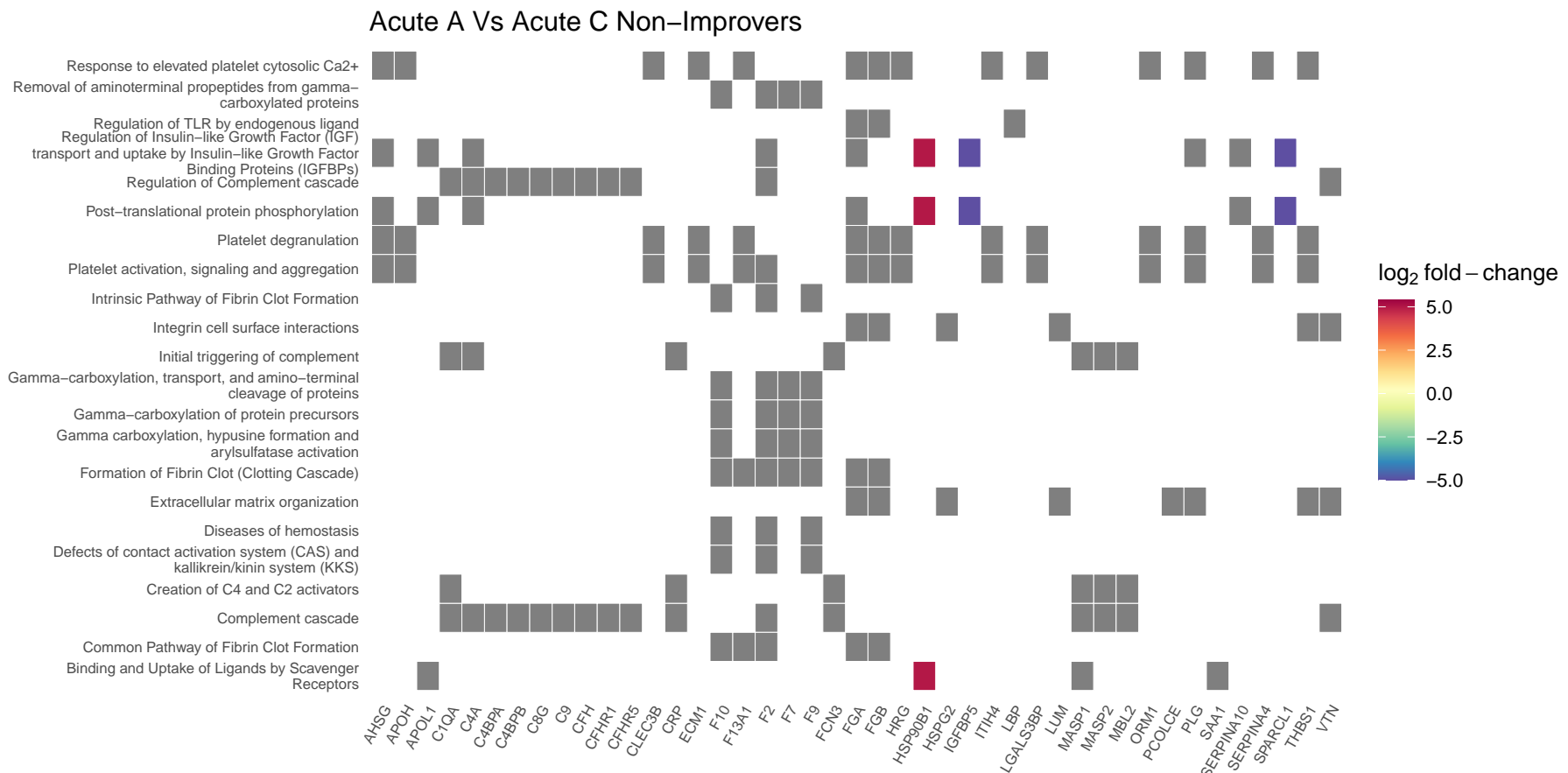


Figure S14. Heatmap denoting the log₂ fold change of proteins in plasma collected 2-weeks post-injury, and the biological pathways these proteins are associated with on Reactome. This compares AIS C SCI patients who did not experience an AIS grade improvement and AIS A patients. Grey blocks denote proteins not present in the comparison.

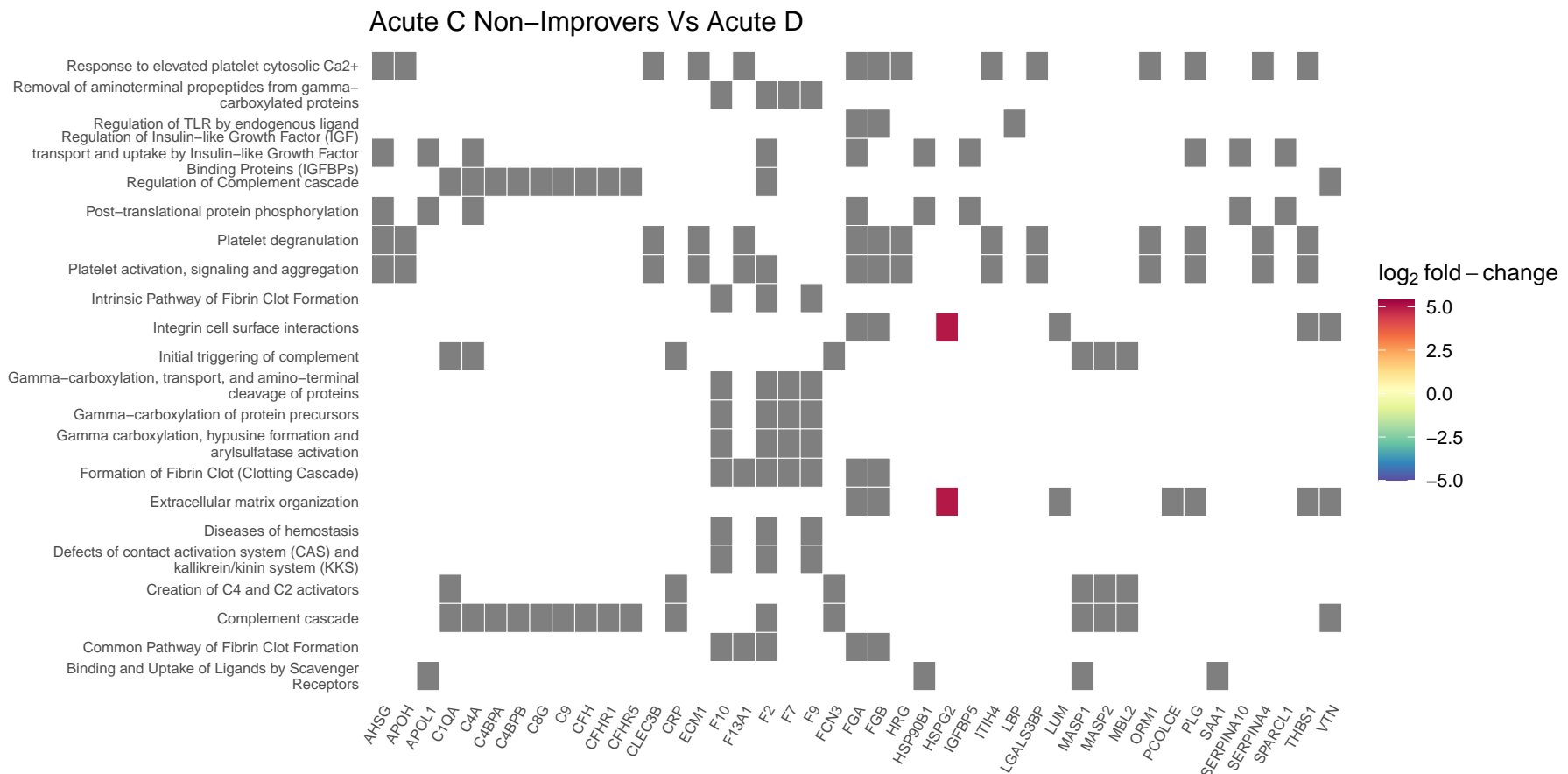


Figure S15. Heatmap denoting the \log_2 fold change of proteins in plasma collected 2-weeks post-injury, and the biological pathways these proteins are associated with on Reactome. This compares AIS C SCI patients who did not experience an AIS grade improvement and AIS D patients. Grey blocks denote proteins not present in the comparison.

553 **5.4 Cnetplots**

554 **5.4.1 iTRAQ data**

AIS C Improvers acute vs subacute

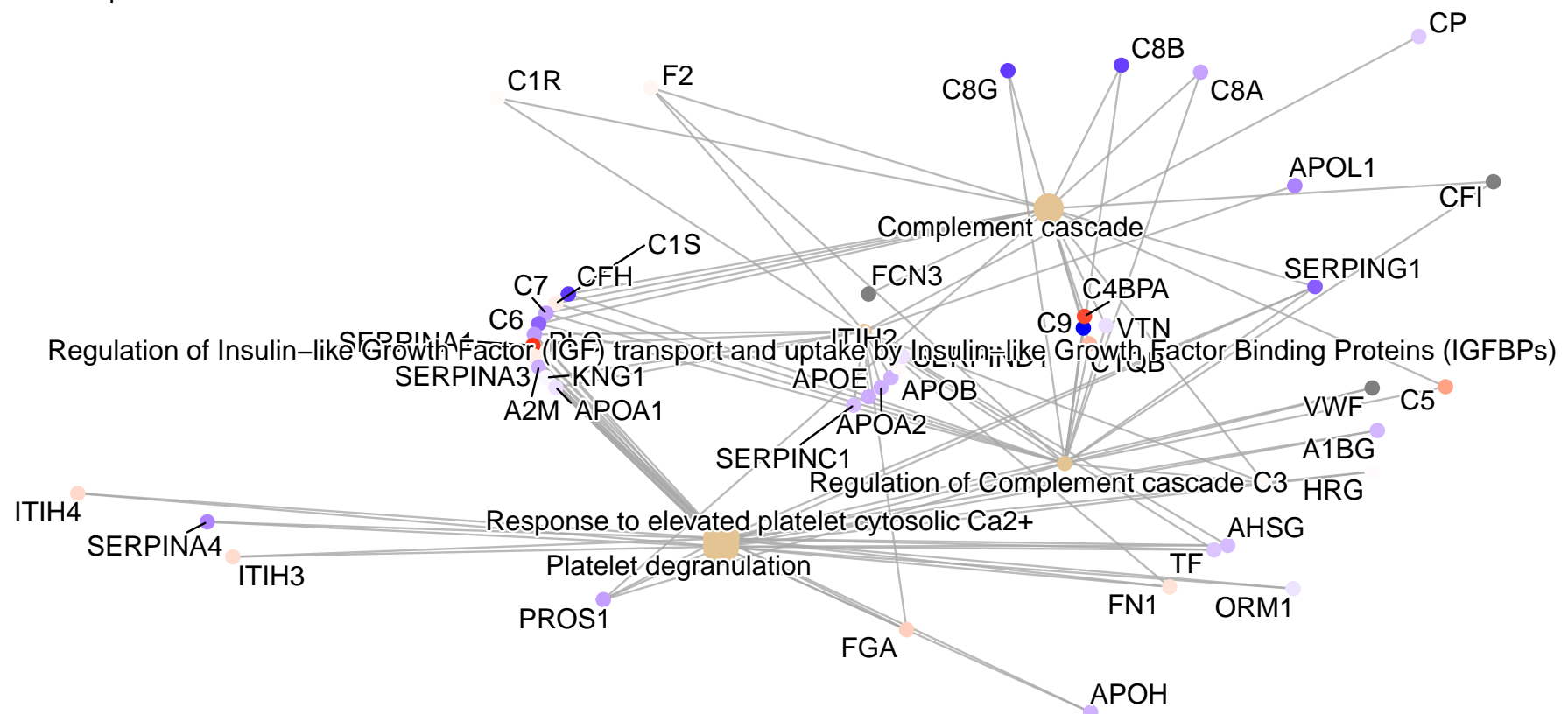


Figure S16. Network plot denoting the log₂ fold change of proteins in plasma collected 2-weeks and 3-months post-injury, and the biological pathways these proteins are associated with on Reactome. This compares AIS C SCI patients who experienced an AIS grade improvement at 2-weeks and 3-months post-injury.

AIS C non-Improvers acute vs subacute

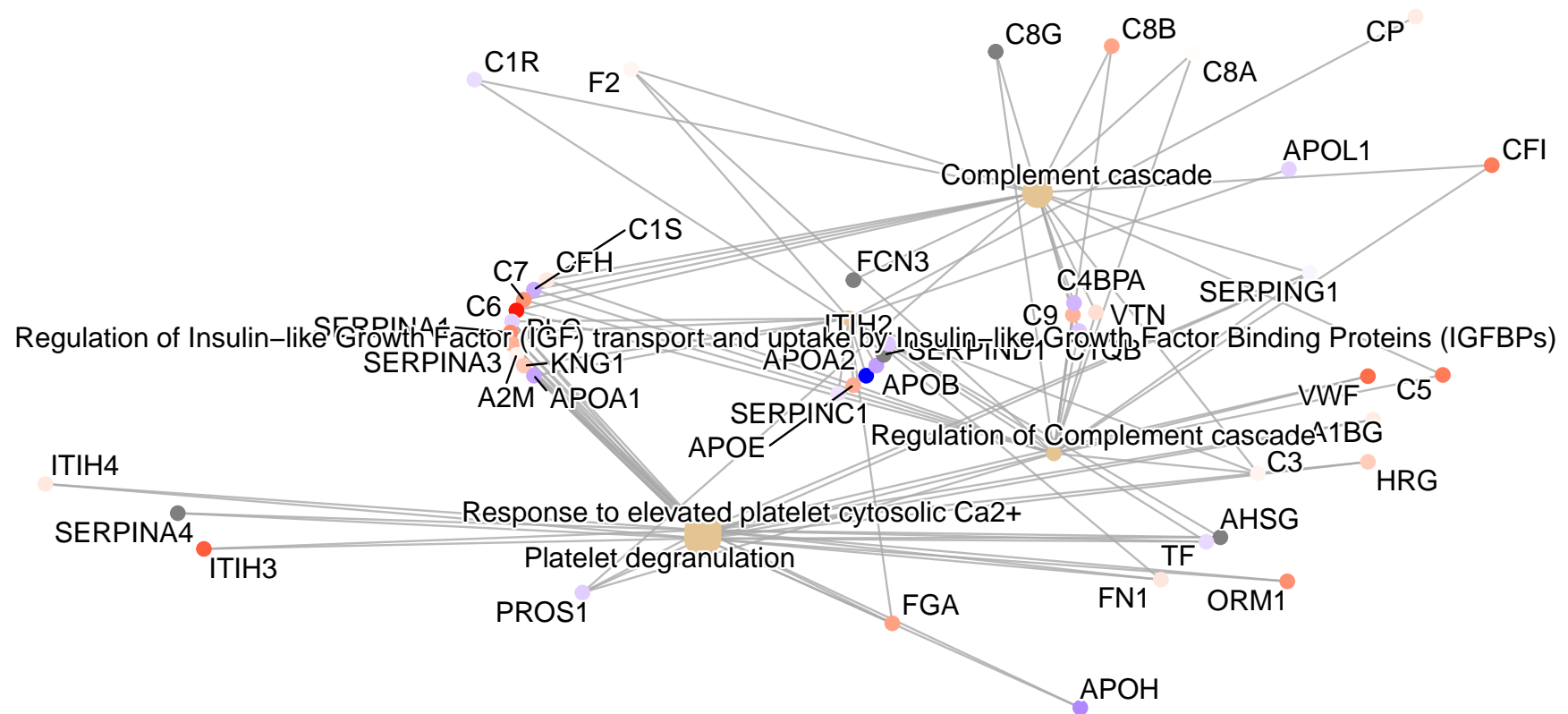


Figure S17. Network plot denoting the \log_2 fold change of proteins in plasma collected 2-weeks and 3-months post-injury, and the biological pathways these proteins are associated with on Reactome. This compares AIS C SCI patients who did not experience an AIS grade improvement at 2-weeks and 3-months post-injury.

Acute AIS C Improvers VS non-Improvers Run 2

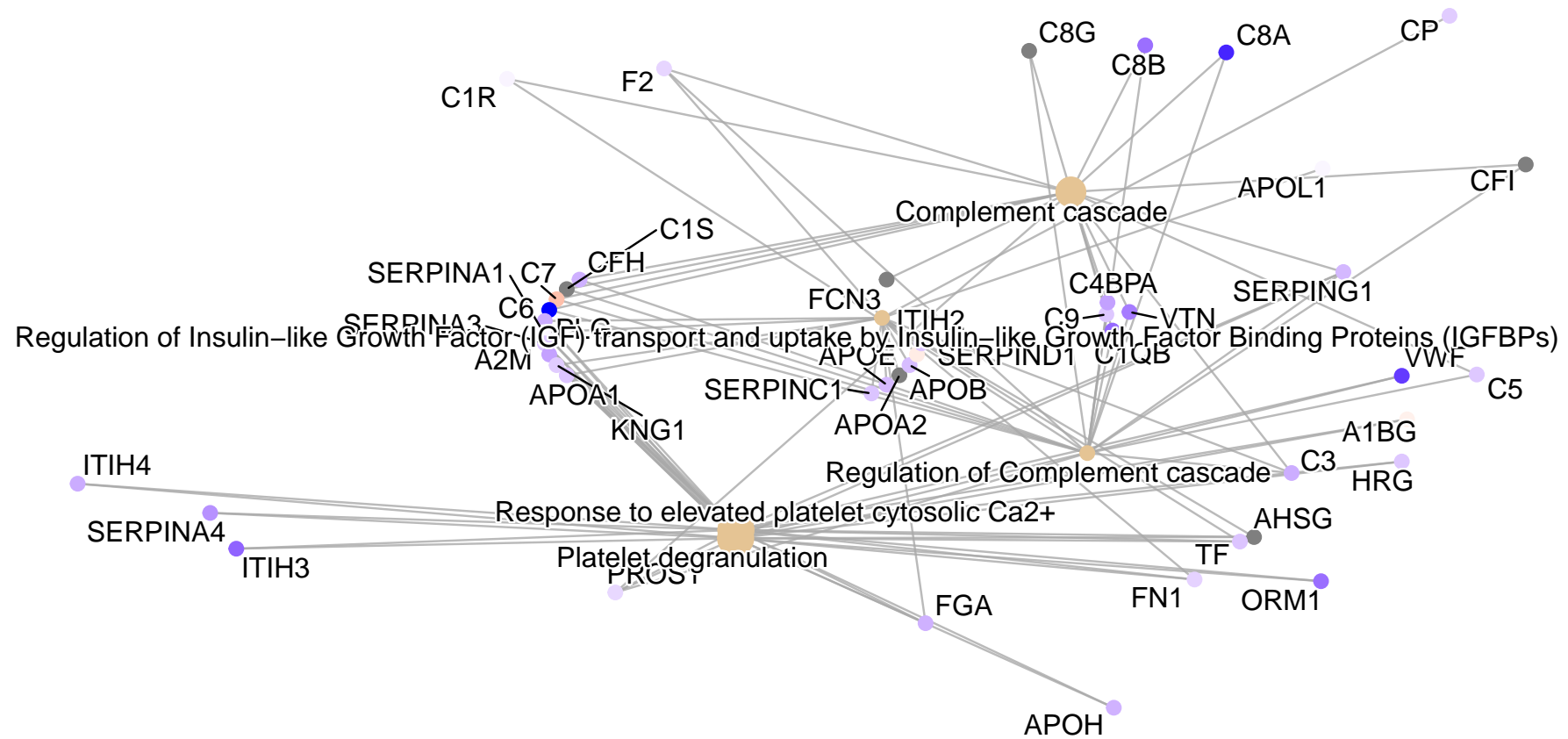


Figure S18. Network plot denoting the \log_2 fold change of proteins in plasma collected 2-weeks post-injury, and the biological pathways these proteins are associated with on Reactome. This compares AIS C SCI patients who experienced an AIS grade improvement and those who did not from the second 4-plex iTRAQ experiment.

AIS A VS AIS D

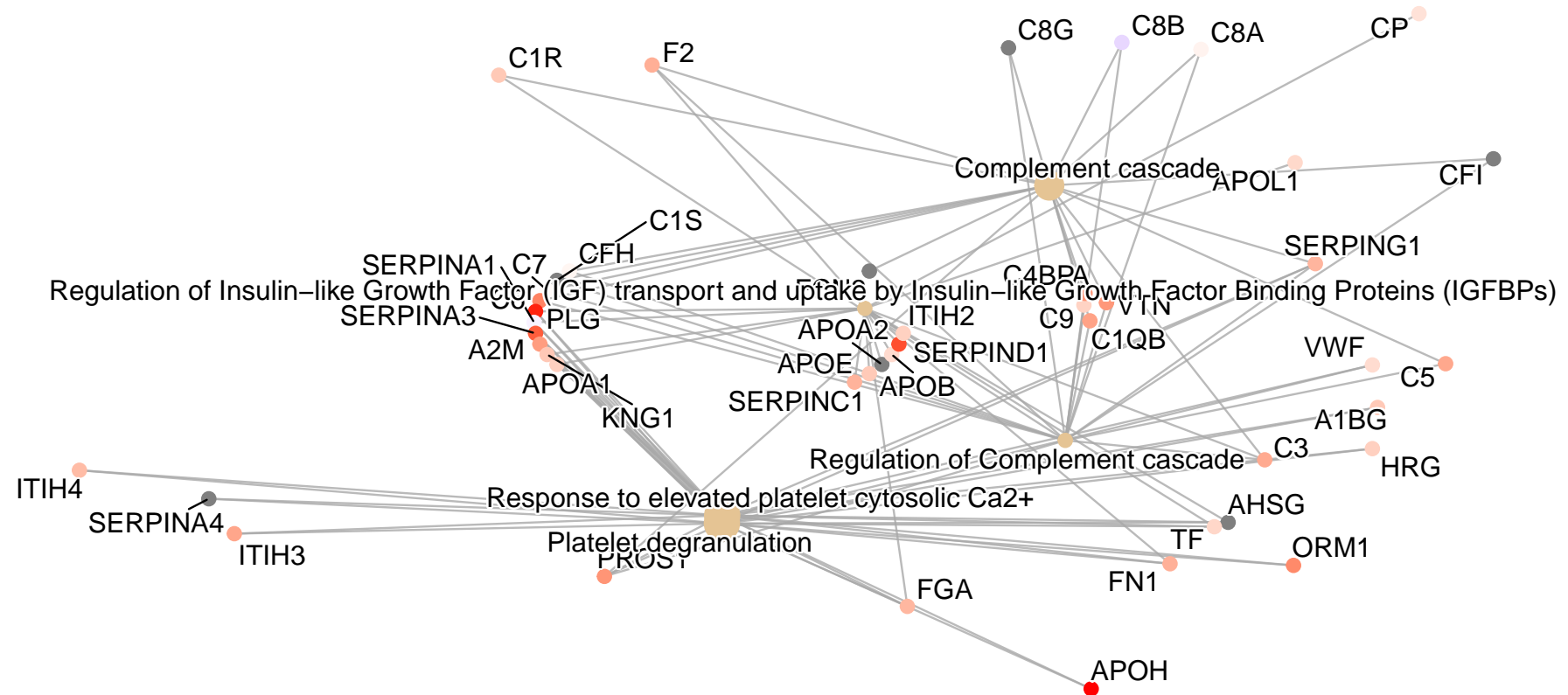


Figure S19. Network plot denoting the \log_2 fold change of proteins in plasma collected 2-weeks post-injury, and the biological pathways these proteins are associated with on Reactome. This compares AIS A and AIS D SCI patients.

Acute AIS C Improvers VS AIS D

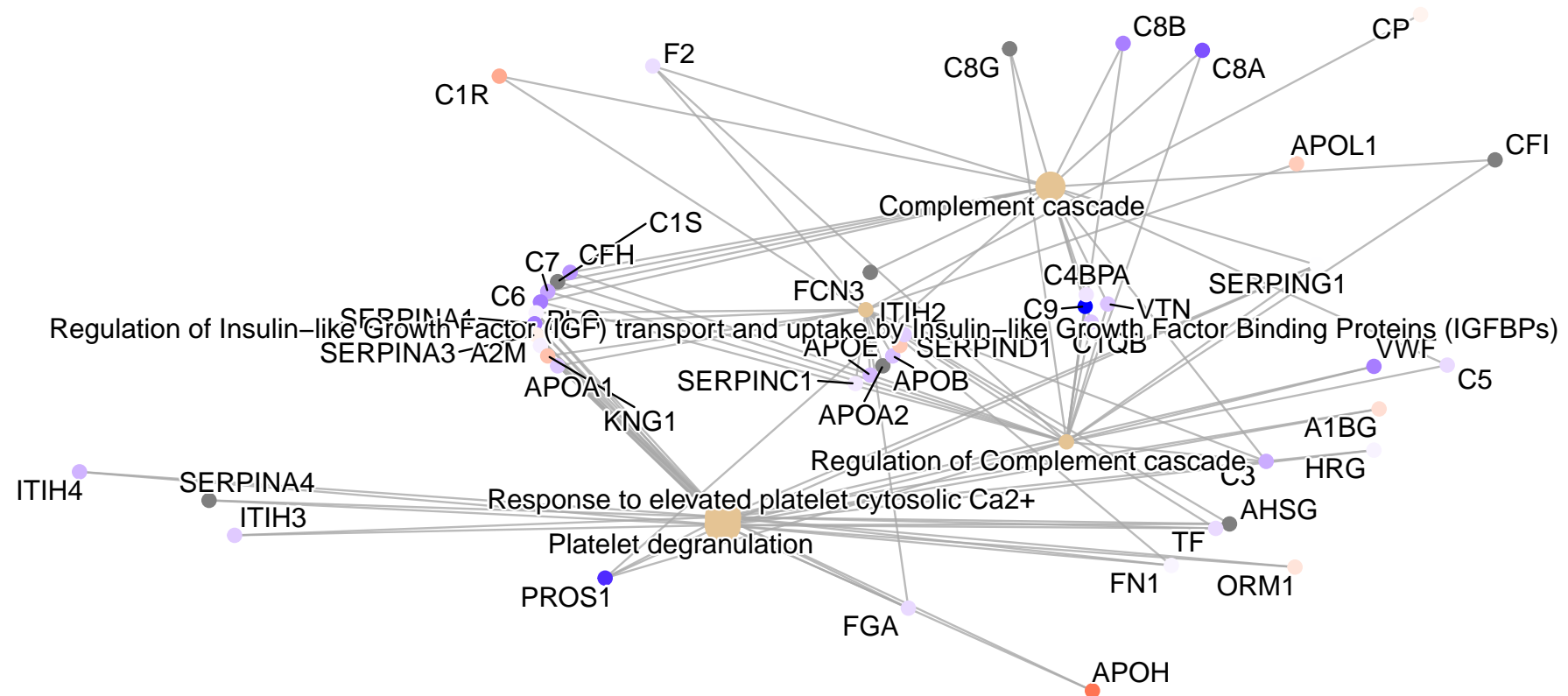


Figure S20. Network plot denoting the \log_2 fold change of proteins in plasma collected 2-weeks post-injury, and the biological pathways these proteins are associated with on Reactome. This compares AIS C SCI patients who experienced an AIS grade improvement and AIS D patients.

Acute AIS C Improvers VS AIS A

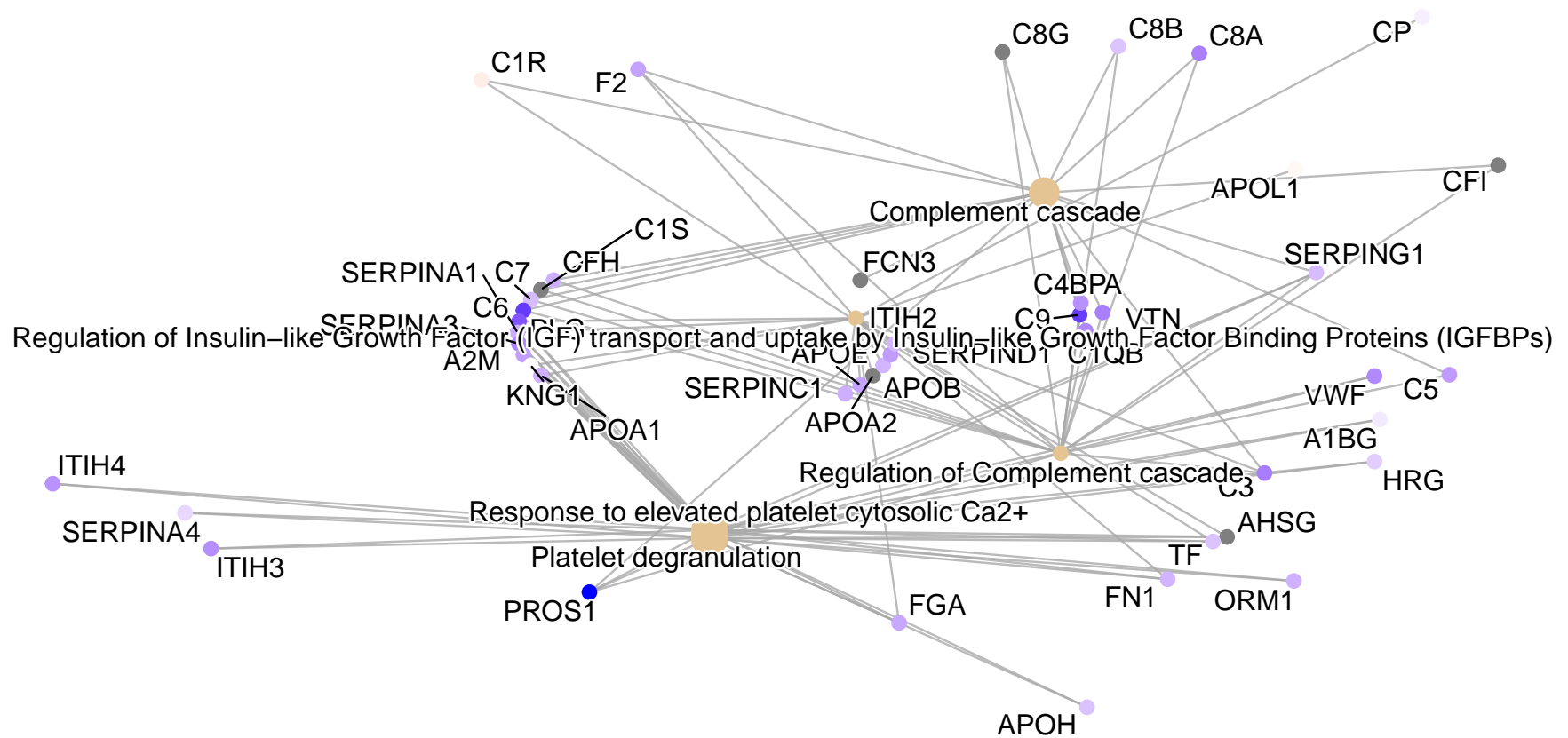


Figure S21. Network plot denoting the log₂ fold change of proteins in plasma collected 2-weeks post-injury, and the biological pathways these proteins are associated with on Reactome. This compares AIS C SCI patients who experienced an AIS grade improvement and AIS A patients.

Acute AIS C non-Improvers VS AIS A

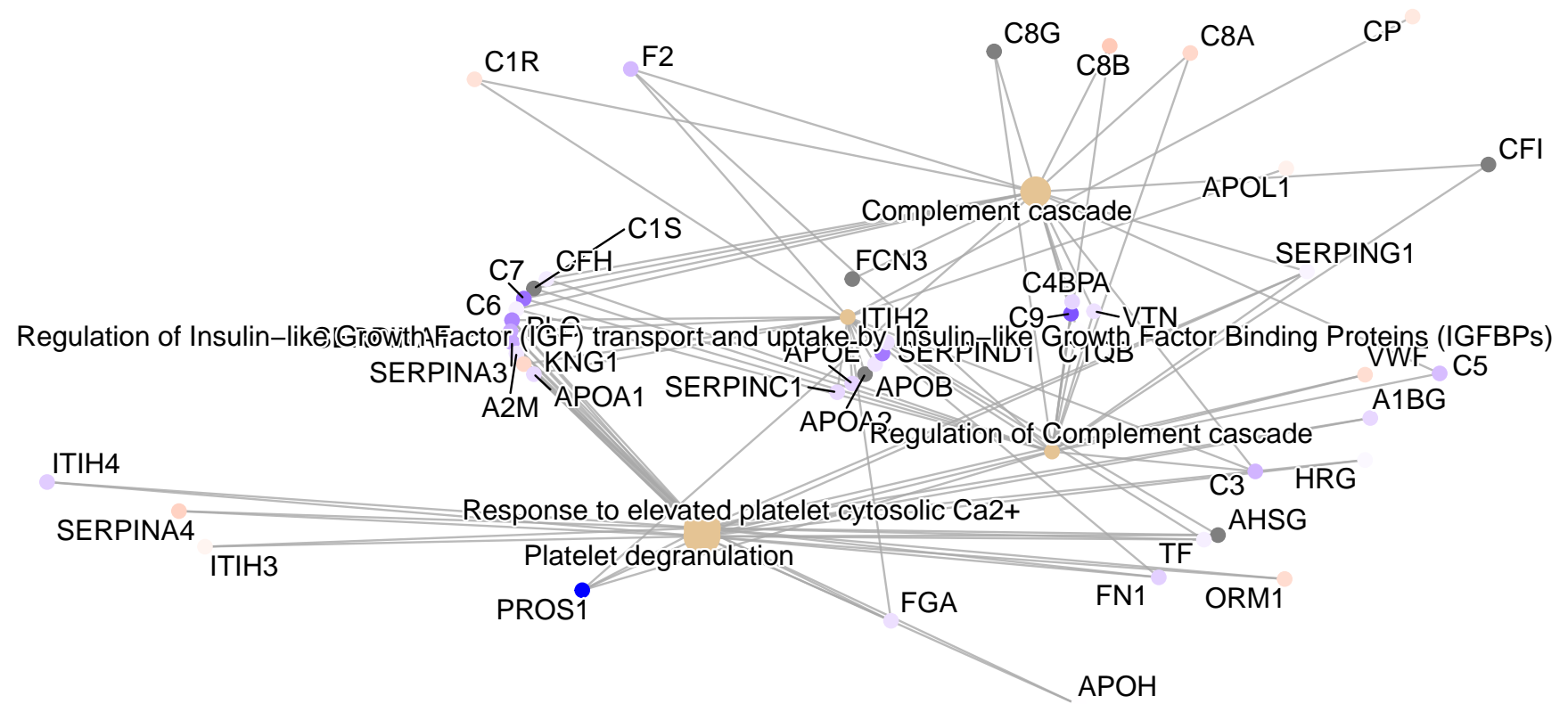


Figure S22. Network plot denoting the log₂ fold change of proteins in plasma collected 2-weeks post-injury, and the biological pathways these proteins are associated with on Reactome. This compares AIS C SCI patients who did not experience an AIS grade improvement and AIS A patients.

Acute AIS C non-Improvers VS AIS D

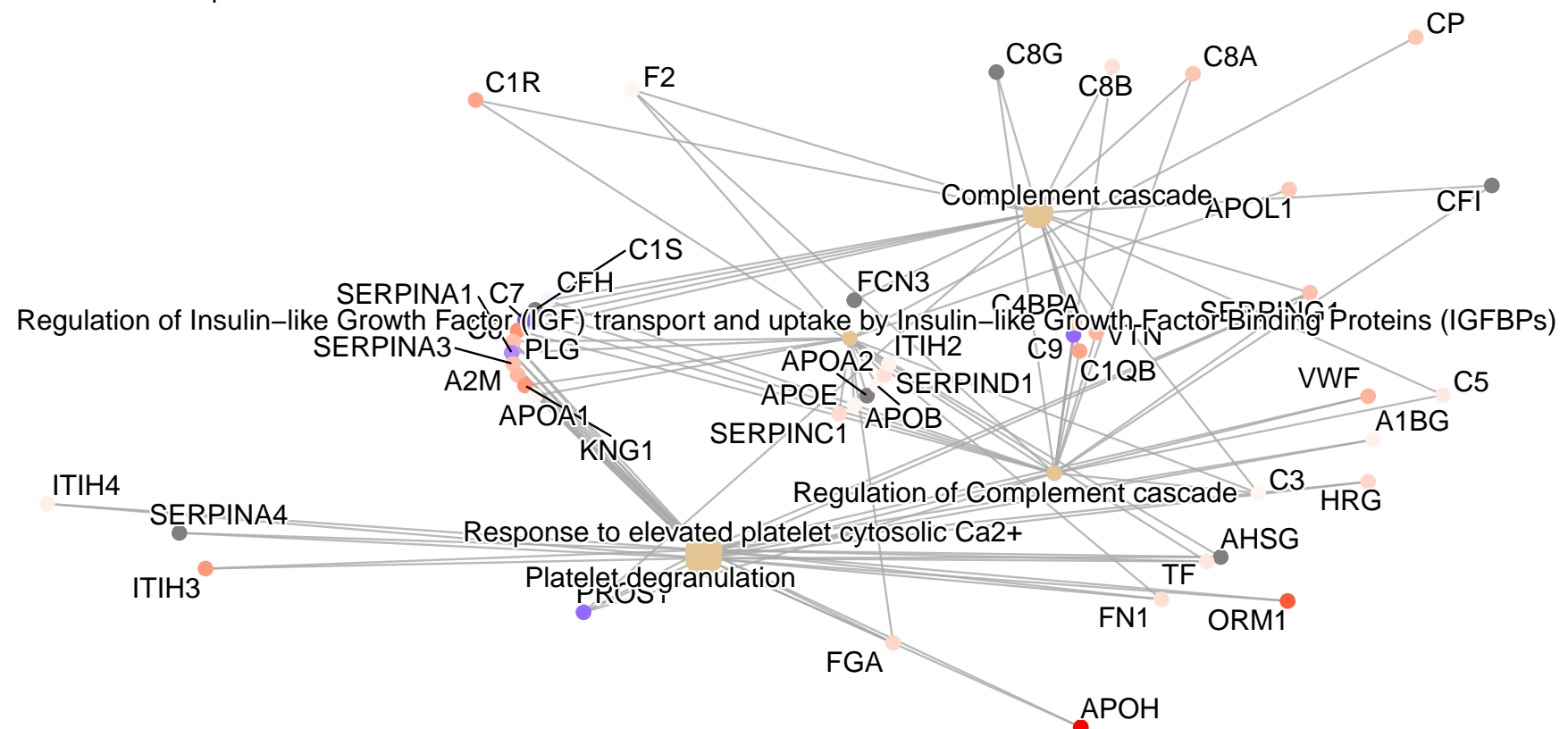


Figure S23. Network plot denoting the \log_2 fold change of proteins in plasma collected 2-weeks post-injury, and the biological pathways these proteins are associated with on Reactome. This compares AIS C SCI patients who did not experience an AIS grade improvement and AIS D patients.

Acute C Improvers Vs Subacute C Improvers

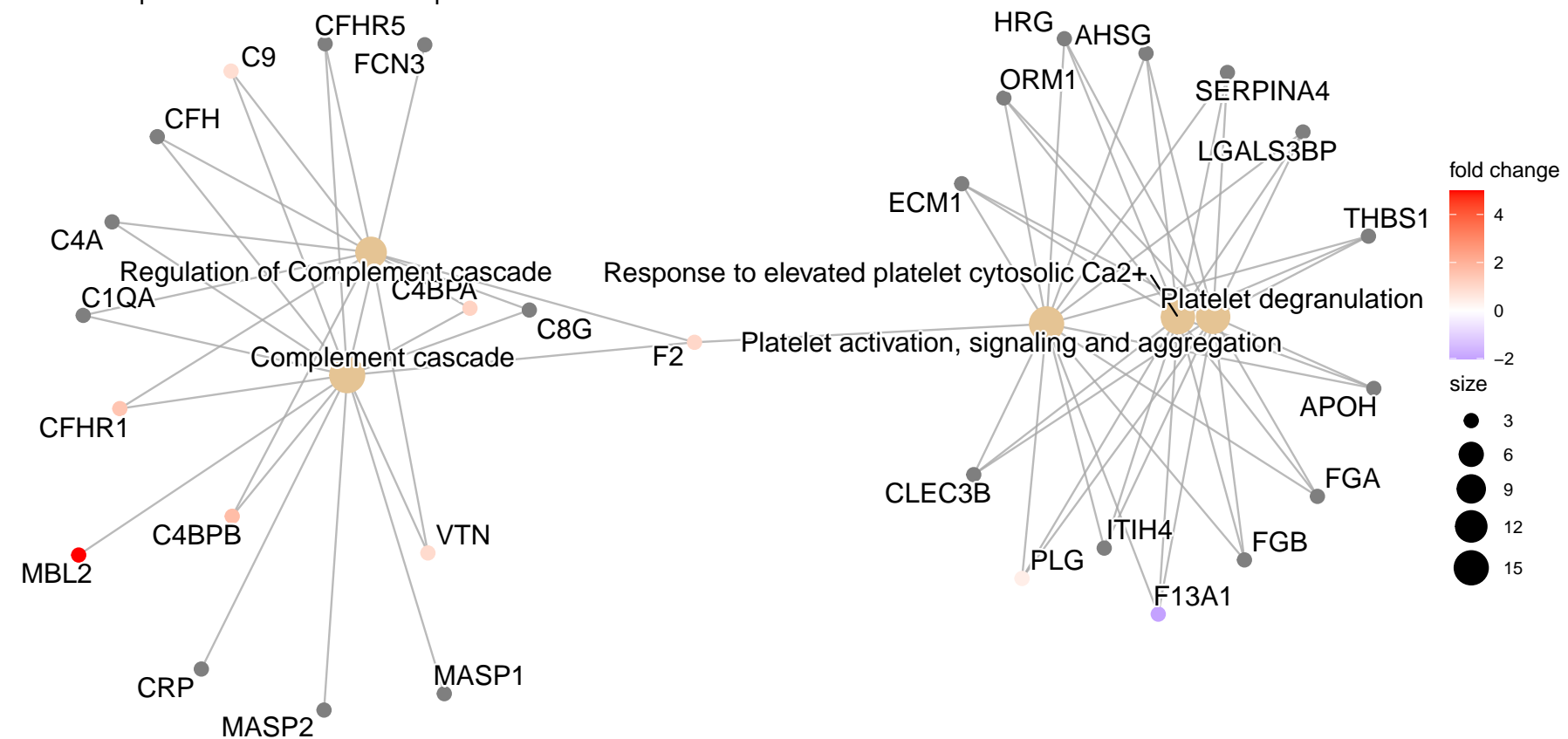


Figure S24. Network plot denoting the \log_2 fold change of proteins in plasma collected 2-weeks and 3-months post-injury, and the biological pathways these proteins are associated with on Reactome. This compares AIS C SCI patients who experienced an AIS grade improvement at 2-weeks and 3-months post-injury.

Acute C Non-Improvers Vs Subacute C Non-Improvers

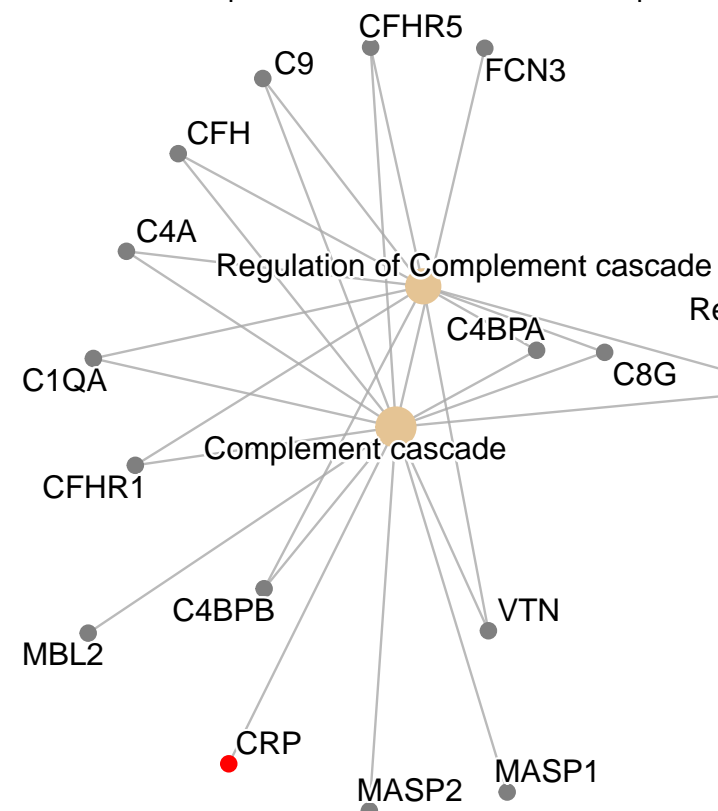


Figure S25. Network plot denoting the \log_2 fold change of proteins in plasma collected 2-weeks and 3-months post-injury, and the biological pathways these proteins are associated with on Reactome. This compares AIS C SCI patients who did not experience an AIS grade improvement at 2-weeks and 3-months post-injury.

Acute A Vs Acute D

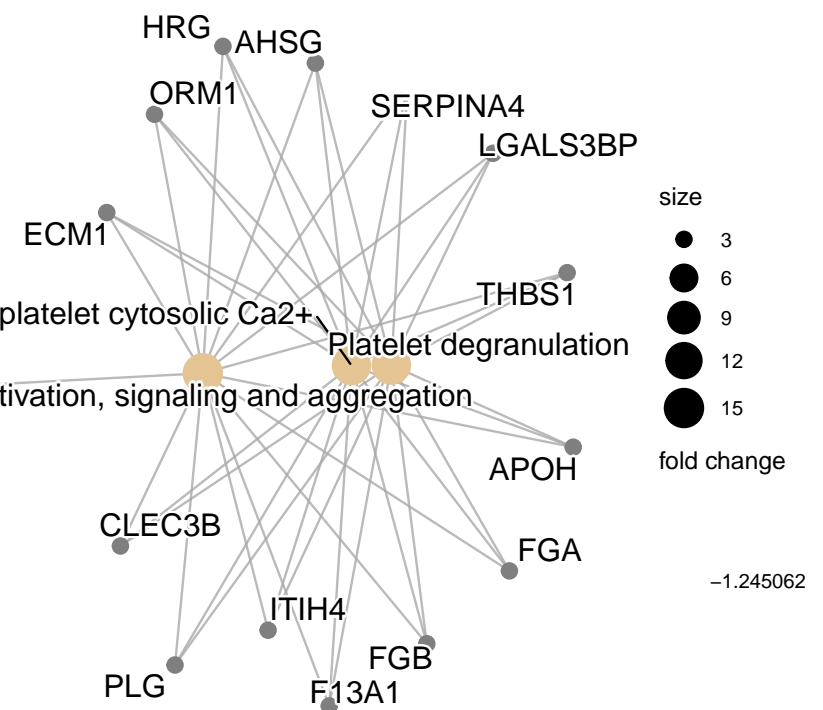
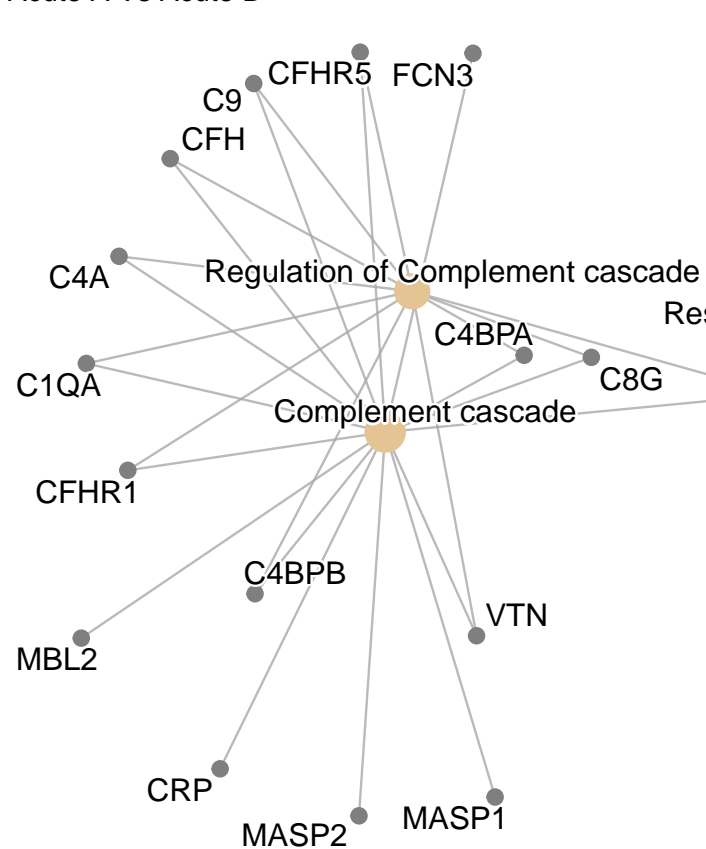


Figure S26. Network plot denoting the \log_2 fold change of proteins in plasma collected 2-weeks post-injury, and the biological pathways these proteins are associated with on Reactome. This compares AIS A and AIS D SCI patients.

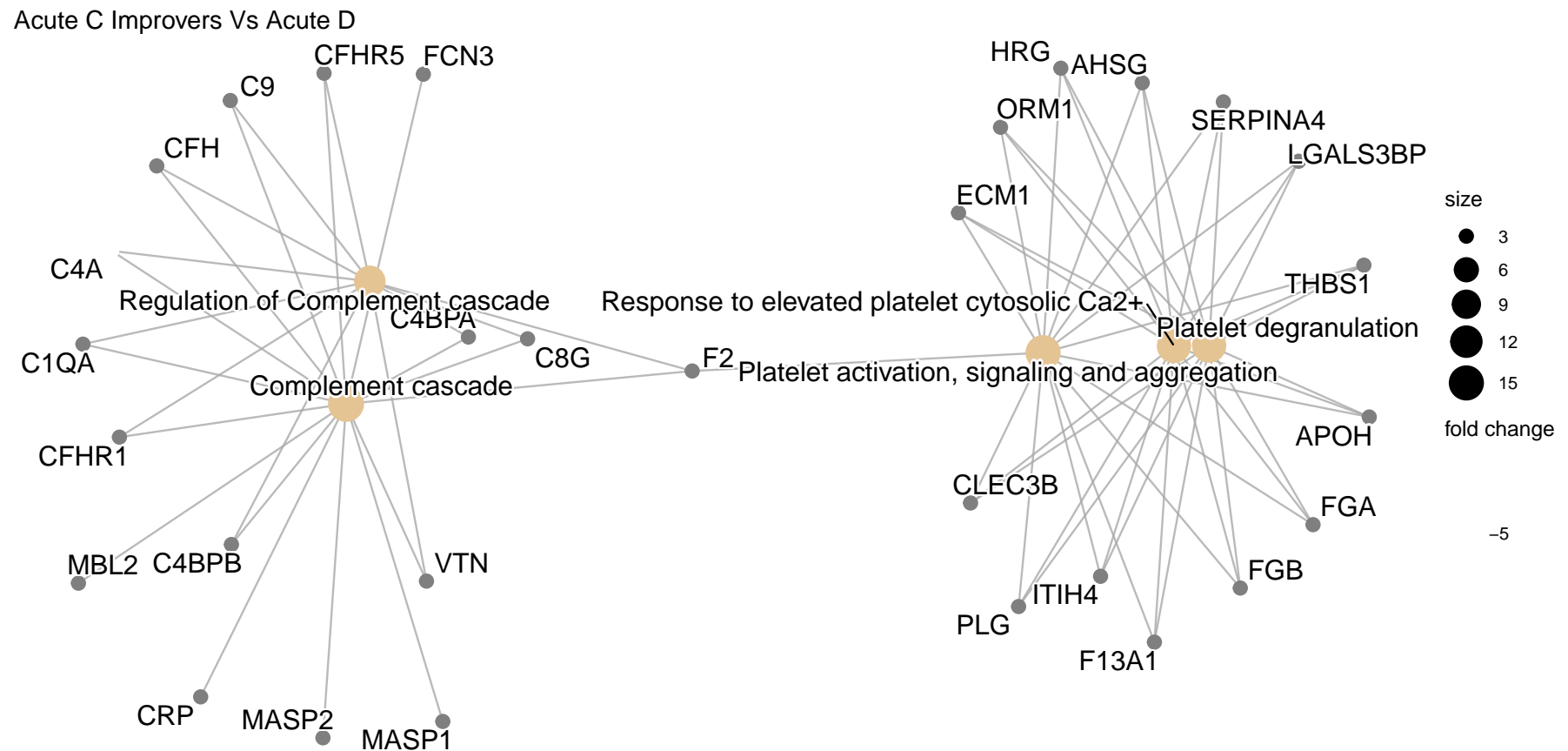


Figure S27. Network plot denoting the \log_2 fold change of proteins in plasma collected 2-weeks post-injury, and the biological pathways these proteins are associated with on Reactome. This compares AIS C SCI patients who experienced an AIS grade improvement and AIS D patients.

Acute A Vs Acute C Improvers

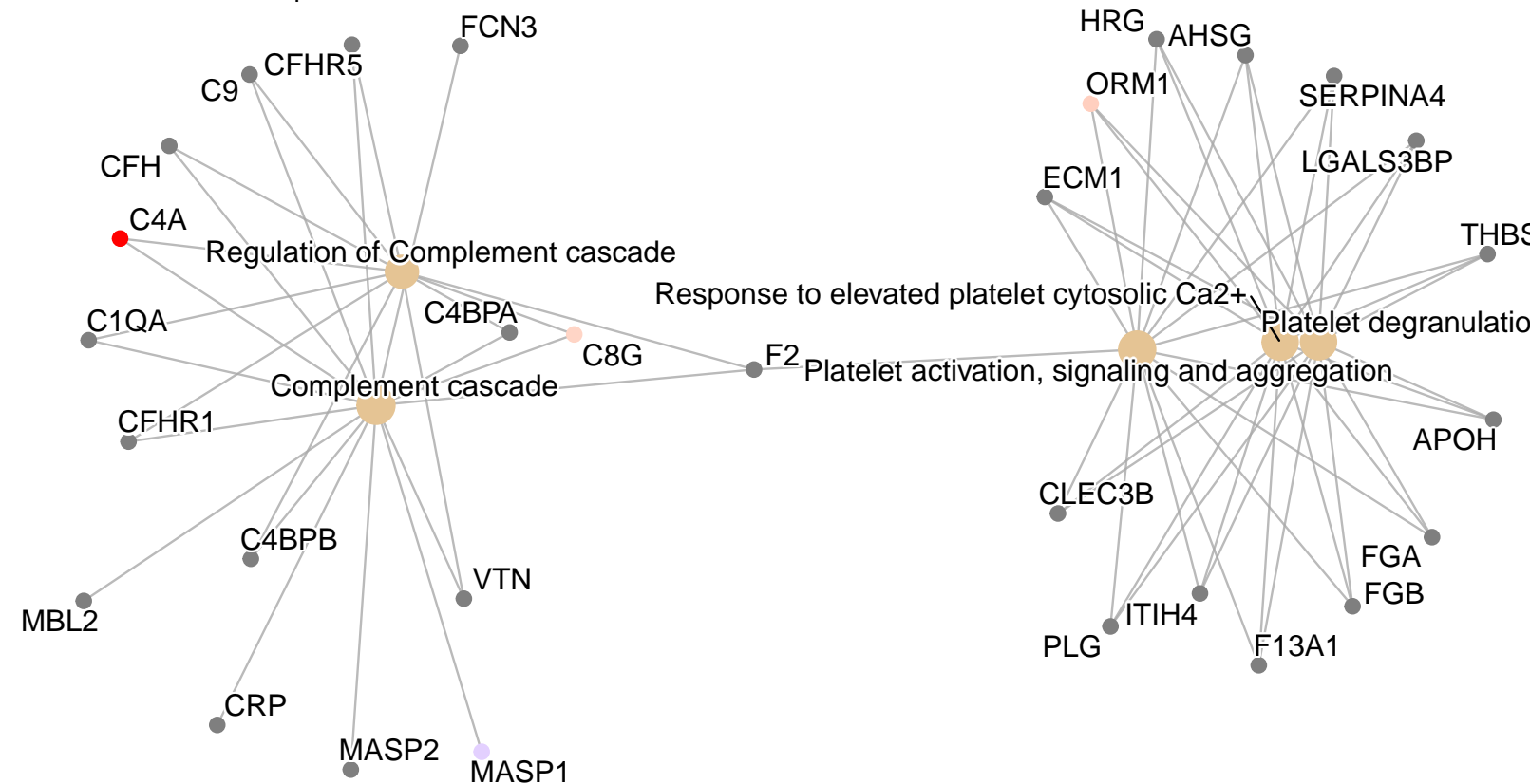


Figure S28. Network plot denoting the \log_2 fold change of proteins in plasma collected 2-weeks post-injury, and the biological pathways these proteins are associated with on Reactome. This compares AIS C SCI patients who experienced an AIS grade improvement and AIS A patients.

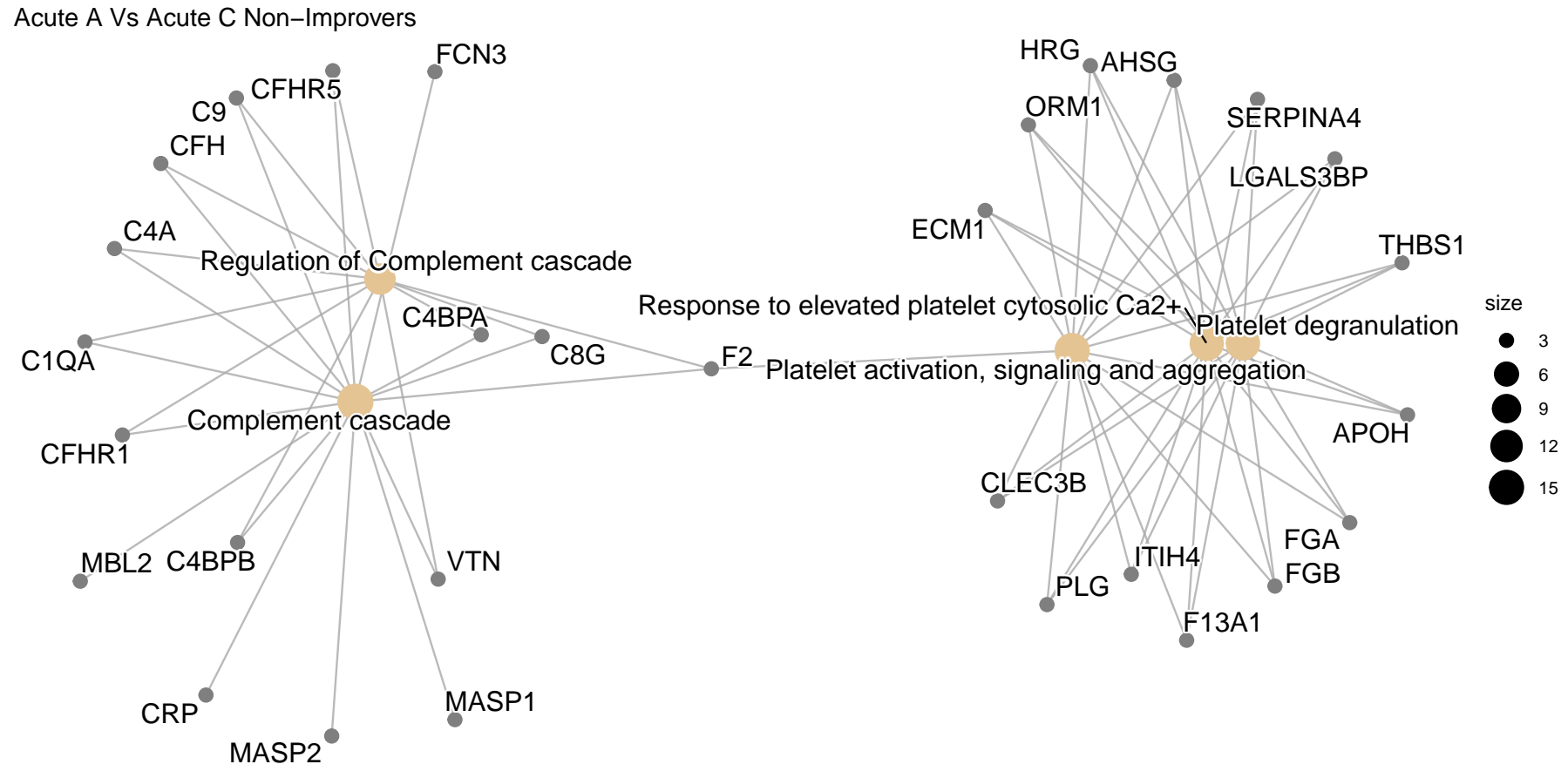


Figure S29. Network plot denoting the \log_2 fold change of proteins in plasma collected 2-weeks post-injury, and the biological pathways these proteins are associated with on Reactome. This compares AIS C SCI patients who did not experience an AIS grade improvement and AIS A patients.

Acute C Non-Improvers Vs Acute D

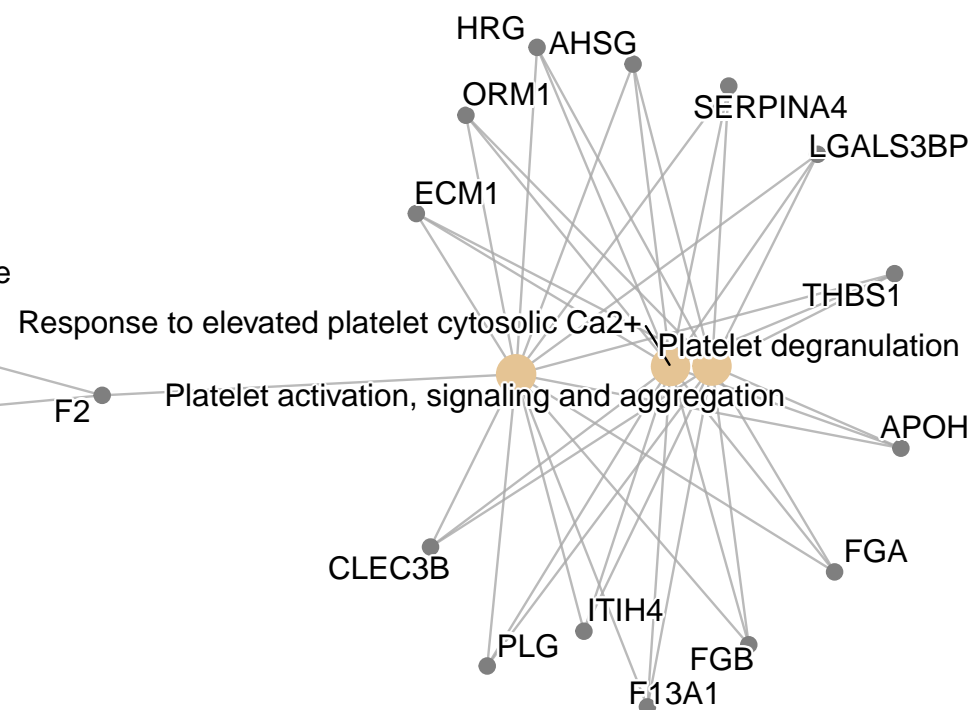
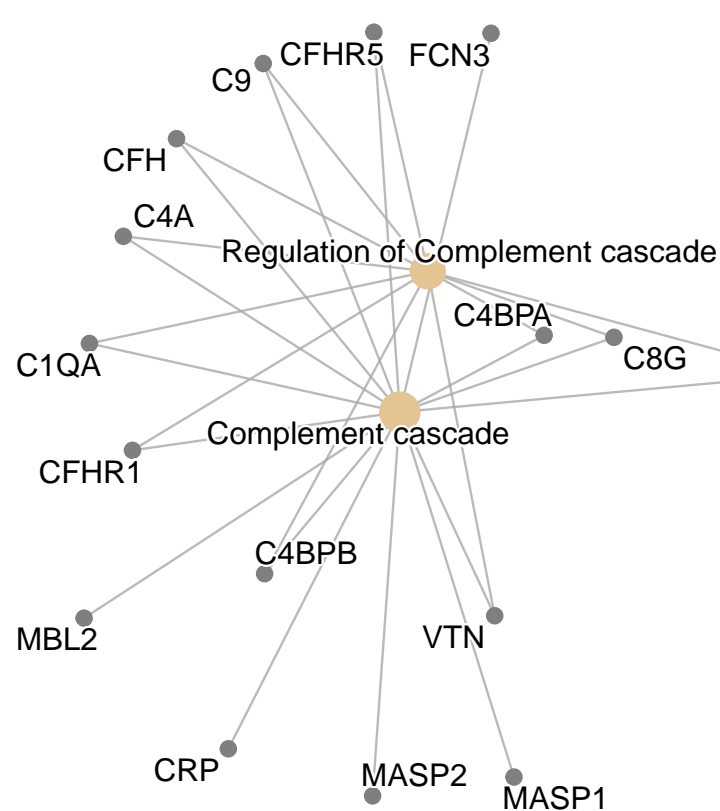


Figure S30. Network plot denoting the log₂ fold change of proteins in plasma collected 2-weeks post-injury, and the biological pathways these proteins are associated with on Reactome. This compares AIS C SCI patients who did not experience an AIS grade improvement and AIS D patients.

556 5.5 STRINGdb network plots

557 5.5.1 iTRAQ data

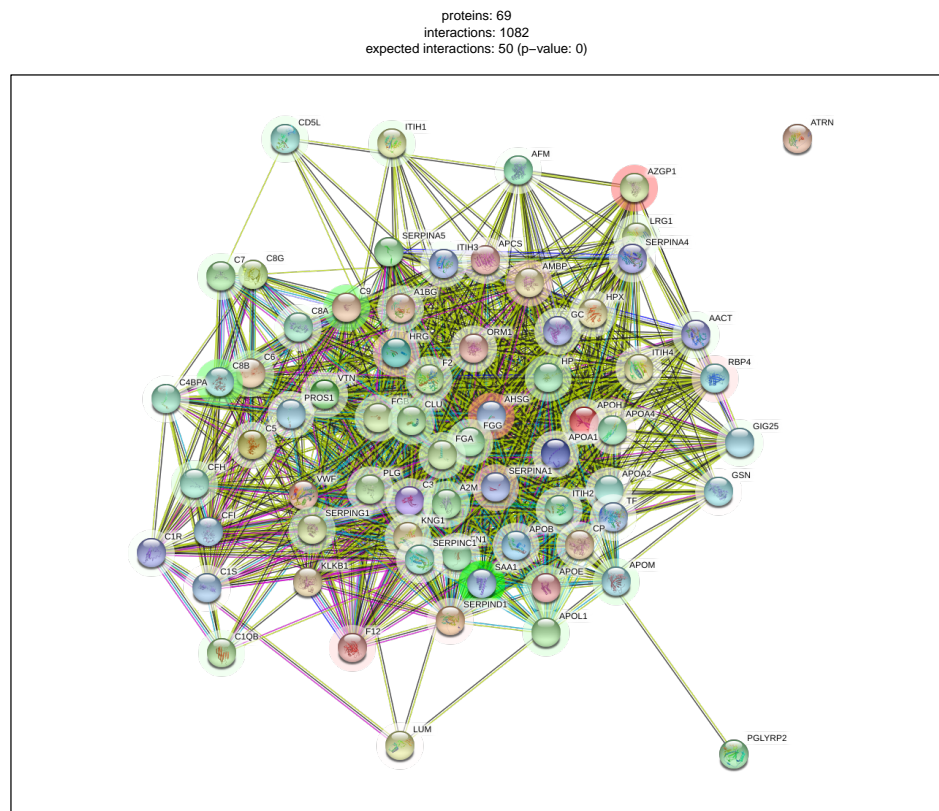


Figure S31. The interaction network of differentially abundant proteins found in plasma 2-weeks post-injury, between AIS C patients who experienced an AIS grade conversion and those who did not. The coloured "halo" denotes fold change whereby green indicates that protein is less abundant and red indicates greater abundance. Edges represent protein-protein associations; these are known interactions from: curated databases and those that are experimentally determined. Predicted interactions from: gene co-occurrence; gene fusions; gene neighbourhood. Others are from gene co-expression; text-mining and protein homology.

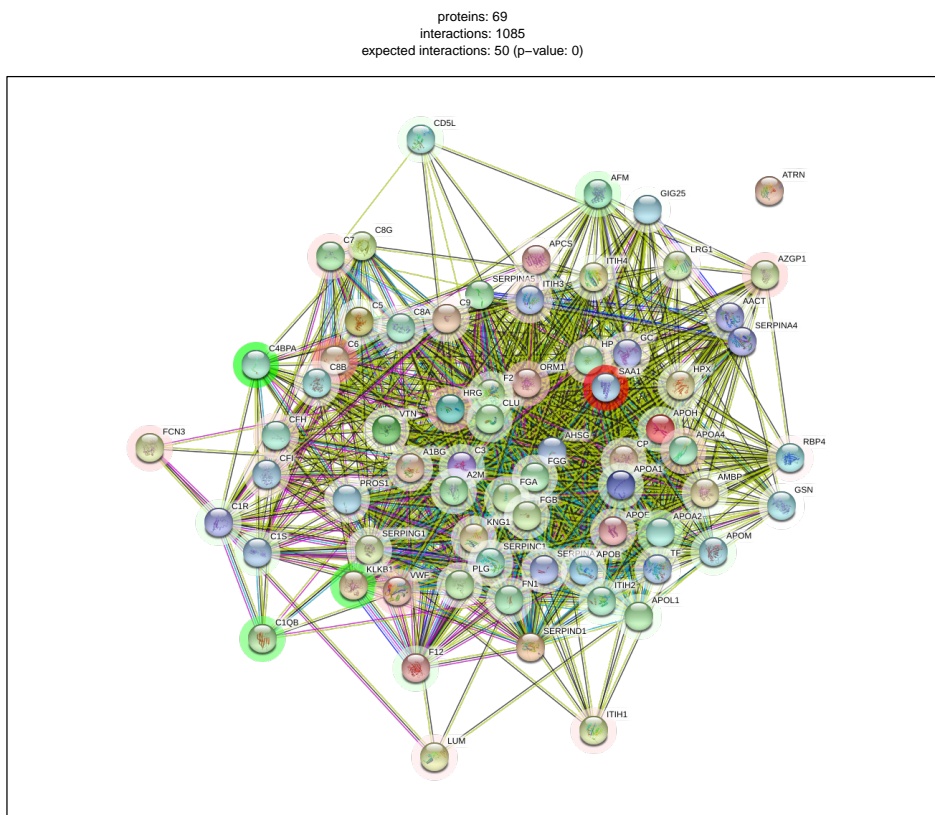


Figure S32. Interaction network of differentially abundant proteins from plasma 3-months post-injury, between AIS C patients who experienced an AIS grade conversion and those who did not. The coloured “halo” denotes fold change whereby green indicates that protein is less abundant and red that there is greater abundance. Edges represent protein-protein associations; these are known interactions from: curated databases  and those that are experimentally determined . Predicted interactions from: gene co-occurrence ; gene fusions ; gene neighbourhood . Others are from gene co-expression ; text-mining  and protein homology .

proteins: 69
interactions: 1064
expected interactions: 50 (p-value: 0)

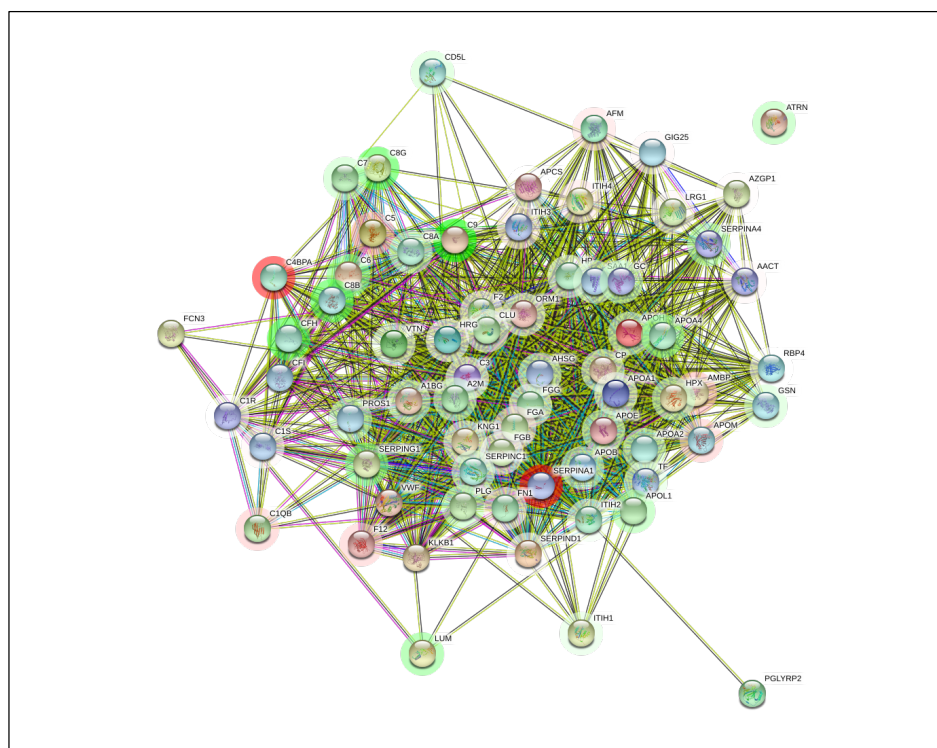


Figure S33. Interaction network of differentially abundant proteins from plasma 2-weeks and 3-months post-injury for AIS C patients who experienced an AIS grade conversion. The coloured "halo" denotes fold change whereby green indicates that protein is less abundant and red that there is greater abundance. Edges represent protein-protein associations; these are known interactions from: curated databases and those that are experimentally determined . Predicted interactions from: gene co-occurrence ; gene fusions ; gene neighbourhood . Others are from gene co-expression ; text-mining and protein homology .

proteins: 67
interactions: 1071
expected interactions: 49 (p-value: 0)

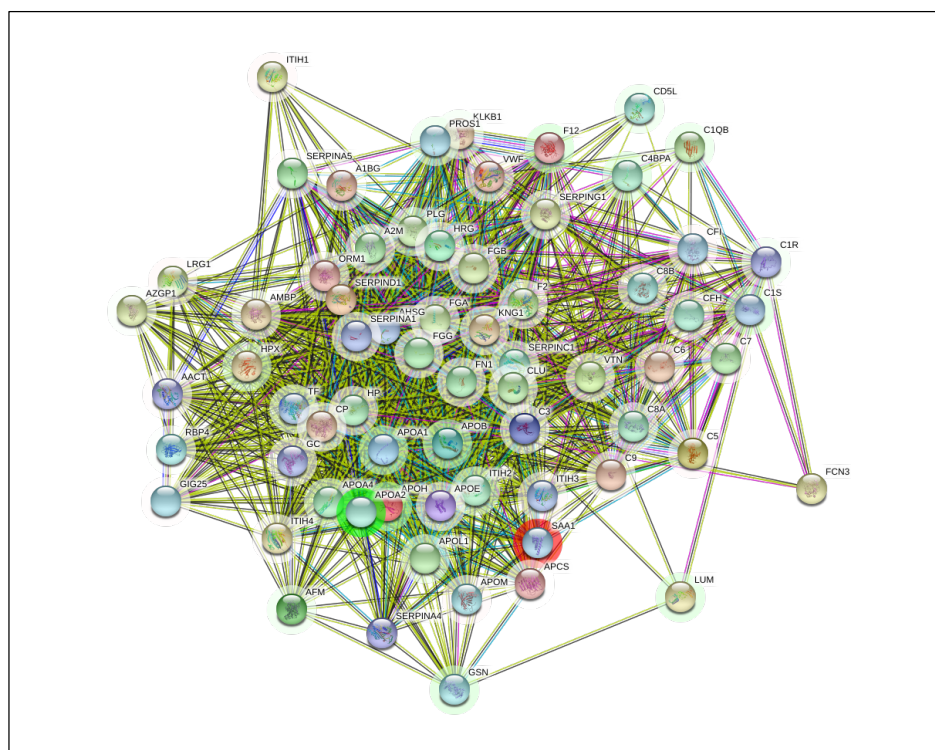


Figure S34. Interaction network of differentially abundant proteins from plasma 2-weeks and 3-months post-injury for AIS C patients who did not experience an AIS grade conversion. The coloured “halo” denotes fold change whereby green indicates that protein is less abundant and red that there is greater abundance. Edges represent protein-protein associations; these are known interactions from: curated databases and those that are experimentally determined. Predicted interactions from: gene co-occurrence; gene fusions; gene neighbourhood. Others are from gene co-expression; text-mining and protein homology.

proteins: 61
interactions: 925
expected interactions: 42 (p-value: 0)

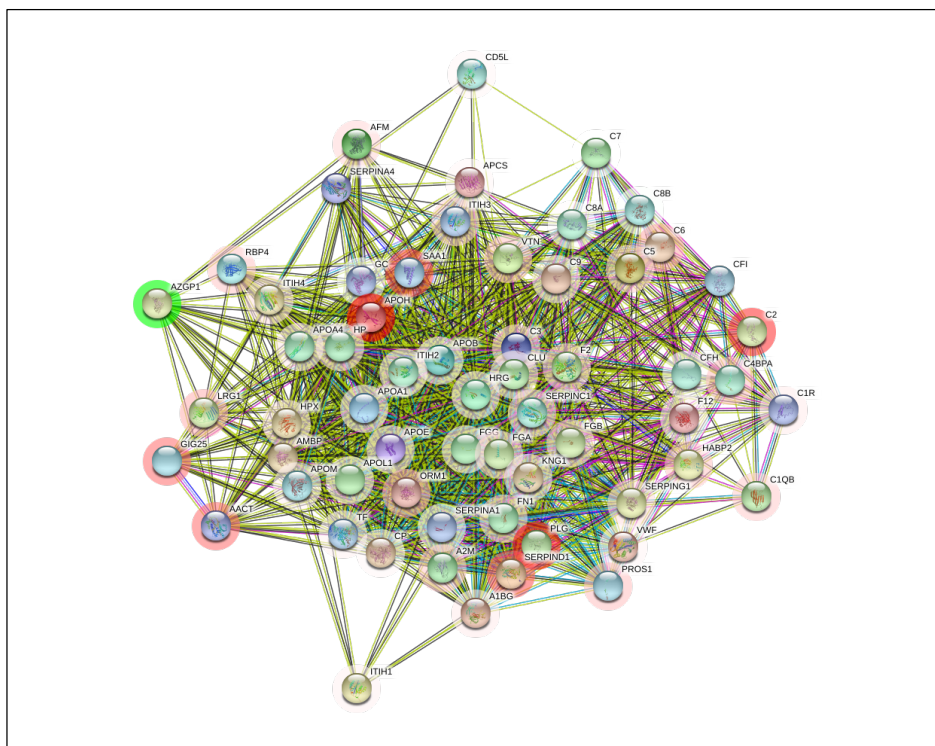


Figure S35. Interaction network of differentially abundant proteins from plasma 2-week post-injury, between AIS A and D. The coloured “halo” denotes fold change whereby green indicates that protein is less abundant and red that there is greater abundance. Edges represent protein-protein associations; these are known interactions from: curated databases and those that are experimentally determined. Predicted interactions from: gene co-occurrence; gene fusions; gene neighbourhood. Others are from gene co-expression; text-mining and protein homology.

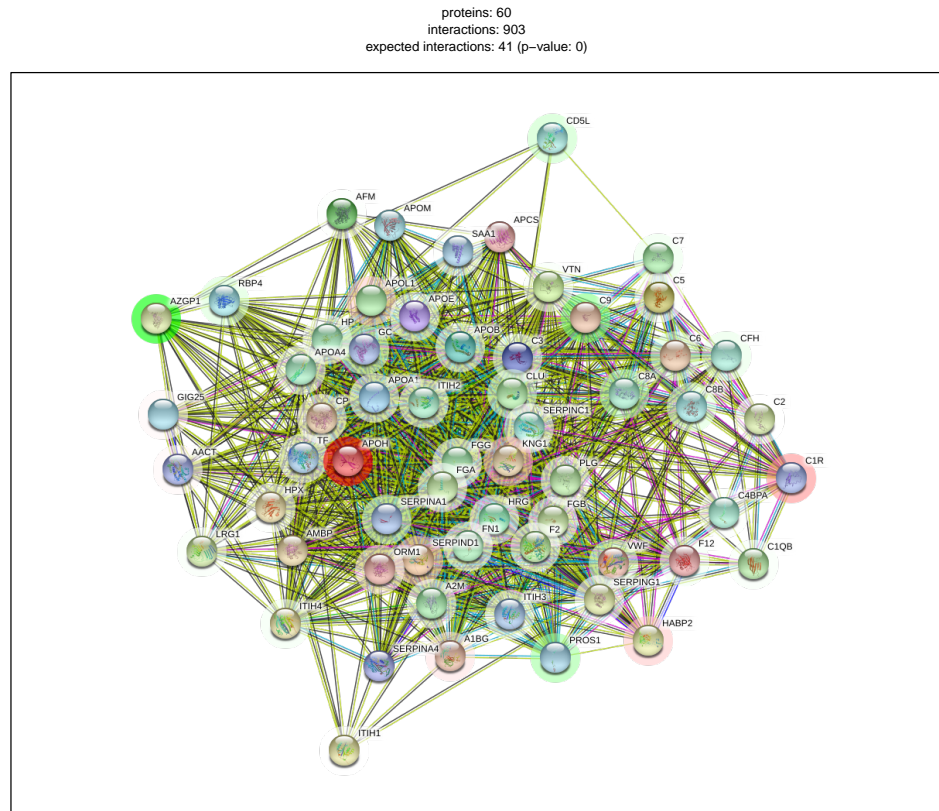


Figure S36. Interaction network of differentially abundant proteins from plasma 2-week post-injury, between AIS C improvers and D. The coloured “halo” denotes fold change whereby green indicates that protein is less abundant and red that there is greater abundance. Edges represent protein-protein associations; these are known interactions from: curated databases  and those that are experimentally determined . Predicted interactions from: gene co-occurrence ; gene fusions ; gene neighbourhood . Others are from gene co-expression ; text-mining  and protein homology .

proteins: 61
interactions: 925
expected interactions: 42 (p-value: 0)

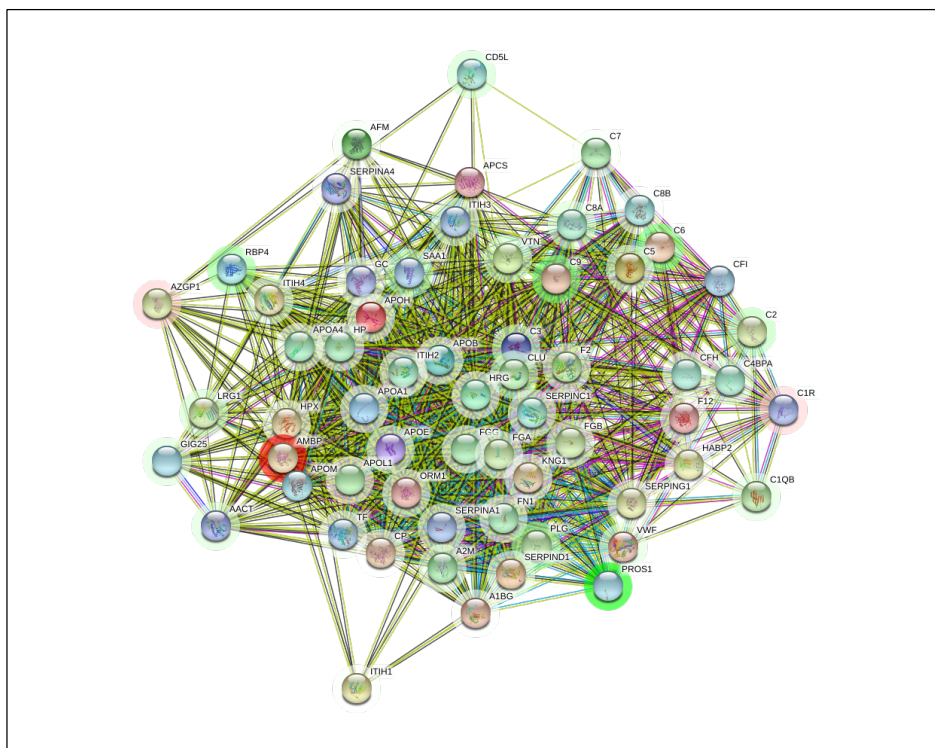


Figure S37. Interaction network of differentially abundant proteins from plasma 2-week post-injury, between AIS C improvers and A. The coloured “halo” denotes fold change whereby green indicates that protein is less abundant and red that there is greater abundance. Edges represent protein-protein associations; these are known interactions from: curated databases and those that are experimentally determined. Predicted interactions from: gene co-occurrence ; gene fusions ; gene neighbourhood . Others are from gene co-expression ; text-mining and protein homology .

proteins: 61
interactions: 925
expected interactions: 42 (p-value: 0)

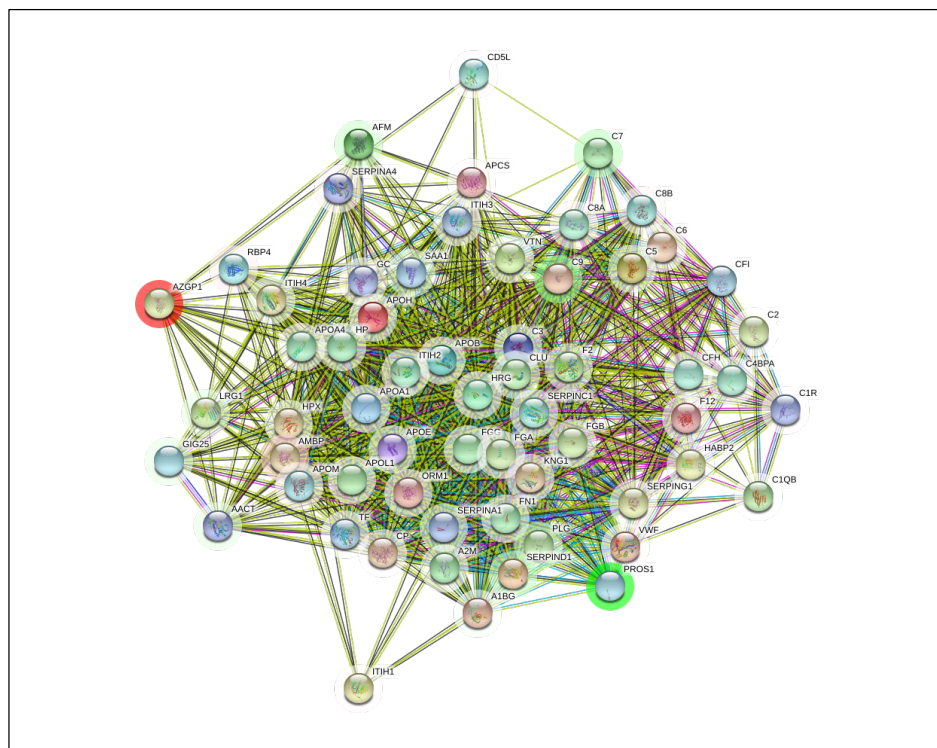


Figure S38. Interaction network of differentially abundant proteins from plasma 2-week post-injury, between AIS C non-improvers and A. The coloured “halo” denotes fold change whereby green indicates that protein is less abundant and red that there is greater abundance. Edges represent protein-protein associations; these are known interactions from: curated databases and those that are experimentally determined . Predicted interactions from: gene co-occurrence ; gene fusions ; gene neighbourhood . Others are from gene co-expression ; text-mining and protein homology .

proteins: 60
interactions: 903
expected interactions: 41 (p-value: 0)

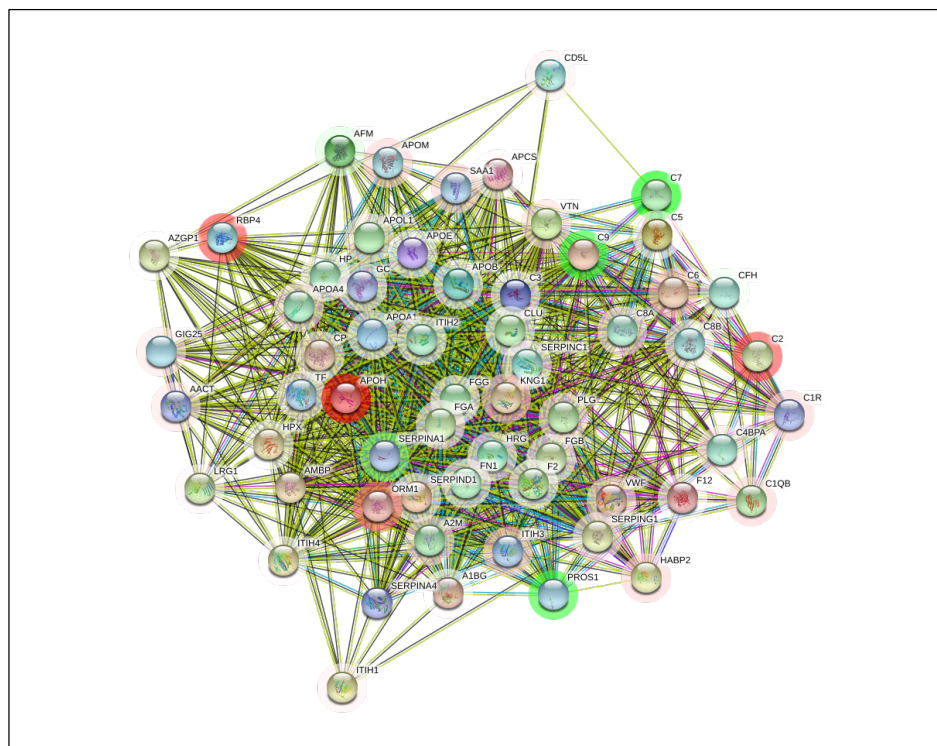


Figure S39. Interaction network of differentially abundant proteins from plasma 2-week post-injury, between AIS C non-improvers and D. The coloured “halo” denotes fold change whereby green indicates that protein is less abundant and red that there is greater abundance. Edges represent protein-protein associations; these are known interactions from: curated databases and those that are experimentally determined . Predicted interactions from: gene co-occurrence ; gene fusions ; gene neighbourhood . Others are from gene co-expression ; text-mining and protein homology .



Figure S40. The interaction network of differentially abundant proteins found in plasma 2-weeks post-injury, between AIS C patients who experienced an AIS grade conversion and those who did not. The coloured “halo” denotes fold change whereby green indicates that protein is less abundant and red indicates greater abundance. Edges represent protein-protein associations; these are known interactions from: curated databases and those that are experimentally determined. Predicted interactions from: gene co-occurrence; gene fusions; gene neighbourhood; others are from gene co-expression; text-mining and protein homology.

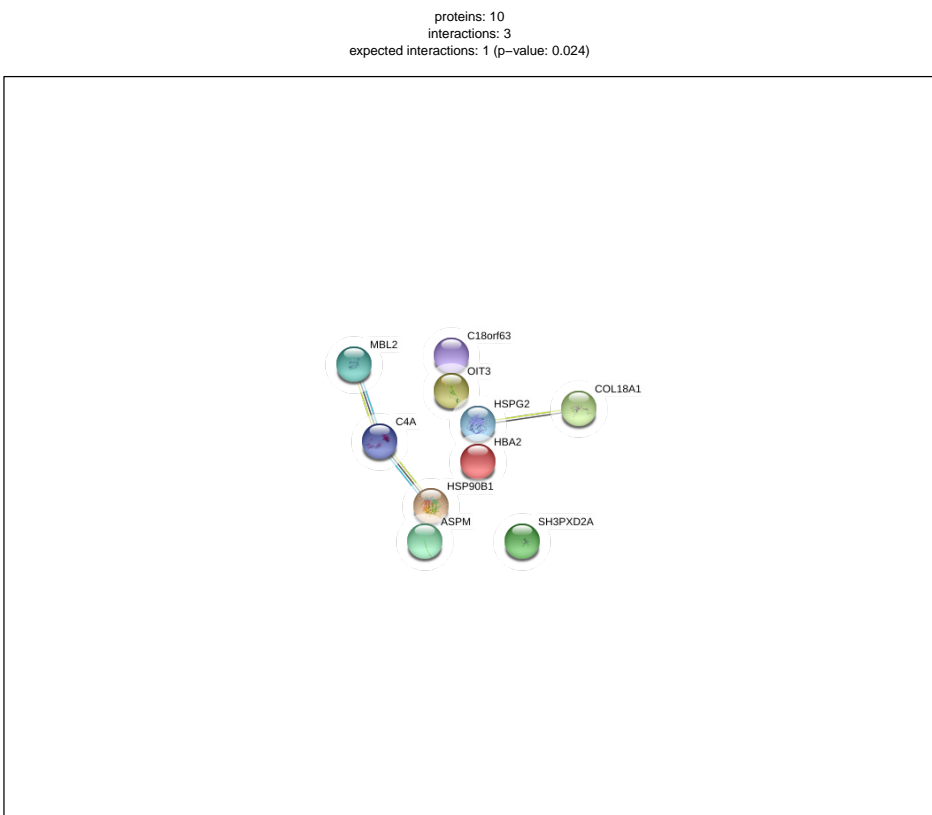


Figure S41. Interaction network of differentially abundant proteins from plasma 3-months post-injury, between AIS C patients who experienced an AIS grade conversion and those who did not. The coloured “halo” denotes fold change whereby green indicates that protein is less abundant and red that there is greater abundance. Edges represent protein-protein associations; these are known interactions from: curated databases and those that are experimentally determined. Predicted interactions from: gene co-occurrence; gene fusions; gene neighbourhood. Others are from gene co-expression; text-mining and protein homology.

proteins: 23
interactions: 40
expected interactions: 3 (p-value: 0)

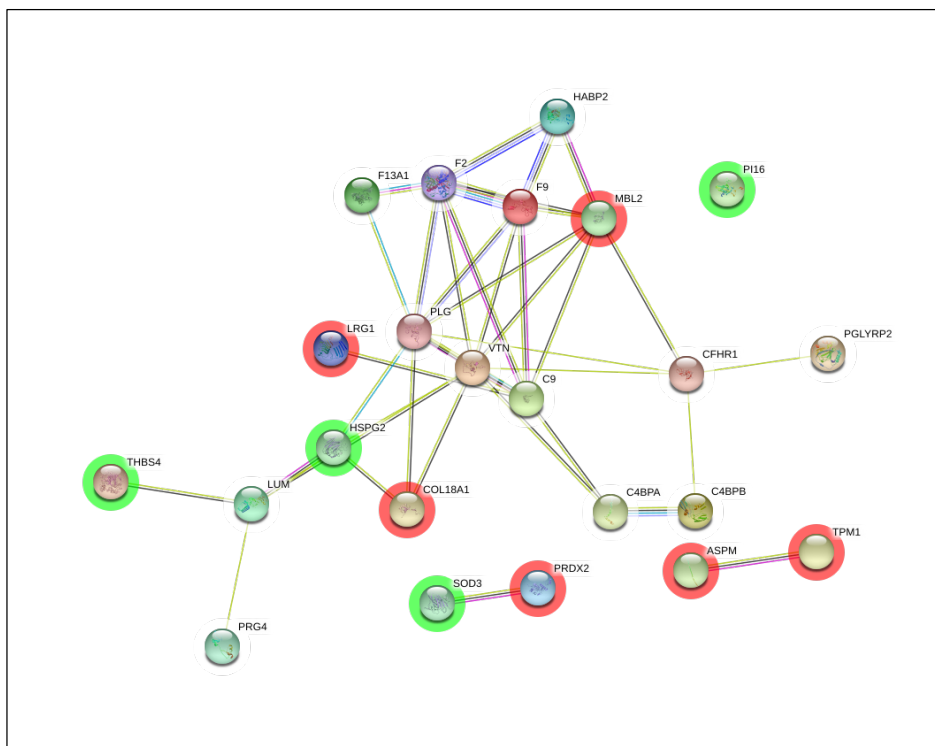


Figure S42. Interaction network of differentially abundant proteins from plasma 2-weeks and 3-months post-injury for AIS C patients who experienced an AIS grade conversion. The coloured "halo" denotes fold change whereby green indicates that protein is less abundant and red that there is greater abundance. Edges represent protein-protein associations; these are known interactions from: curated databases and those that are experimentally determined. Predicted interactions from: gene co-occurrence ; gene fusions ; gene neighbourhood . Others are from gene co-expression ; text-mining and protein homology .

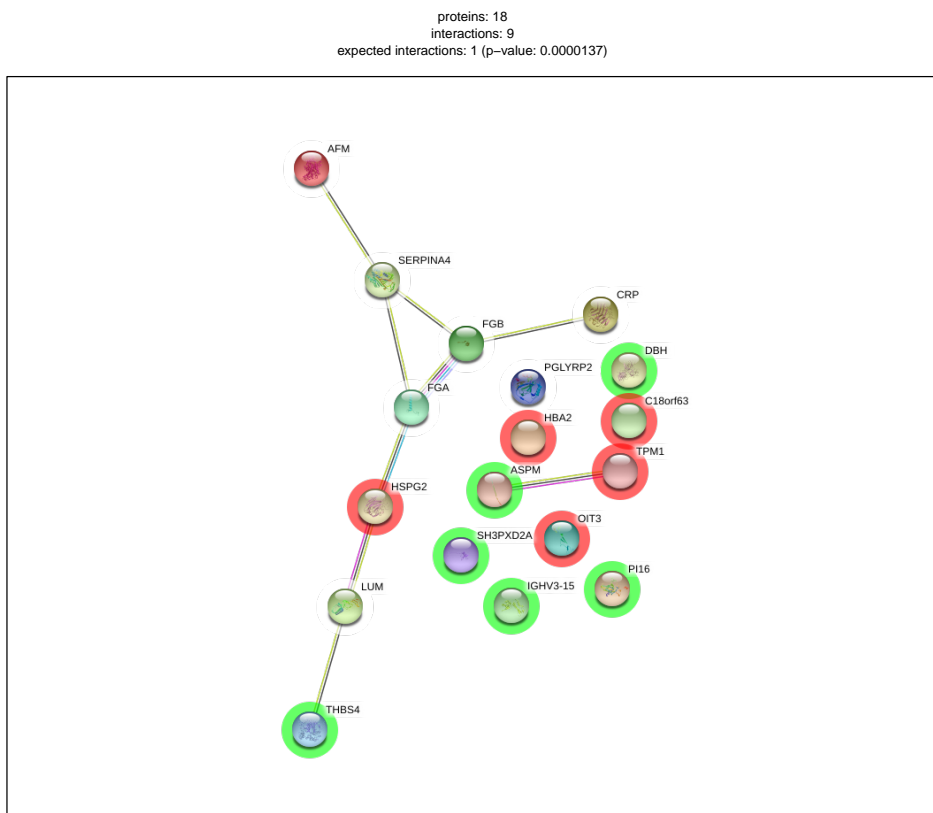


Figure S43. Interaction network of differentially abundant proteins from plasma 2-weeks and 3-months post-injury for AIS C patients who did not experience an AIS grade conversion. The coloured “halo” denotes fold change whereby green indicates that protein is less abundant and red that there is greater abundance. Edges represent protein-protein associations; these are known interactions from: curated databases and those that are experimentally determined. Predicted interactions from: gene co-occurrence; gene fusions; gene neighbourhood. Others are from gene co-expression; text-mining and protein homology.

proteins: 20
interactions: 15
expected interactions: 3 (p-value: 0.00000243)

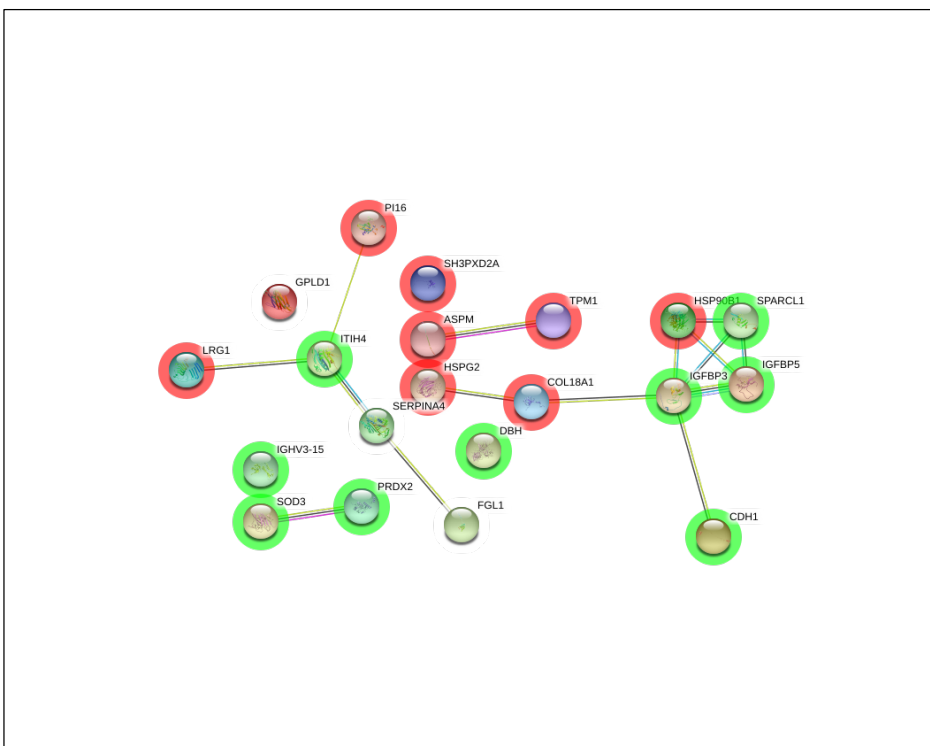


Figure S44. Interaction network of differentially abundant proteins from plasma 2-week post-injury, between AIS A and D. The coloured “halo” denotes fold change whereby green indicates that protein is less abundant and red that there is greater abundance. Edges represent protein-protein associations; these are known interactions from: curated databases and those that are experimentally determined. Predicted interactions from: gene co-occurrence; gene fusions; gene neighbourhood. Others are from gene co-expression; text-mining and protein homology.



Figure S45. Interaction network of differentially abundant proteins from plasma 2-week post-injury, between AIS C improvers and D. The coloured “halo” denotes fold change whereby green indicates that protein is less abundant and red that there is greater abundance. Edges represent protein-protein associations; these are known interactions from: curated databases and those that are experimentally determined. Predicted interactions from: gene co-occurrence ; gene fusions ; gene neighbourhood . Others are from gene co-expression ; text-mining and protein homology .

proteins: 21
interactions: 21
expected interactions: 2 (p-value: 1.64e-13)

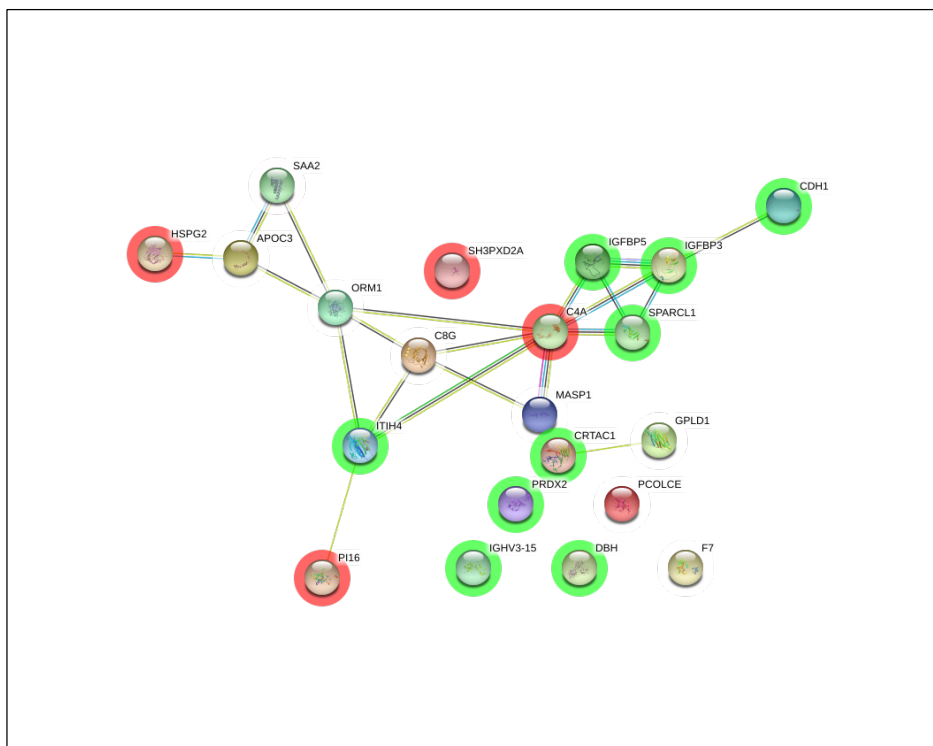


Figure S46. Interaction network of differentially abundant proteins from plasma 2-week post-injury, between AIS C improvers and A. The coloured “halo” denotes fold change whereby green indicates that protein is less abundant and red that there is greater abundance. Edges represent protein-protein associations; these are known interactions from: curated databases and those that are experimentally determined. Predicted interactions from: gene co-occurrence ; gene fusions ; gene neighbourhood . Others are from gene co-expression ; text-mining and protein homology .

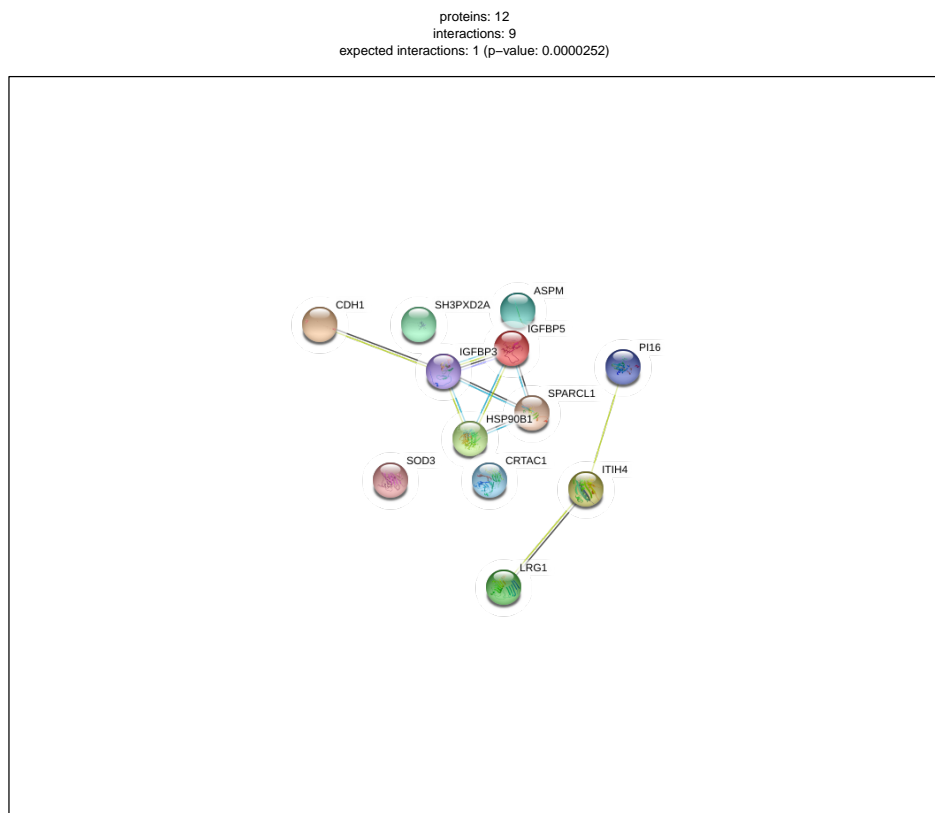


Figure S47. Interaction network of differentially abundant proteins from plasma 2-week post-injury, between AIS C non-improvers and A. The coloured “halo” denotes fold change whereby green indicates that protein is less abundant and red that there is greater abundance. Edges represent protein-protein associations; these are known interactions from: curated databases and those that are experimentally determined. Predicted interactions from: gene co-occurrence ; gene fusions ; gene neighbourhood . Others are from gene co-expression ; text-mining and protein homology .

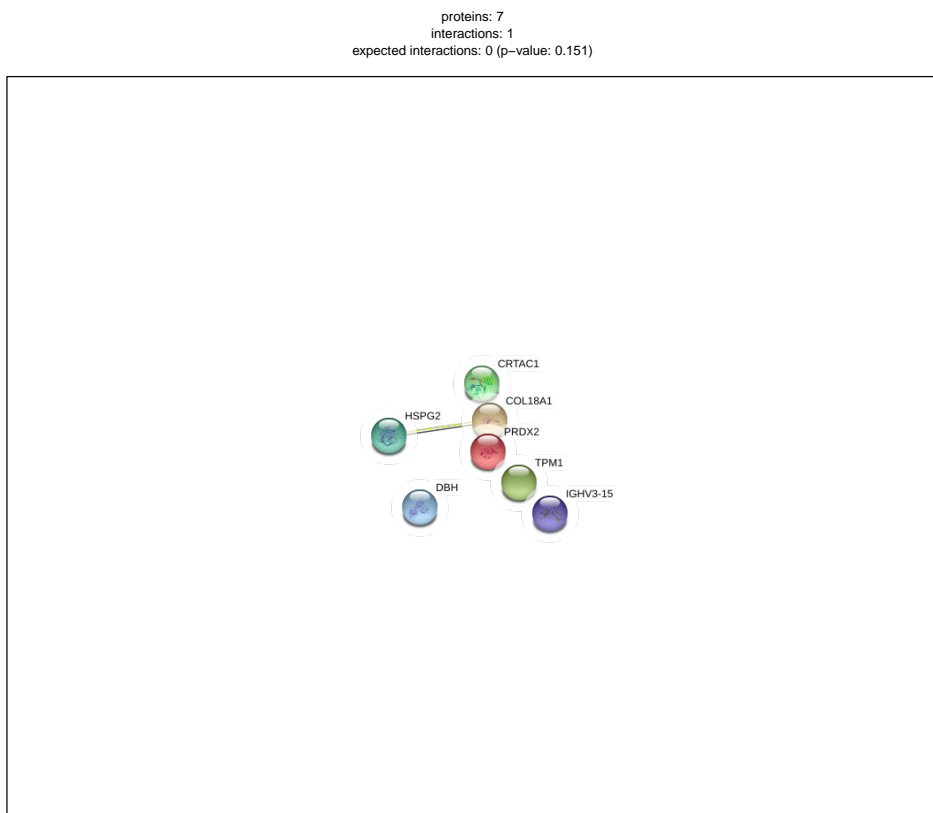


Figure S48. Interaction network of differentially abundant proteins from plasma 2-week post-injury, between AIS C non-improvers and D. The coloured “halo” denotes fold change whereby green indicates that protein is less abundant and red that there is greater abundance. Edges represent protein-protein associations; these are known interactions from: curated databases and those that are experimentally determined . Predicted interactions from: gene co-occurrence ; gene fusions ; gene neighbourhood . Others are from gene co-expression ; text-mining and protein homology .

Acute C Improvers Vs Acute C Non-Improvers

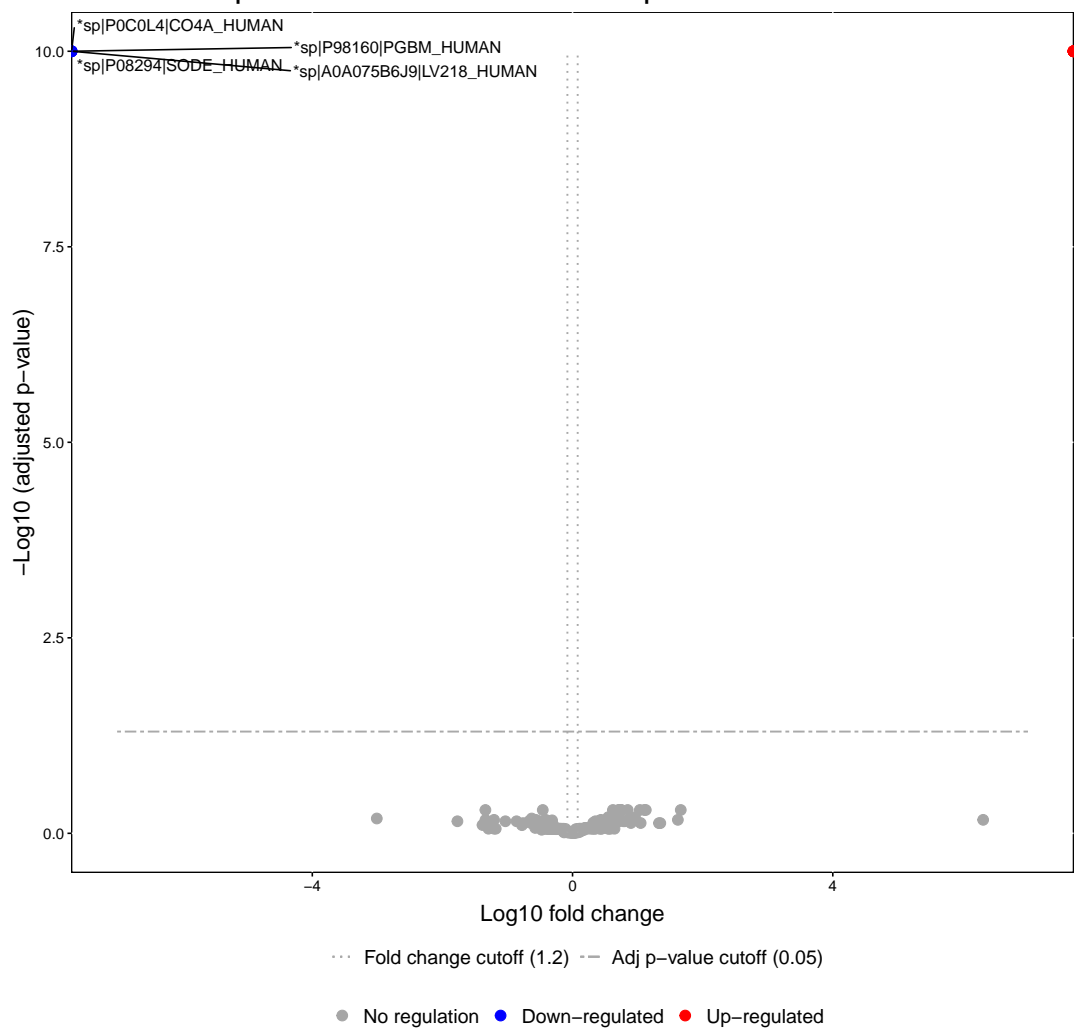


Figure S49. Volcano plot of \log_{10} fold change and \log_{10} adjusted p-value for plasma proteins from 2-weeks post-injury between AIS C patients who experienced an AIS grade conversion and those who did not. Proteins with a fold changes beyond >1.2 and an adjusted p-value less than 0.05 are labelled.

Subacute C Improvers Vs Subacute C Non-Improvers

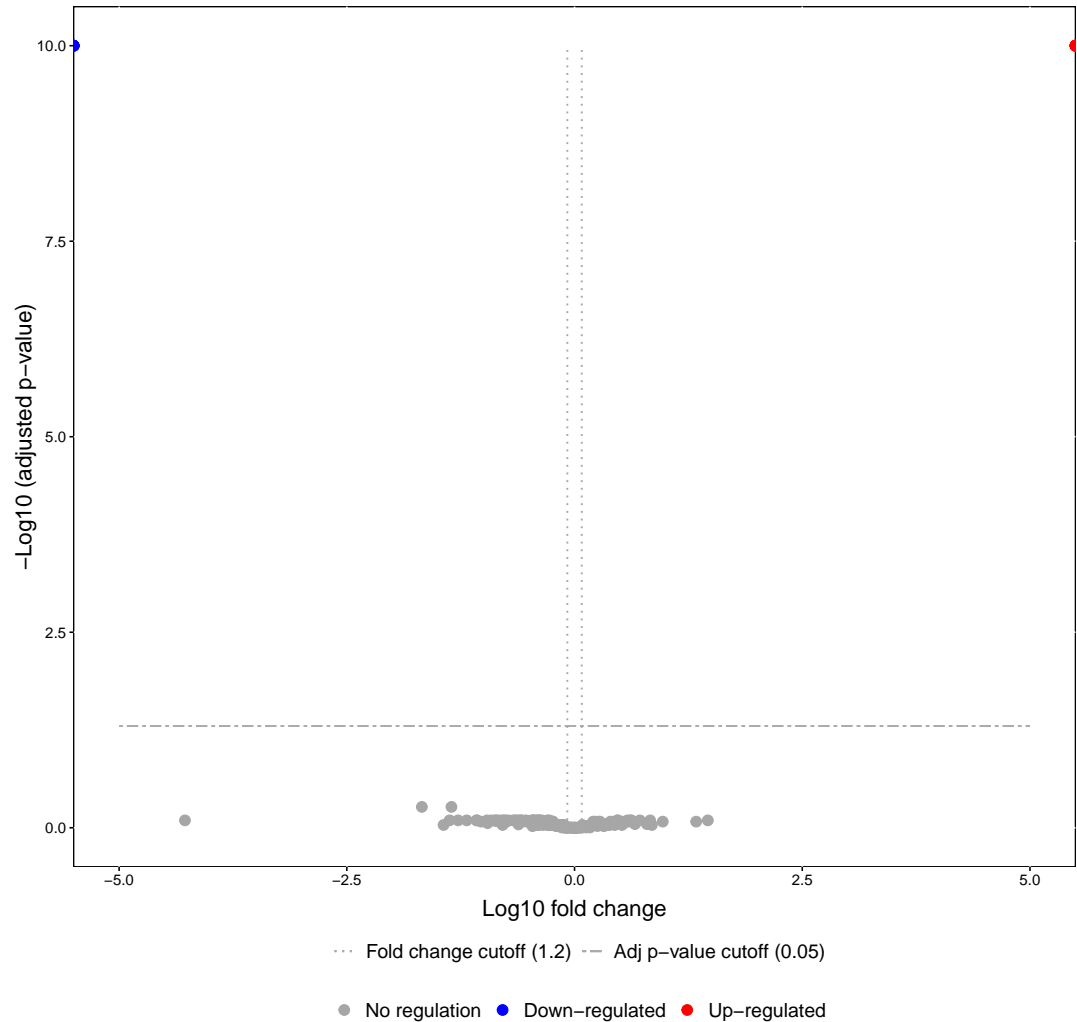


Figure S50. Volcano plot of \log_{10} fold change and \log_{10} adjusted p-value for plasma proteins from 3-months post-injury between AIS C patients who experienced an AIS grade conversion and those who did not. Proteins with a fold changes beyond ± 1.2 and an adjusted p-value less than 0.05 are labelled.

Acute C Improvers Vs Subacute C Improvers

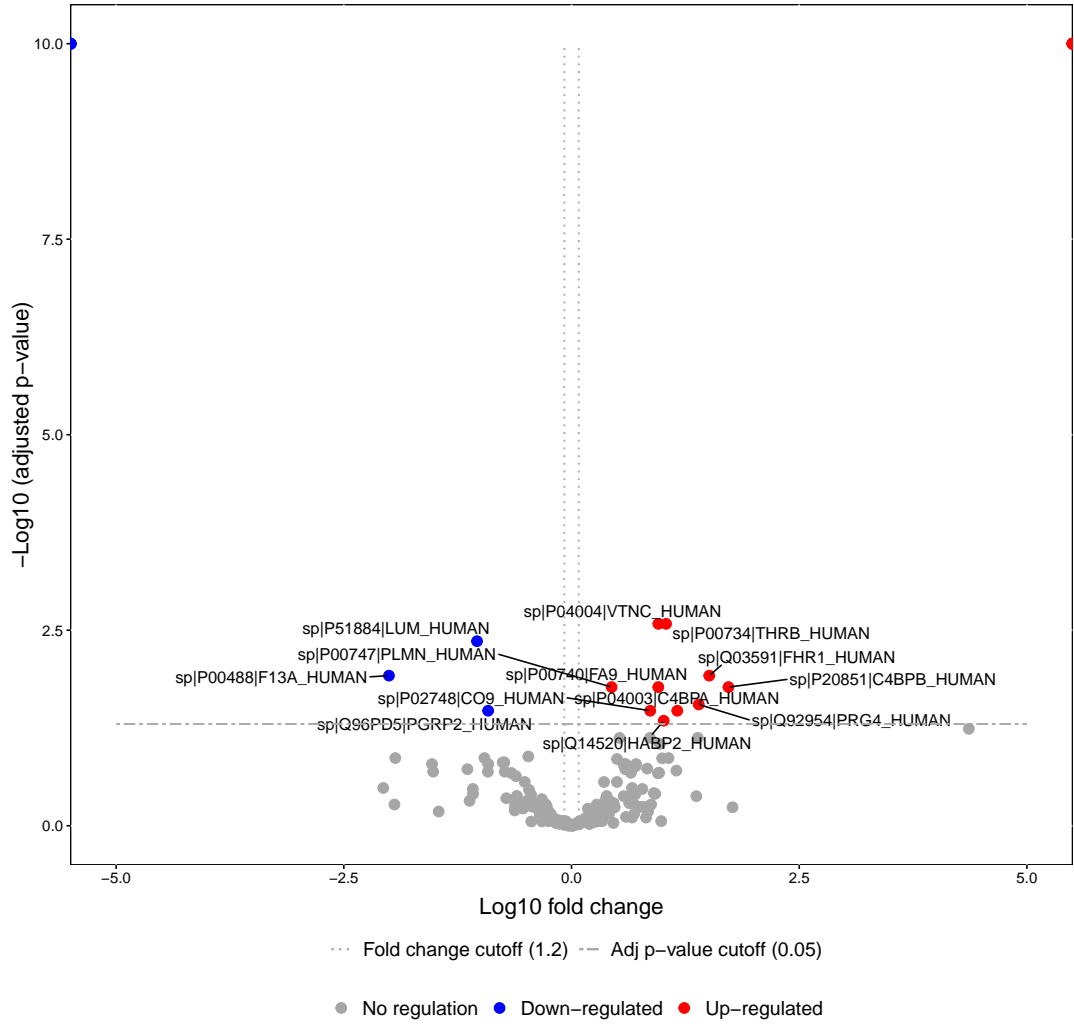


Figure S51. Volcano plot of \log_{10} fold change and \log_{10} adjusted p-value for plasma proteins from 2-weeks and 3-months post-injury from AIS C patients who experienced an AIS grade conversion. Proteins with a fold changes beyond 1.2 and an adjusted p-value less than 0.05 are labelled.

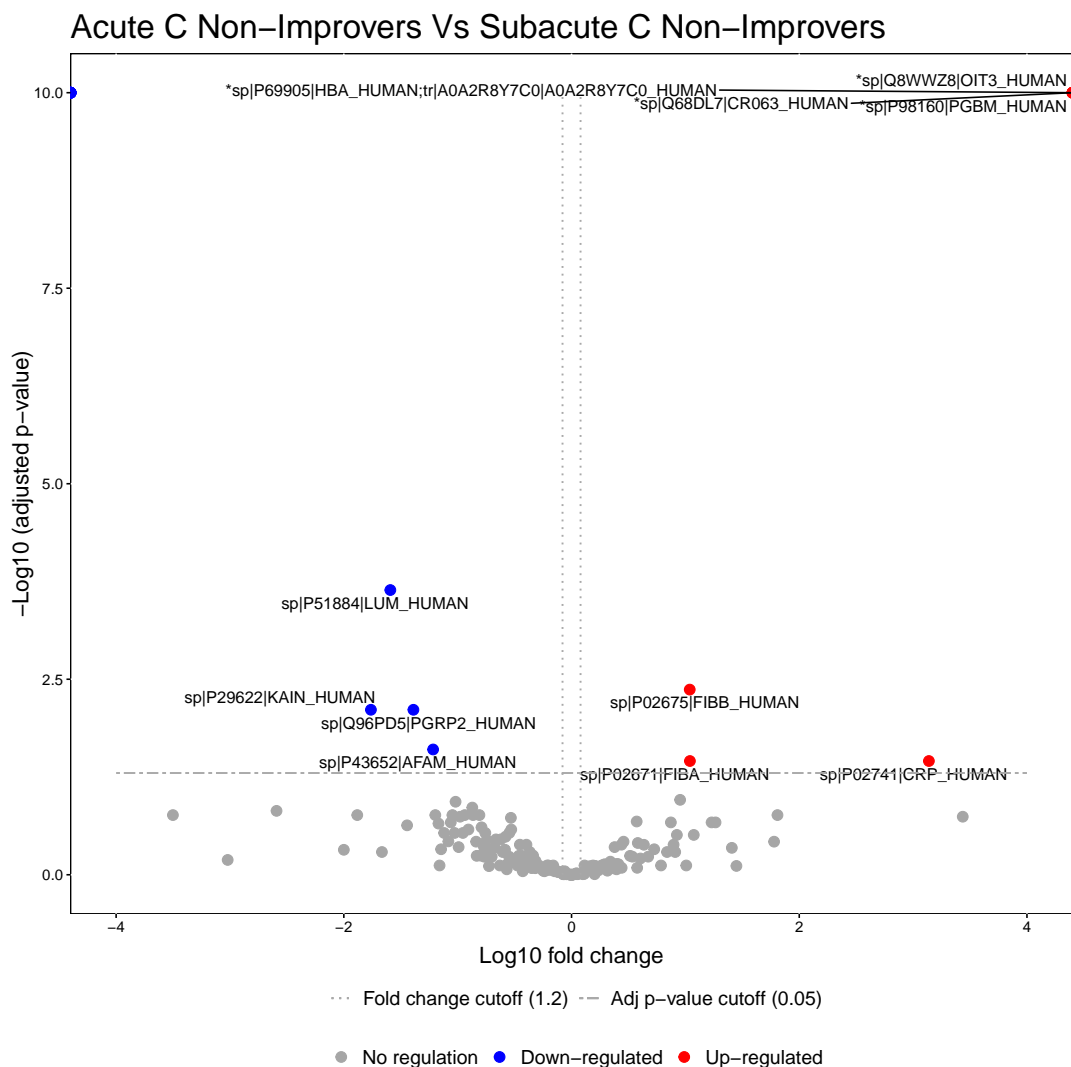


Figure S52. Volcano plot of \log_{10} fold change and \log_{10} adjusted p-value for plasma proteins from 2-weeks and 3-months post-injury from AIS C patients who did not experience an AIS grade conversion. Proteins with a fold changes beyond >1.2 and an adjusted p-value less than 0.05 are labelled.

Acute A Vs Acute D

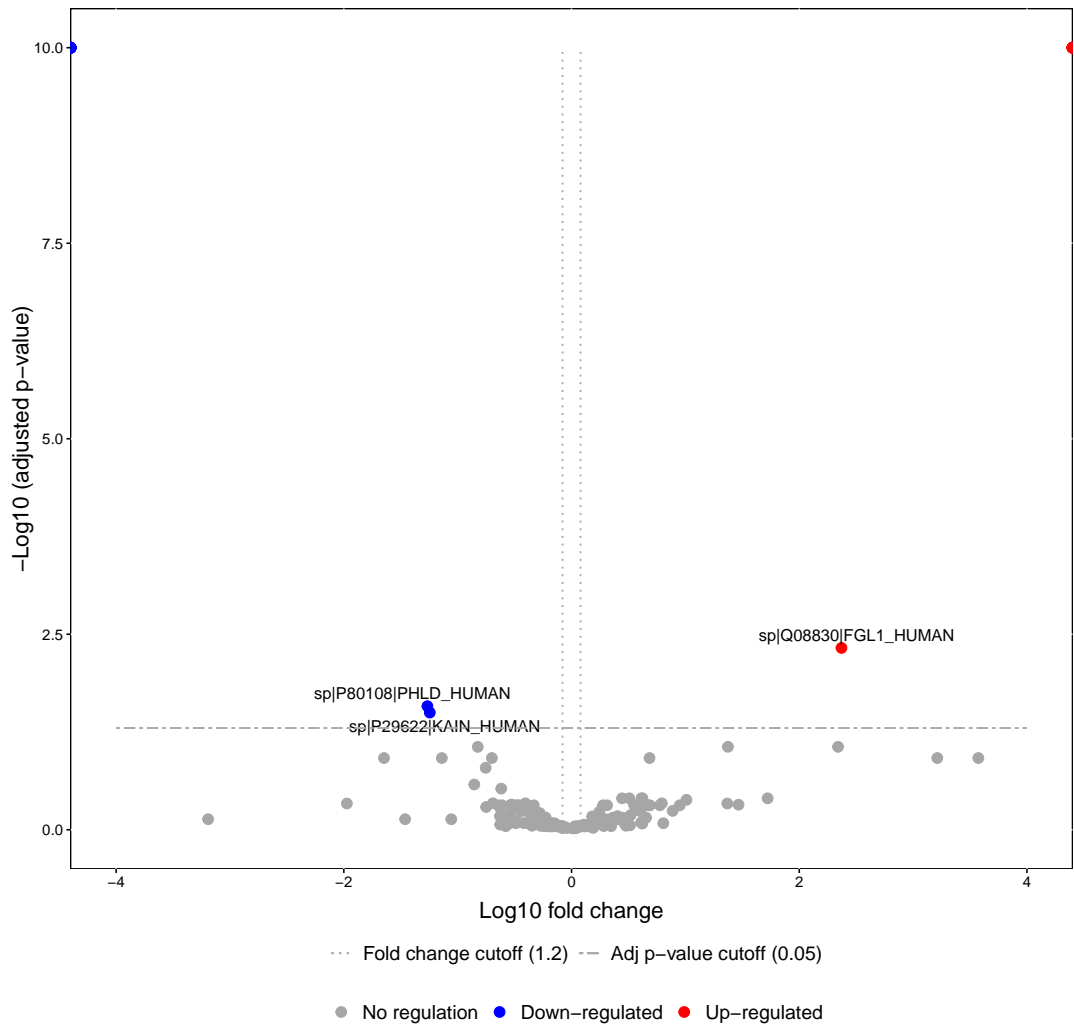


Figure S53. Volcano plot of \log_{10} fold change and \log_{10} adjusted p-value for plasma proteins from 2-weeks post-injury between AIS A and AIS D patients. Proteins with a fold changes beyond 1.2 and an adjusted p-value less than 0.05 are labelled.

Acute A Vs Subacute A

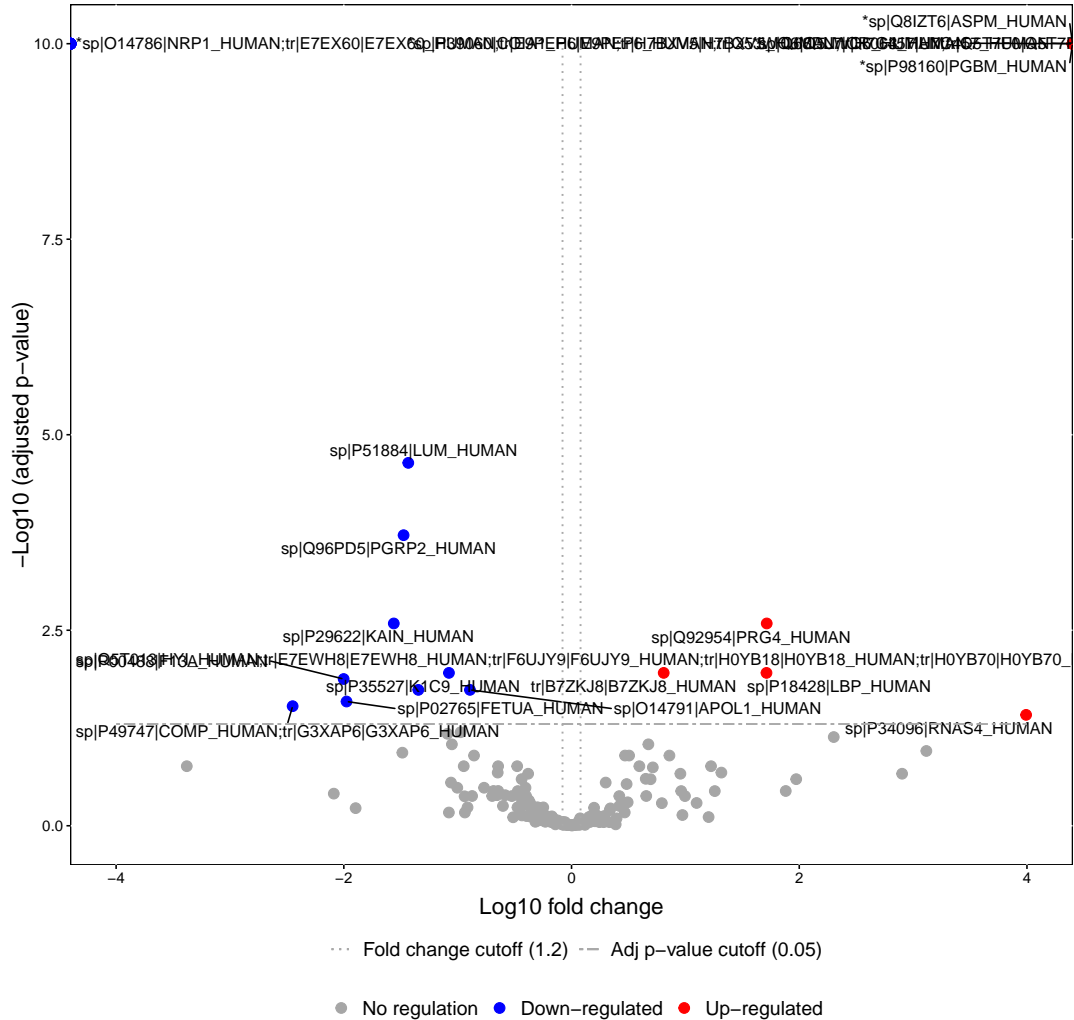


Figure S54. Volcano plot of \log_{10} fold change and \log_{10} adjusted p-value for plasma proteins from 2-weeks and 3-months post-injury from AIS A patients. Proteins with a fold changes beyond >1.2 and an adjusted p-value less than 0.05 are labelled.

Acute D Vs Subacute D

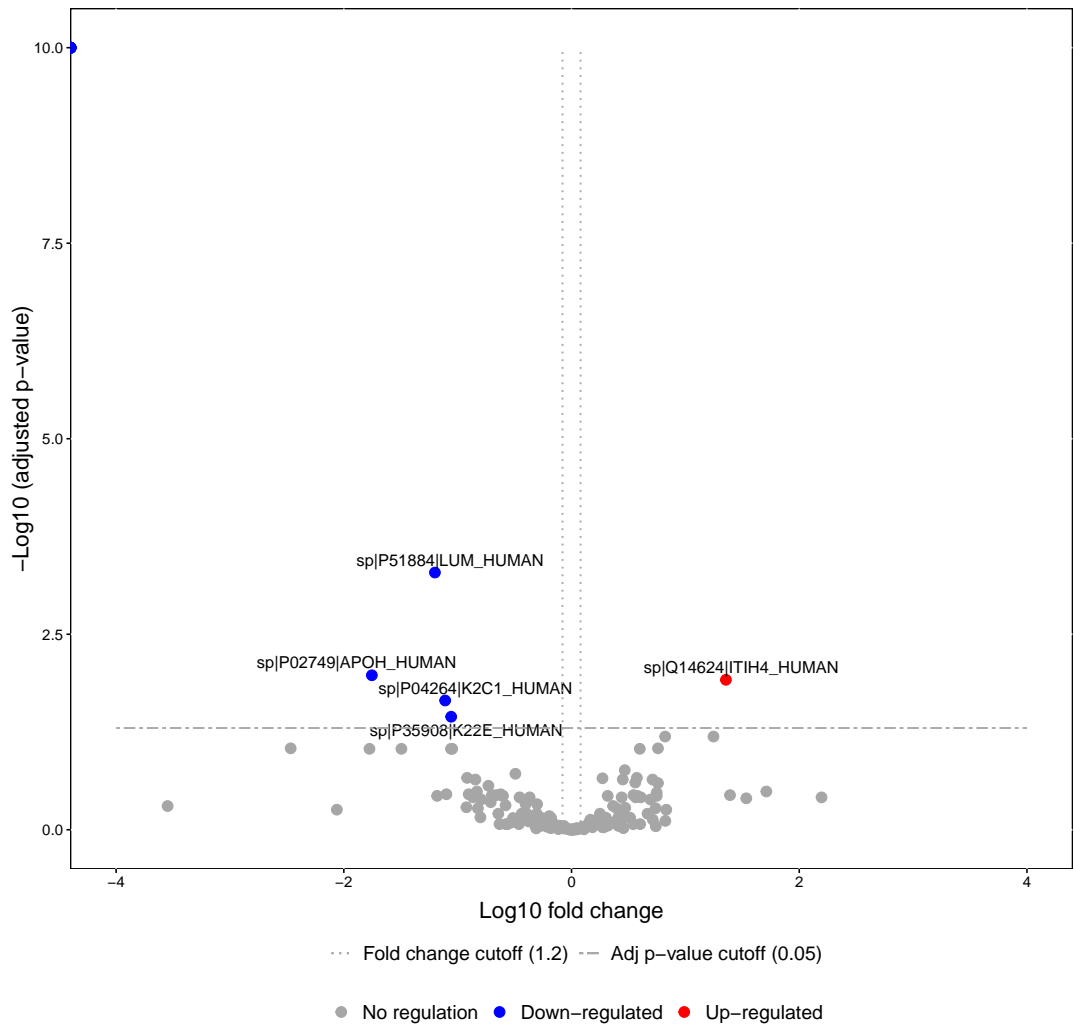


Figure S55. Volcano plot of \log_{10} fold change and \log_{10} adjusted p-value for plasma proteins from 2-weeks and 3-months post-injury from AIS D patients. Proteins with a fold changes beyond >1.2 and an adjusted p-value less than 0.05 are labelled.

Acute C Improvers Vs Acute D

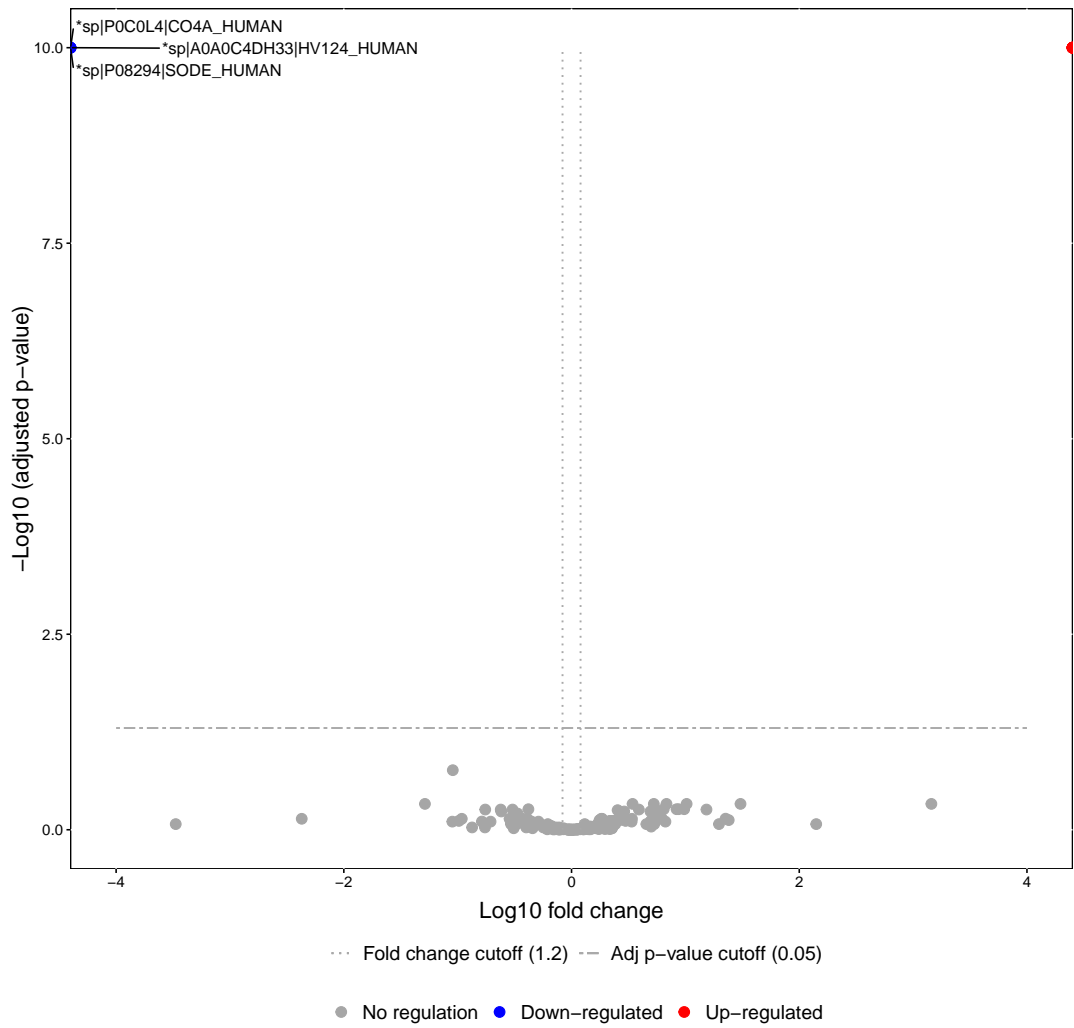


Figure S56. Volcano plot of \log_{10} fold change and \log_{10} adjusted p-value for plasma proteins from 2-weeks post-injury between AIS C patients who experienced an AIS grade conversion and AIS D patients. Proteins with a fold changes beyond ,1.2 and an adjusted p-value less than 0.05 are labelled.

Acute A Vs Acute C Improvers

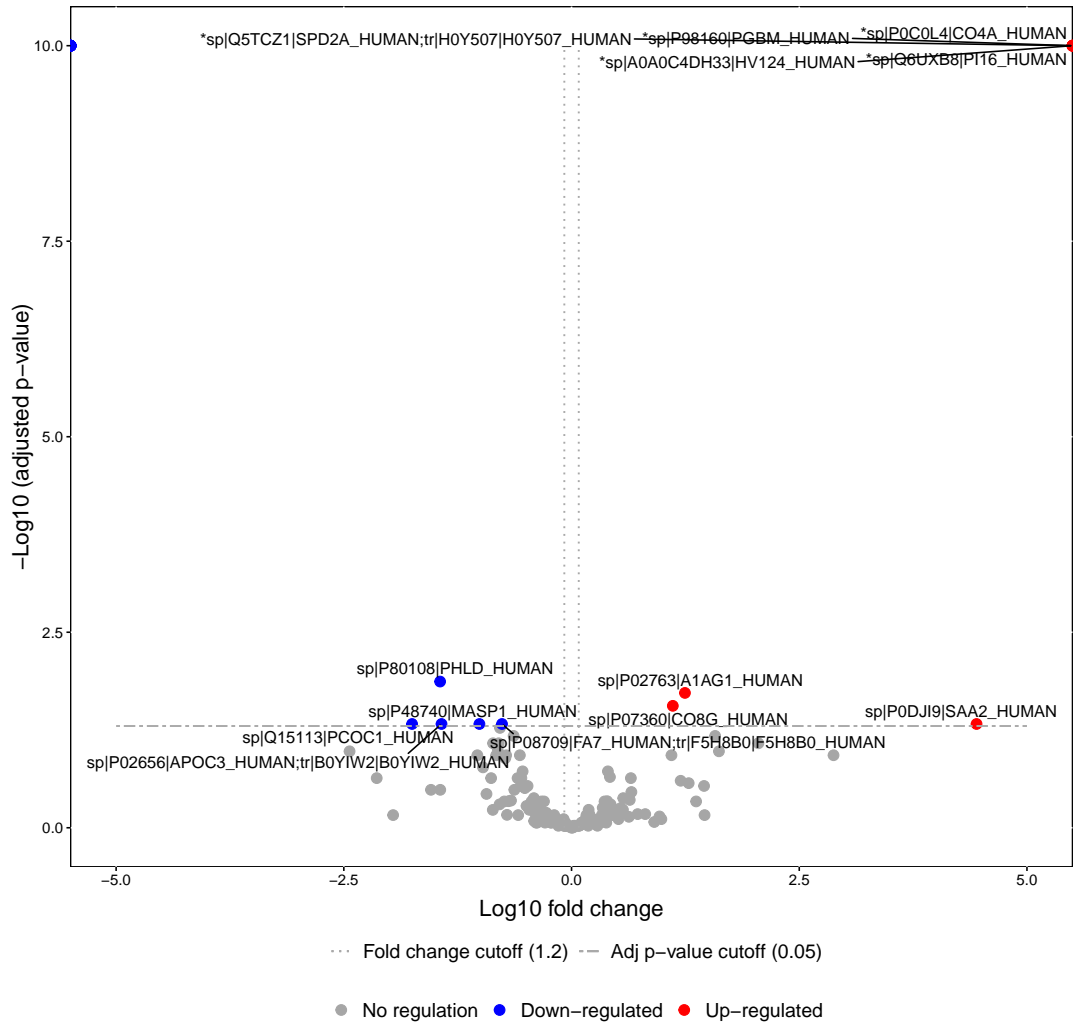


Figure S57. Volcano plot of \log_{10} fold change and \log_{10} adjusted p-value for plasma proteins from 2-weeks post-injury between AIS A patients and AIS C patients who experienced an AIS grade conversion. Proteins with a fold changes beyond 1.2 and an adjusted p-value less than 0.05 are labelled.

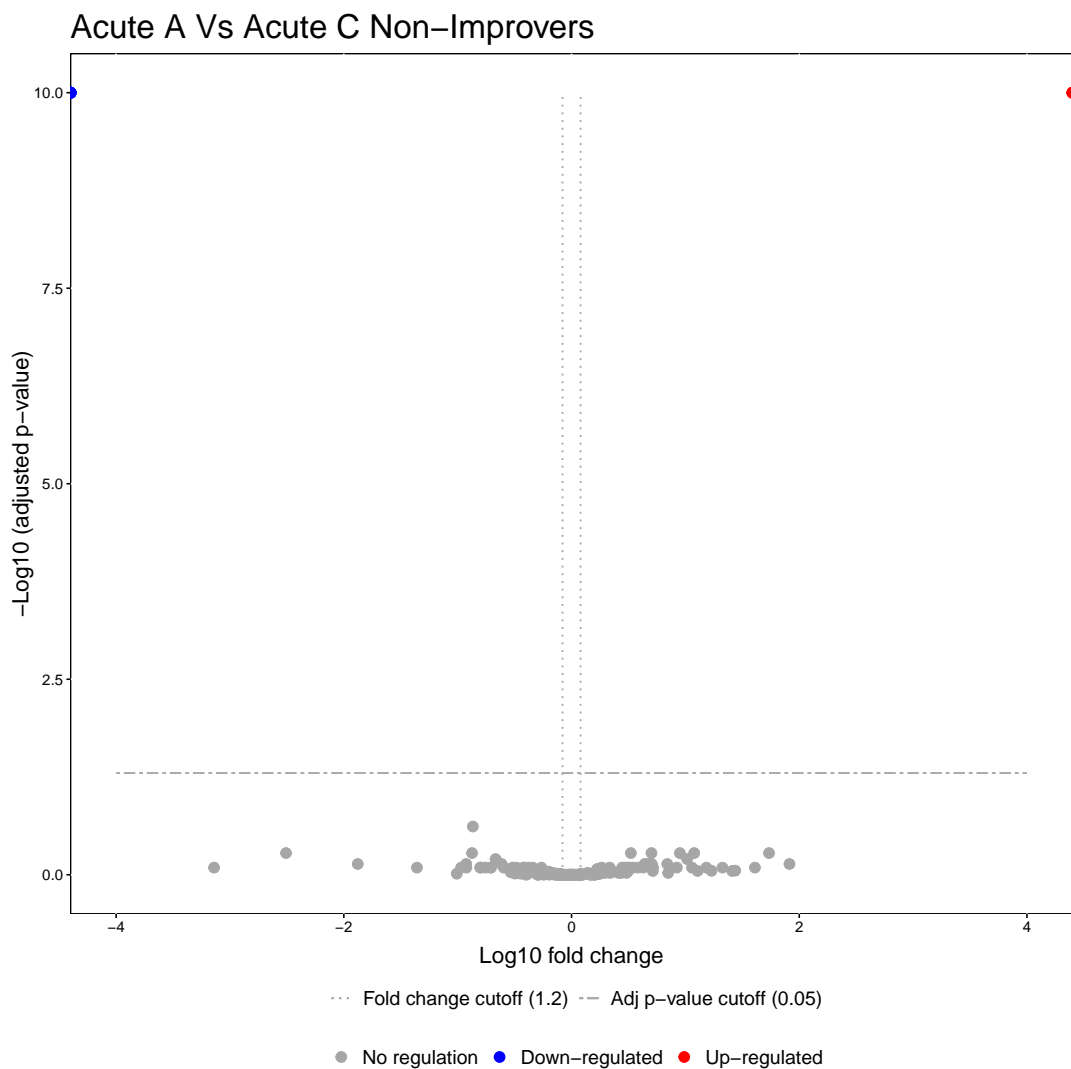


Figure S58. Volcano plot of \log_{10} fold change and \log_{10} adjusted p-value for plasma proteins from 2-weeks post-injury between AIS A patients and AIS C patients who did not experience an AIS grade conversion. Proteins with a fold changes beyond >1.2 and an adjusted p-value less than 0.05 are labelled.

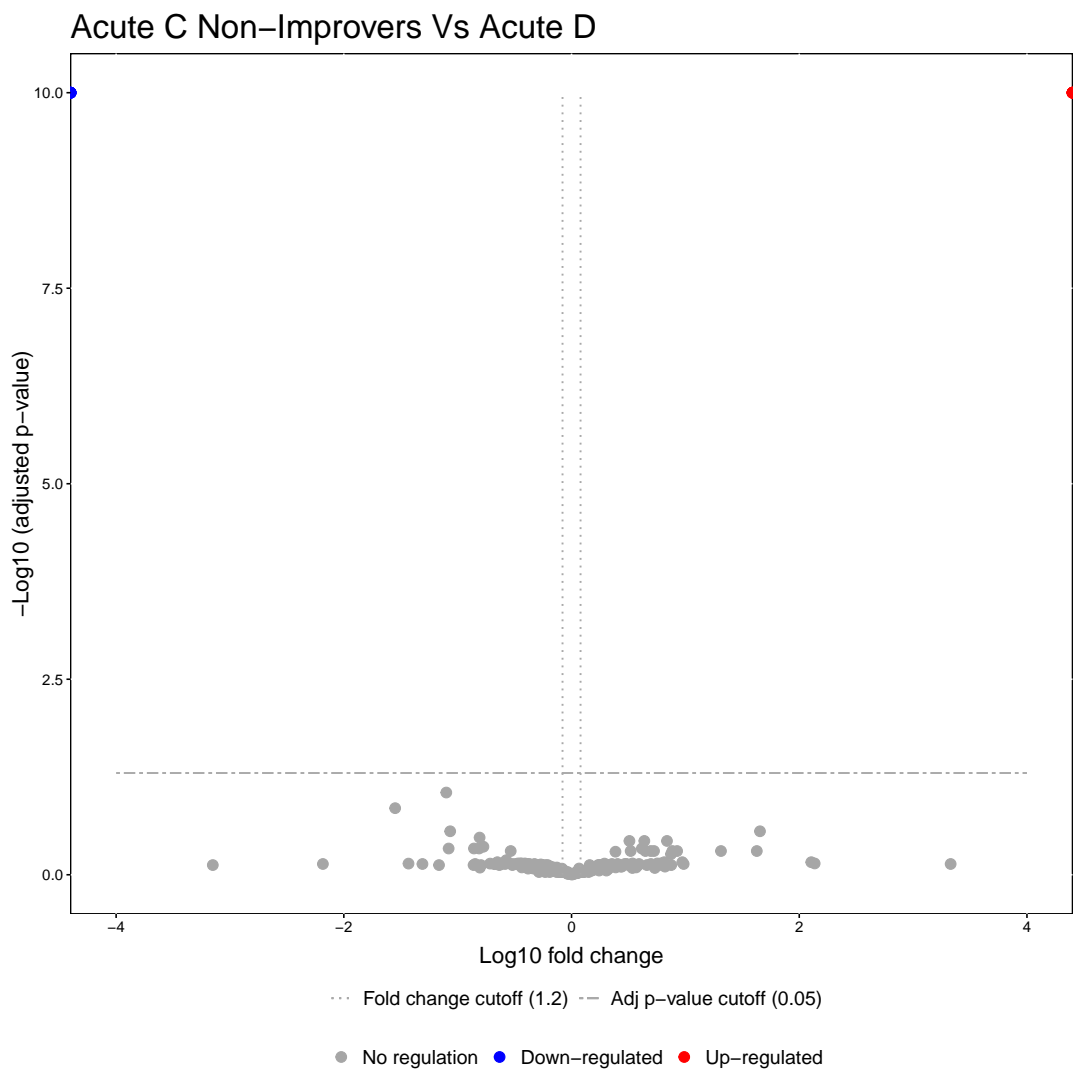


Figure S59. Volcano plot of log₁₀ fold change and log₁₀ adjusted p-value for plasma proteins from 2-weeks post-injury between AIS C patients who did not experience an AIS grade conversion and AIS D patients. Proteins with a fold changes beyond ,1.2 and an adjusted p-value less than 0.05 are labelled.

560 References

- 561 Anthony, Daniel C., and Yvonne Couch. 2014. "The Systemic Response to CNS Injury." *Experimental*
 562 *Neurology*, Special Issue: Neuroimmunology of spinal cord injury, 258 (August): 105–11. <https://doi.org/10.1016/j.expneurol.2014.03.013>.
- 563 Balmer, James E., and Rune Blomhoff. 2002. "Gene Expression Regulation by Retinoic Acid." *Journal*
 564 *of Lipid Research* 43 (11): 1773–1808. <https://doi.org/10.1194/jlr.R100015-JLR200>.
- 565 Bao, Feng, Vanessa Omana, Arthur Brown, and Lynne C. Weaver. 2012. "The Systemic Inflam-
 566 matory Response After Spinal Cord Injury in the Rat Is Decreased by a4B1 Integrin Blockade." *Journal*
 567 *of Neurotrauma* 29 (8): 1626–37. <https://doi.org/10.1089/neu.2011.2190>.
- 568 Bernardo Harrington, Gabriel Mateus, Paul Cool, Charlotte Hulme, Aheed Osman, Joy Chowdhury,
 569 Naveen Kumar, Srinivasa Budithi, and Karina Wright. 2020. "Routinely Measured Haematologi-
 570 cal Markers Can Help to Predict AIS Scores Following Spinal Cord Injury." *Journal of Neurotrauma*,
 571 July. <https://doi.org/10.1089/neu.2020.7144>.
- 572 Boschetti, Egisto, and Pier Giorgio Righetti. 2008. "The ProteoMiner in the Proteomic Arena: A

- 574 Non-Depleting Tool for Discovering Low-Abundance Species." *Journal of Proteomics*, Proteomic
575 Technologies, 71 (3): 255–64. <https://doi.org/10.1016/j.jprot.2008.05.002>.
- 576 Brown, Sharon J., Gabriel M. B. Harrington, Charlotte H. Hulme, Rachel Morris, Anna Bennett, Wai-
577 Hung Tsang, Aheed Osman, Joy Chowdhury, Naveen Kumar, and Karina T. Wright. 2019. "A
578 Preliminary Cohort Study Assessing Routine Blood Analyte Levels and Neurological Outcome
579 After Spinal Cord Injury." *Journal of Neurotrauma*, July. <https://doi.org/10.1089/neu.2019.6495>.
- 580 Campbell, Sandra J., Daniel C. Anthony, Fiona Oakley, Harald Carlsen, Ahmed M. Elsharkawy, Rune
581 Blomhoff, and Derek A. Mann. 2008. "Hepatic Nuclear Factor kB Regulates Neutrophil Recruit-
582 ment to the Injured Brain." *Journal of Neuropathology & Experimental Neurology* 67 (3): 223–30.
583 <https://doi.org/10.1097/NEN.0b013e3181654957>.
- 584 Campbell, Sandra J., V. Hugh Perry, Fernando J. Pitossi, Angus G. Butchart, Mariela Chertoff, Sara
585 Waters, Robert Dempster, and Daniel C. Anthony. 2005. "Central Nervous System Injury Trig-
586 gers Hepatic CC and CXC Chemokine Expression That Is Associated with Leukocyte Mobilization
587 and Recruitment to Both the Central Nervous System and the Liver." *The American Journal of
588 Pathology* 166 (5): 1487–97. [https://doi.org/10.1016/S0002-9440\(10\)62365-6](https://doi.org/10.1016/S0002-9440(10)62365-6).
- 589 Campbell, Sandra J., Imran Zahid, Patrick Losey, Shing Law, Yanyan Jiang, Mehmet Bilgen, Nico van
590 Rooijen, Damineh Morsali, Andrew E. M. Davis, and Daniel C. Anthony. 2008. "Liver Kupffer Cells
591 Control the Magnitude of the Inflammatory Response in the Injured Brain and Spinal Cord." *Neuropharmacology* 55 (5): 780–87. <https://doi.org/10.1016/j.neuropharm.2008.06.074>.
- 592 Chambers, Matthew C., Brendan Maclean, Robert Burke, Dario Amodei, Daniel L. Ruderman, Stef-
593 fen Neumann, Laurent Gatto, et al. 2012. "A Cross-Platform Toolkit for Mass Spectrometry and
594 Proteomics." *Nature Biotechnology* 30 (10): 918–20. <https://doi.org/10.1038/nbt.2377>.
- 595 Choi, Meena, Ching-Yun Chang, Timothy Clough, Daniel Brody, Trevor Killeen, Brendan MacLean,
596 and Olga Vitek. 2014. "MSstats: An R Package for Statistical Analysis of Quantitative Mass
597 Spectrometry-Based Proteomic Experiments." *Bioinformatics* 30 (17): 2524–26. <https://doi.org/10.1093/bioinformatics/btu305>.
- 598 Chow, Diana S. L., Yang Teng, Elizabeth G. Toups, Bizhan Aarabi, James S. Harrop, Christopher I.
599 Shaffrey, Michele M. Johnson, et al. 2012. "Pharmacology of Riluzole in Acute Spinal Cord Injury."
600 *Journal of Neurosurgery: Spine* 17 (Suppl1): 129–40. <https://doi.org/10.3171/2012.5.AOSPINE12>
601 112.
- 602 Colbert, Melissa C., William W. Rubin, Elwood Linney, and Anthony-Samuel LaMantia. 1995.
603 "Retinoid signaling and the generation of regional and cellular diversity in the embryonic mouse
604 spinal cord." *Developmental Dynamics* 204 (1): 1–12. <https://doi.org/10.1002/aja.1002040102>.
- 605 Crispe, Ian N. 2016. "Hepatocytes as Immunological Agents." *The Journal of Immunology* 196 (1):
606 17–21. <https://doi.org/10.4049/jimmunol.1501668>.
- 607 Crozier-Shaw, Geoff, Hazel Denton, and Seamus Morris. 2020. "Management Strategies in Acute
608 Traumatic Spinal Cord Injury: A Narrative Review." *Neuroimmunology and Neuroinflammation* 7
609 (September). <https://doi.org/10.20517/2347-8659.2019.005>.
- 610 DeLeve, Laurie D. 2007. "Hepatic Microvasculature in Liver Injury." *Seminars in Liver Disease* 27 (04):
611 390–400. <https://doi.org/10.1055/s-2007-991515>.
- 612 Eng, Jimmy K., Tahmina A. Jahan, and Michael R. Hoopmann. 2013. "Comet: An Open-Source
613 MS/MS Sequence Database Search Tool." *PROTEOMICS* 13 (1): 22–24. <https://doi.org/10.1002/pmic.201200439>.
- 614 Farkas, Gary J., and David R. Gater. 2018. "Neurogenic Obesity and Systemic Inflammation Fol-
615 lowing Spinal Cord Injury: A Review." *The Journal of Spinal Cord Medicine* 41 (4): 378–87. <https://doi.org/10.1080/10790268.2017.1357104>.
- 616 Fleming, Jennifer C., Christopher S. Bailey, Hans Hundt, Kevin R. Gurr, Stewart I. Bailey, Gediminas
617 Cepinskas, Abdel-rahman Lawandy, and Amit Badhwar. 2012. "Remote Inflammatory Response
618 in Liver Is Dependent on the Segmental Level of Spinal Cord Injury." *Journal of Trauma and Acute
619 Care Surgery* 72 (5): 1194–1201. <https://doi.org/10.1097/ta.0b013e31824d68bd>.
- 620 Frost, Frederick, Mary Jo Roach, Irving Kushner, and Peter Schreiber. 2005. "Inflammatory C-
- 621
- 622
- 623
- 624

- 625 reactive Protein and Cytokine Levels in Asymptomatic People with Chronic Spinal Cord Injury."
626 *Archives of Physical Medicine and Rehabilitation* 86 (2): 312-17. <https://doi.org/10.1016/j.apmr.2004.02.009>.
- 627 Fuller, Heidi R., Robert Slade, Nataša Jovanov-Milošević, Mirjana Babić, Goran Sedmak, Goran Šimić,
628 Matthew A. Fuszard, Sally L. Shirran, Catherine H. Botting, and Monte A. Gates. 2015. "Stathmin Is Enriched in the Developing Corticospinal Tract." *Molecular and Cellular Neuroscience* 69
629 (November): 12-21. <https://doi.org/10.1016/j.mcn.2015.09.003>.
- 630 Furlan, Julio C, Sivakumar Gulasingam, and B Catharine Craven. 2017. "The Health Economics of
631 the Spinal Cord Injury or Disease Among Veterans of War : A Systematic Review." *The Journal of
632 Spinal Cord Medicine* 40 (6): 649-64. <https://doi.org/10.1080/10790268.2017.1368267>.
- 633 Gan, Yu, Xunming Ji, Xiaoming Hu, Yumin Luo, Lili Zhang, Peiying Li, Xiangrong Liu, et al. 2012.
634 "Transgenic Overexpression of Peroxiredoxin-2 Attenuates Ischemic Neuronal Injury Via Sup-
635 pression of a Redox-Sensitive Pro-Death Signaling Pathway." *Antioxidants & Redox Signaling* 17
636 (5): 719-32. <https://doi.org/10.1089/ars.2011.4298>.
- 637 Garcia-Bonilla, Lidia, and Costantino Iadecola. 2012. "Peroxiredoxin Sets the Brain on Fire After
638 Stroke." *Nature Medicine* 18 (6): 858-59. <https://doi.org/10.1038/nm.2797>.
- 639 García-López, P., A. Martínez-Cruz, G. Guízar-Sahagún, and G. Castañeda-Hernández. 2007. "Acute
640 Spinal Cord Injury Changes the Disposition of Some, but Not All Drugs Given Intravenously."
641 *Spinal Cord* 45 (9): 603-8. <https://doi.org/10.1038/sj.sc.3102001>.
- 642 Goodus, Matthew T., Andrew D. Sauerbeck, Phillip G. Popovich, Richard S. Bruno, and Dana M.
643 McTigue. 2018. "Dietary Green Tea Extract Prior to Spinal Cord Injury Prevents Hepatic Iron
644 Overload but Does Not Improve Chronic Hepatic and Spinal Cord Pathology in Rats." *Journal of
645 Neurotrauma* 35 (24): 2872-82. <https://doi.org/10.1089/neu.2018.5771>.
- 646 Gris, Denis, Ellis F. Hamilton, and Lynne C. Weaver. 2008. "The Systemic Inflammatory Response
647 After Spinal Cord Injury Damages Lungs and Kidneys." *Experimental Neurology* 211 (1): 259-70.
648 <https://doi.org/10.1016/j.expneurol.2008.01.033>.
- 649 Guo, Qiang, Shurong Li, Yajie Liang, Yanling Zhang, Jiqiang Zhang, Can Wen, Sen Lin, Hanzhi Wang,
650 and Bingyin Su. 2010. "Effects of C3 Deficiency on Inflammation and Regeneration Following
651 Spinal Cord Injury in Mice." *Neuroscience Letters* 485 (1): 32-36. <https://doi.org/10.1016/j.neulet.2010.08.056>.
- 652 Hagen, Ellen Merete. 2015. "Acute Complications of Spinal Cord Injuries." *World Journal of Ortho-
653 pedics* 6 (1): 17-23. <https://doi.org/10.5312/wjo.v6.i1.17>.
- 654 Haskell, Gloria Thompson, Thomas Michael Maynard, Ron Andrew Shatzmiller, and Anthony-
655 Samuel Lamantia. 2002. "Retinoic Acid Signaling at Sites of Plasticity in the Mature
656 Central Nervous System." *Journal of Comparative Neurology* 452 (3): 228-41. <https://doi.org/10.1002/cne.10369>.
- 657 Hayes, K.c., T.c.l. Hull, G.a. Delaney, P.j. Potter, K.a.j. Sequeira, K. Campbell, and P.g. Popovich.
658 2002. "Elevated Serum Titers of Proinflammatory Cytokines and CNS Autoantibodies in Patients
659 with Chronic Spinal Cord Injury." *Journal of Neurotrauma* 19 (6): 753-61. <https://doi.org/10.1089/08977150260139129>.
- 660 Hulme, C. H., S. J. Brown, H. R. Fuller, J. Riddell, A. Osman, J. Chowdhury, N. Kumar, W. E. Johnson,
661 and K. T. Wright. 2017. "The Developing Landscape of Diagnostic and Prognostic Biomarkers
662 for Spinal Cord Injury in Cerebrospinal Fluid and Blood." *Spinal Cord* 55 (2): 114-25. <https://doi.org/10.1038/sc.2016.174>.
- 663 Hulstaert, Niels, Jim Shofstahl, Timo Sachsenberg, Mathias Walzer, Harald Barsnes, Lennart
664 Martens, and Yasset Perez-Riverol. 2020. "ThermoRawFileParser: Modular, Scalable,
665 and Cross-Platform RAW File Conversion." *Journal of Proteome Research* 19 (1): 537-42.
666 <https://doi.org/10.1021/acs.jproteome.9b00328>.
- 667 Hundt, H., J. C. Fleming, J. T. Phillips, A. Lawandy, K. R. Gurr, S. I. Bailey, D. Sanders, et al. 2011. "As-
668 sessment of Hepatic Inflammation After Spinal Cord Injury Using Intravital Microscopy." *Injury*
669 42 (7): 691-96. <https://doi.org/10.1016/j.injury.2010.12.013>.

- 676 Hurst, Robert E., Przemyslaw Waliszewski, Miroslawa Waliszewska, Rebecca B. Bonner, Doris M.
677 Benbrook, Arindam Dar, and George P. Hemstreet. 1999. "Complexity, Retinoid-Responsive
678 Gene Networks, and Bladder Carcinogenesis." In *Advances in Bladder Research*, edited by Lau-
679 rence S. Baskin and Simon W. Hayward, 462:449–67. Advances in Experimental Medicine and
680 Biology. Boston, MA: Springer US. https://doi.org/10.1007/978-1-4615-4737-2_35.
- 681 Jassal, Bijay, Lisa Matthews, Guilherme Viteri, Chuqiao Gong, Pascual Lorente, Antonio Fabregat,
682 Konstantinos Sidiropoulos, et al. 2020. "The Reactome Pathway Knowledgebase." *Nucleic Acids*
683 *Research* 48 (D1): D498–503. <https://doi.org/10.1093/nar/gkz1031>.
- 684 Jogia, Trisha, Marcel A. Kopp, Jan M. Schwab, and Marc J. Ruitenberg. 2021. "Peripheral White Blood
685 Cell Responses as Emerging Biomarkers for Patient Stratification and Prognosis in Acute Spinal
686 Cord Injury." *Current Opinion in Neurology* 34 (6): 796–803. <https://doi.org/10.1097/WCO.0000000000000995>.
- 688 Kim, So Yong, Tae Jin Kim, and Ki-Young Lee. 2008. "A Novel Function of Peroxiredoxin 1 (Prx-1) in
689 Apoptosis Signal-Regulating Kinase 1 (Ask1)-Mediated Signaling Pathway." *FEBS Letters* 582 (13):
690 1913–18. <https://doi.org/10.1016/j.febslet.2008.05.015>.
- 691 Kwon, Brian K., Ona Bloom, Ina-Beate Wanner, Armin Curt, Jan M. Schwab, James Fawcett, and
692 Kevin K. Wang. 2019. "Neurochemical Biomarkers in Spinal Cord Injury." *Spinal Cord* 57 (10):
693 819–31. <https://doi.org/10.1038/s41393-019-0319-8>.
- 694 Kwon, Brian K, Anthea M T Stammers, Lise M Belanger, Arlene Bernardo, Donna Chan, Carole M
695 Bishop, Gerard P Slobogean, et al. 2010. "Cerebrospinal Fluid Inflammatory Cytokines and
696 Biomarkers of Injury Severity in Acute Human Spinal Cord Injury." *Journal of Neurotrauma* 27
697 (4): 669–82. <https://doi.org/10.1089/neu.2009.1080>.
- 698 Lane, Michelle A., and Sarah J. Bailey. 2005. "Role of Retinoid Signalling in the Adult Brain." *Progress*
699 *in Neurobiology* 75 (4): 275–93. <https://doi.org/10.1016/j.pneurobio.2005.03.002>.
- 700 Low, Felicia M., Mark B. Hampton, and Christine C. Winterbourn. 2008. "Peroxiredoxin 2 and Per-
701 oxide Metabolism in the Erythrocyte." *Antioxidants & Redox Signaling* 10 (9): 1621–30. <https://doi.org/10.1089/ars.2008.2081>.
- 703 Lu, Yue, Xiang-Sheng Zhang, Zi-Huan Zhang, Xiao-Ming Zhou, Yong-Yue Gao, Guang-Jie Liu, Han
704 Wang, Ling-Yun Wu, Wei Li, and Chun-Hua Hang. 2018. "Peroxiredoxin 2 Activates Microglia by
705 Interacting with Toll-like Receptor 4 After Subarachnoid Hemorrhage." *Journal of Neuroinflammation* 15 (1): 87. <https://doi.org/10.1186/s12974-018-1118-4>.
- 707 Lu, Yue, Xiang-Sheng Zhang, Xiao-Ming Zhou, Yong-Yue Gao, Chun-Lei Chen, Jing-Peng Liu, Zhen-
708 Nan Ye, et al. 2019. "Peroxiredoxin 1/2 Protects Brain Against H2O2-induced Apoptosis After
709 Subarachnoid Hemorrhage." *The FASEB Journal* 33 (2): 3051–62. <https://doi.org/10.1096/fj.201801150R>.
- 711 Malaspina, Andrea, Narendra Kaushik, and Jackie De Belleroche. 2001. "Differential Expression of
712 14 Genes in Amyotrophic Lateral Sclerosis Spinal Cord Detected Using Gridded cDNA Arrays." *Journal of Neurochemistry* 77 (1): 132–45. <https://doi.org/10.1046/j.1471-4159.2001.00231.x>.
- 714 Matsuzawa, Atsushi, Kaoru Saegusa, Takuya Noguchi, Chiharu Sadamitsu, Hideki Nishi-
715 toh, Shigenori Nagai, Shigeo Koyasu, Kunihiro Matsumoto, Kohsuke Takeda, and Hide-
716 nori Ichijo. 2005. "ROS-dependent Activation of the TRAF6-ASK1-p38 Pathway Is Selec-
717 tively Required for TLR4-mediated Innate Immunity." *Nature Immunology* 6 (6): 587–92.
718 <https://doi.org/10.1038/ni1200>.
- 719 McDaid, David, A.-La Park, Angela Gall, Mariel Purcell, and Mark Bacon. 2019. "Understanding and
720 Modelling the Economic Impact of Spinal Cord Injuries in the United Kingdom." *Spinal Cord* 57
721 (9): 778–88. <https://doi.org/10.1038/s41393-019-0285-1>.
- 722 Peffers, M. J., B. McDermott, P. D. Clegg, and C. M. Riggs. 2015. "Comprehensive Protein Profiling
723 of Synovial Fluid in Osteoarthritis Following Protein Equalization." *Osteoarthritis and Cartilage*
724 23 (7): 1204–13. <https://doi.org/10.1016/j.joca.2015.03.019>.
- 725 Peterson, P. A. 1971. "Studies on the Interaction Between Prealbumin, Retinol-Binding Protein, and
726 Vitamin A." *The Journal of Biological Chemistry* 246 (1): 44–49.

- 727 Qiao, Fei, Carl Atkinson, Hongbin Song, Ravinder Pannu, Inderjit Singh, and Stephen Tomlinson.
728 2006. "Complement Plays an Important Role in Spinal Cord Injury and Represents a Therapeutic
729 Target for Improving Recovery Following Trauma." *The American Journal of Pathology* 169 (3):
730 1039–47. <https://doi.org/10.2353/ajpath.2006.060248>.
- 731 Rhee, Sue Goo, and Hyun Ae Woo. 2011. "Multiple Functions of Peroxiredoxins: Peroxidases, Sen-
732 sors and Regulators of the Intracellular Messenger H₂O₂, and Protein Chaperones." *Antioxidants*
733 & Redox Signaling
- 734 Röst, Hannes L., Timo Sachsenberg, Stephan Aiche, Chris Bielow, Hendrik Weisser, Fabian Aicheler,
735 Sandro Andreotti, et al. 2016. "OpenMS: A Flexible Open-Source Software Platform for Mass
736 Spectrometry Data Analysis." *Nature Methods* 13 (9): 741–48. <https://doi.org/10.1038/nmeth.3959>.
- 737 Salzano, Sonia, Paola Checconi, Eva-Maria Hanschmann, Christopher Horst Lillig, Lucas D. Bowler,
738 Philippe Chan, David Vaudry, et al. 2014. "Linkage of Inflammation and Oxidative Stress via
739 Release of Glutathionylated Peroxiredoxin-2, Which Acts as a Danger Signal." *Proceedings of the*
740 *National Academy of Sciences* 111 (33): 12157–62. <https://doi.org/10.1073/pnas.1401712111>.
- 741 Segal, J. L., E. Gonzales, S. Yousefi, L. Jamshidipour, and S. R. Brunnemann. 1997. "Circulating Levels
742 of IL-2r, ICAM-1, and IL-6 in Spinal Cord Injuries." *Archives of Physical Medicine and Rehabilitation*
743 78 (1): 44–47. [https://doi.org/10.1016/s0003-9993\(97\)90008-3](https://doi.org/10.1016/s0003-9993(97)90008-3).
- 744 Shichita, Takashi, Eiichi Hasegawa, Akihiro Kimura, Rimpei Morita, Ryota Sakaguchi, Ichiro Takada,
745 Takashi Sekiya, et al. 2012. "Peroxiredoxin Family Proteins Are Key Initiators of Post-Ischemic
746 Inflammation in the Brain." *Nature Medicine* 18 (6): 911–17. <https://doi.org/10.1038/nm.2749>.
- 747 Sockanathan, Shanthini, and Thomas M Jessell. 1998. "Motor Neuron-Derived Retinoid Signaling
748 Specifies the Subtype Identity of Spinal Motor Neurons." *Cell* 94 (4): 503–14. [https://doi.org/10.1016/S0092-8674\(00\)81591-3](https://doi.org/10.1016/S0092-8674(00)81591-3).
- 749 Song, Guoqing, Cate Cechvala, Daniel K. Resnick, Robert J. Dempsey, and Vermuganti L. Raghavendra Rao. 2001. "GeneChip Analysis After Acute Spinal Cord Injury in Rat." *Journal of Neurochemistry*
750 79 (4): 804–15. <https://doi.org/10.1046/j.1471-4159.2001.00626.x>.
- 751 Spiess, Martina R., Roland M. Müller, Rüdiger Rupp, Christian Schuld, and Hubertus J. A. van Hedel.
752 2009. "Conversion in ASIA Impairment Scale During the First Year After Traumatic Spinal Cord
753 Injury." *Journal of Neurotrauma* 26 (11): 2027–36. <https://doi.org/10.1089/neu.2008.0760>.
- 754 Stoscheck, Christa M. 1987. "Protein Assay Sensitive at Nanogram Levels." *Analytical Biochemistry*
755 160 (2): 301–5. [https://doi.org/10.1016/0003-2697\(87\)90051-0](https://doi.org/10.1016/0003-2697(87)90051-0).
- 756 Sun, Xin, Zachary B. Jones, Xiao-ming Chen, Libing Zhou, Kwok-Fai So, and Yi Ren. 2016. "Multiple
757 Organ Dysfunction and Systemic Inflammation After Spinal Cord Injury: A Complex Relation-
758 ship." *Journal of Neuroinflammation* 13 (1): 260. <https://doi.org/10.1186/s12974-016-0736-y>.
- 759 Szalai, Alexander J., Frederik W. van Ginkel, Yue Wang, Jerry R. McGhee, and John E. Volanakis. 2000.
760 "Complement-Dependent Acute-Phase Expression of C-Reactive Protein and Serum Amyloid P-
761 Component." *The Journal of Immunology* 165 (2): 1030–35. <https://doi.org/10.4049/jimmunol.165.2.1030>.
- 762 The UniProt Consortium. 2021. "UniProt: The Universal Protein Knowledgebase in 2021." *Nucleic
763 Acids Research* 49 (D1): D480–89. <https://doi.org/10.1093/nar/gkaa1100>.
- 764 Wang, Kevin K., Zhihui Yang, Tian Zhu, Yuan Shi, Richard Rubenstein, J. Adrian Tyndall, and Geoff T.
765 Manley. 2018. "An Update on Diagnostic and Prognostic Biomarkers for Traumatic Brain Injury."
766 *Expert Review of Molecular Diagnostics* 18 (2): 165–80. <https://doi.org/10.1080/14737159.2018.1428089>.
- 767 Yang, Chih-Ya, Jiun-Bo Chen, Ting-Fen Tsai, Yi-Chen Tsai, Ching-Yen Tsai, Pi-Hui Liang, Tsui-Ling Hsu,
768 et al. 2013. "Clec4f Is an Inducible C-Type Lectin in F4/80-Positive Cells and Is Involved in Alpha-
769 Galactosylceramide Presentation in Liver." *PLOS ONE* 8 (6): e65070. <https://doi.org/10.1371/journal.pone.0065070>.
- 770 Yu, Guangchuang, and Qing-Yu He. 2016. "ReactomePA: An R/Bioconductor Package for Reactome
771 Pathway Analysis and Visualization." *Molecular BioSystems* 12 (2): 477–79. <https://doi.org/10.1039/c5mb00530a>.

